Effective Field Theory for Doubly Heavy Baryons and Lattice QCD

by

Jie Hu

Department of Physics
Duke University

Date: _____

Approved:

_____

Thomas C. Mehen, Supervisor

_____

Shailesh Chandrasekharan

_____

Albert M. Chang

_____

Haiyan Gao

_____

Mark C. Kruse

Dissertation submitted in partial fulfillment of the
requirements for the degree of Doctor of Philosophy
in the Department of Physics
in the Graduate School of
Duke University

2009

ABSTRACT

Effective Field Theory for Doubly Heavy Baryons and Lattice QCD

by

Jie Hu

Department of Physics
Duke University

Date: _____

Approved:

_____
Thomas C. Mehen, Supervisor

_____
Shailesh Chandrasekharan

_____
Albert M. Chang

_____
Haiyan Gao

_____
Mark C. Kruse

An abstract of a dissertation submitted in partial fulfillment of the
requirements for the degree of Doctor of Philosophy
in the Department of Physics
in the Graduate School of
Duke University

2009

Abstract

In this thesis, we study effective field theories for doubly heavy baryons and lattice QCD. We construct a chiral Lagrangian for doubly heavy baryons and heavy mesons that is invariant under heavy quark-diquark symmetry at leading order and includes the leading $O(1/m_Q)$ symmetry violating operators. The theory is used to predict the electromagnetic decay width of the $J = \frac{3}{2}$ member of the ground state doubly heavy baryon doublet. Numerical estimates are provided for doubly charm baryons. We also calculate chiral corrections to doubly heavy baryon masses and strong decay widths of low lying excited doubly heavy baryons. We derive the couplings of heavy diquarks to weak currents in the limit of heavy quark-diquark symmetry, and construct the chiral Lagrangian for doubly heavy baryons coupled to weak currents. Chiral corrections to doubly heavy baryon zero-recoil semileptonic decay for both unquenched and partially quenched QCD are calculated. This theory is used to derive chiral extrapolation formulae for measurements of the doubly heavy baryon zero-recoil semileptonic decay form factors in lattice QCD simulations. Additionally, we study the pion physics on lattice using chiral perturbation theory. For finite

volume field theories with discrete translational invariance, conserved currents can obtain additional corrections from infrared effects. We demonstrate this for pions using chiral perturbation theory coupled to electromagnetism in a periodic box. Gauge invariant single particle effective theories are constructed to explain these results. We use chiral perturbation theory to study the extraction of pion electromagnetic polarizabilities from lattice QCD. Chiral extrapolation formulae are derived for partially quenched and quenched QCD simulations. We determine finite volume corrections to the Compton scattering tensor of pions.

Dedicated to my mother and father.

Contents

List of Tables

List of Figures

Acknowledgements

I would like to express my gratitude to all those who made it possible to complete this thesis. First, I want to thank Physics Department at Duke University for allowing me to do the necessary research work.

I am deeply indebted to my advisor and mentor Prof. Thomas C. Mehen, whose encouragement, invaluable guidance, and stimulating suggestions helped me in all the time of my research. During the past years, I have acquired a great deal from him of technical knowledge, philosophical insights, and art of dealing with complicated situations both in research and in life. It is a great honor to be his student. I am also grateful to Prof. Shailesh Chandrasekharan, Prof. Albert M. Chang, Prof. Haiyan Gao and Prof. Mark C. Kruse for kindly serving on my committee.

I would like to express my appreciation to the members of the theoretical nuclear and particle physics group at Physics Department for their support, encouragement, valuable comments and help with questions: Prof. Roxanne P. Springer, Prof. Berndt Müller, Prof. Shailesh Chandrasekharan, Prof. M. Ronen Plesser; as well as Dr. Brian Tiburzi, Dr. Fu-Jiun Jiang, Dr. Brian Bunton and Dr. D. J. Cecile. I would also like to thank my classmates for their valuable friendship and support to me during these years, especially Matthew Blackston and Cortney Blackston, Zheng Gao, Dean Hidas, Le Luo and Qiang Ye, who have been good friends. I am especially thankful to have met Carolyn Berger and Jianrong Deng, who shared a lot of happy or sad moments together and would be there whenever needed.

Last but not least, I want to thank my husband Lingchu Yu for his selfless love, patience, and understanding; thanks to my parents and my parents in law for their constant encouragement and support; and thanks to my close friends, Yiping Liu, Jiefeng Liu, Zhenglei Gao, Peidong Yu, Lian Hong, Xiangqian Hu, Junhua Liu, Yu Wang, Zhen Li, and Xin Lv, whose support and enthusiasm for life helped me in many ways.

For all those mentioned above, I will be eternally grateful.

Chapter 1

Introduction

Quantum Chromodynamics (QCD) is a nonabelian gauge field theory describing the strong interactions which bind quarks and gluons inside hadrons. Asymptotic freedom [1] is the most important feature of QCD: the coupling constant of the strong interaction, α_s, decreases at shorter distance scales. A rough sketch of the strong coupling constant is shown in Fig. 1.1. Λ_{QCD} is the energy scale of QCD, which locates at the pole of the one-loop running coupling constant and is about a few hundred MeV, and $\Lambda_\chi \approx 1.5$ GeV is the chiral symmetry breaking scale which we will discuss in the next section. In the high energy regime, where $\ln(q^2/\Lambda_{QCD}^2) \gg 1$, $\alpha_s \ll 1$, therefore perturbation theory is very useful to describe high energy collisions characterized by large momentum transfer. However, as the energy approaches Λ_{QCD} the QCD coupling becomes so large, perturbation theory breaks down and nonperturbative effects become important. Effective field theory is a useful method for describing the low energy dynamics of QCD and providing analytic results which can be tested directly by experiments. In this thesis, the relevant tools which we will use are chiral symmetry and chiral perturbation theory, heavy quark symmetry, non-relativistic QCD, and lattice QCD.

$$\alpha_s(q^2) = \frac{2\pi}{b_0 \log(q^2/\Lambda^2_{QCD})} + \cdots$$
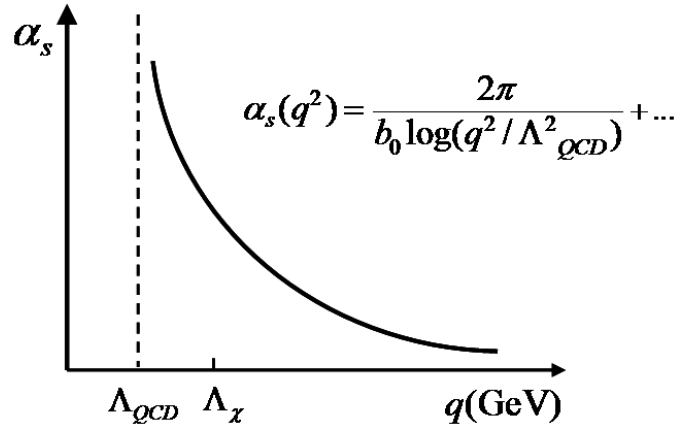
Figure 1.1: The strong coupling constant, α_s, as a function of q, the momentum transfer in the processes. Here $b_0 = \frac{1}{2}(11 - \frac{2}{3}n_f)$, where n_f = number of flavors and the ellipsis denotes higher order terms.

1.1   Chiral Symmetries and Chiral Lagrangian

The QCD Lagrangian of light quarks and gluons is [2]

$$\mathcal{L}_{QCD} = -\frac{1}{4}G^A_{\mu\nu}G^{A\mu\nu} + \bar{q}(i\not{D} - m_q)q, \tag{1.1}$$

where q is the triplet of light quark fields,

$$q = \begin{pmatrix} u \\ d \\ s \end{pmatrix}, \tag{1.2}$$

and m_q is the light quark mass matrix,

$$m_q = \begin{pmatrix} m_u & 0 & 0 \\ 0 & m_d & 0 \\ 0 & 0 & m_s \end{pmatrix}. \tag{1.3}$$

The color index on the quarks is suppressed. Here D_μ denotes the $SU(3)$ color covariant derivative,

$$D_\mu = \partial_\mu + ig_s A_\mu^A T^A \ , \tag{1.4}$$

where g_s is the strong coupling, A_μ^A are the eight color gauge fields, and T^A are the eight generators of color $SU(3)$. $G_{\mu\nu}^A$ is the gluon field strength tensor,

$$G_{\mu\nu}^A = \partial_\mu A_\nu^A - \partial_\nu A_\mu^A - g_s f^{ABC} A_\mu^B A_\nu^C, \tag{1.5}$$

where the structure constants f^{ABC} are defined by $[T^A, T^B] = if^{ABC}T^C$. Here $\displaystyle{\not{D}} = D_\mu \gamma^\mu$ and we use the standard "Bjorken and Drell" convention for gamma matrices,

$\gamma^0 = \begin{pmatrix} 1 & 0 \\ 0 & -1 \end{pmatrix}$, $\gamma^i = \begin{pmatrix} 0 & \sigma^i \\ -\sigma^i & 0 \end{pmatrix}$, and $\gamma^5 = \begin{pmatrix} 0 & 1 \\ 1 & 0 \end{pmatrix}$, where σ^i is the Pauli matrix.

In order to explore the chiral symmetry in the limit of $m_q \to 0$, we write the QCD Lagrangian of massless light quarks in terms of left-handed fields and right-handed fields,

$$q_L = \frac{1}{2} \left(1 - \gamma_5 \right) q \ , \quad q_R = \frac{1}{2} \left(1 + \gamma_5 \right) q \ , \tag{1.6}$$

yielding

$$\mathcal{L}_{l.q.} = \bar{q} i \not{D} q = \bar{q}_L i \not{D} q_L + \bar{q}_R i \not{D} q_R \ . \tag{1.7}$$

In the limit of zero quark mass, $\mathcal{L}_{l.q.}$ has the global chiral symmetry $SU(3)_L \times SU(3)_R$,

$$q_L \quad \to \quad L q_L, \ L \in SU(3)_L \ ,$$

$$q_R \quad \to \quad R q_R, \ R \in SU(3)_R \ . \tag{1.8}$$

Note that the strong interactions conserve chirality. Under the $SU(3)_L \times SU(3)_R$ chiral transformation, the right-handed and left handed quark fields can transform differently. The mass terms in the QCD Lagrangian breaks chiral symmetry explicitly,

$$\mathcal{L}_{mass} = -\bar{q}_L m_q q_R - \bar{q}_R m_q q_L \ . \tag{1.9}$$

Even for massless light quarks, chiral symmetry is not an exact symmetry. The non-vanishing vacuum expectation value of the quark bilinear, $\langle 0|\bar{q}_R^j q_L^k|0\rangle = v\delta^{kj}$, spontaneously breaks the chiral symmetry. Here j and k are flavor indices, and v is of order Λ_{QCD}^3. The vacuum expectation value is not changed under transformations with $L = R$, therefore the $SU(3)_L \times SU(3)_R$ chiral symmetry is broken to the subgroup $SU(3)_{L+R}$. As a consequence of this spontaneous symmetry breaking eight Goldstone bosons are produced according to Goldstone's theorem [3, 4]. The Goldstone boson fields can be described by a 3×3 special unitary matrix Σ [5, 6]. Σ represents the low energy excitations of quark bilinear, and transforms as $\Sigma \to L\Sigma R^\dagger$ under $SU(3)_L \times SU(3)_R$ chiral transformations. The Goldstone boson fields are written as

$$\Sigma = exp\left(\frac{2iM}{f}\right) \ , \tag{1.10}$$

where f is the pion decay constant and M is a traceless 3×3 Hermitian matrix,

$$M = \begin{pmatrix} \frac{1}{\sqrt{2}}\pi^0 + \frac{1}{\sqrt{6}}\eta & \pi^+ & K^+ \\ \pi^- & -\frac{1}{\sqrt{2}}\pi^0 + \frac{1}{\sqrt{6}}\eta & K^0 \\ K^- & \bar{K}^0 & -\frac{2}{\sqrt{6}}\eta \end{pmatrix} \ . \tag{1.11}$$

4

Under the unbroken $SU(3)_{L+R}$ transformation $L = R = V$, M transforms as the adjoint representation, $M \to VMV^{\dagger}$, therefore, the π, k and η transform as an $SU(3)_V$ octet. On the other hand we expect M to transform nonlinearly under the broken $SU(3)_L \times SU(3)_R$ transformations, $L = R^{\dagger} = A$. Considering an infinitesimal transformation $L = R^{\dagger} = A = 1 + i\epsilon^a T^a$ as an example, M transforms nonlinearly: $M \to M + f\epsilon^a T^a$.

The effective Lagrangian for the Goldstone bosons is

$$\mathcal{L} = \frac{f^2}{8}\mathrm{Tr}[\partial_{\mu}\Sigma\partial^{\mu}\Sigma^{\dagger}] + v\mathrm{Tr}[m_q^{\dagger}\Sigma + \Sigma^{\dagger}m_q] + \cdots , \qquad (1.12)$$

where the ellipsis denotes terms with more derivatives and factors of m_q. The factor $f^2/8$ is chosen so that the kinetic terms of the Goldstone bosons are properly normalized. The first term is invariant under the chiral symmetry transformation. The higher derivative terms are suppressed by powers of p^2/Λ_{χ}^2, where p is the typical momentum and $\Lambda_{\chi} = 4\pi f$ is the chiral symmetry breaking scale. Tree-level four-pion interactions can be obtained from the Lagrangian in Eq.(1.12) and are of order $\sim p^2/f^2$. The next order contribution from one loop diagrams is of order $\sim p^4/(4\pi)^2 f^4$ where the $(4\pi)^2$ comes from the loop integration. Comparing tree level and one-loop contributions shows the expansion is in $p^2/(4\pi)^2 f^2 = p^2/\Lambda_{\chi}^2$. Also in-

cluded are the leading $O(m_q)$ corrections which give masses to the Goldstone bosons

$$
\begin{aligned}
m^2_{\pi^\pm} &= \frac{4v}{f^2}(m_u + m_d), \\
m^2_{k^\pm} &= \frac{4v}{f^2}(m_u + m_s), \\
m^2_{k^0} &= m^2_{\bar{k}^0} = \frac{4v}{f^2}(m_d + m_s), \\
m^2_{(\pi^0,\eta)} &= \frac{4v}{f^2}
\begin{bmatrix}
(m_u + m_d) & \frac{1}{\sqrt{3}}(m_u - m_d) \\[2mm]
\frac{1}{\sqrt{3}}(m_u - m_d) & \frac{1}{3}(4m_s + m_u + m_d)
\end{bmatrix}.
\end{aligned}
\tag{1.13}
$$

This Lagrangian can be used to analyze Goldstone boson interactions in an expansion in p/Λ_χ and m_π/Λ_χ.

1.2 Heavy Quark Symmetries and Heavy Hadron Chiral Perturbation Theory

Isgur and Wise first discovered the heavy quark symmetry of QCD in 1989 [7, 8]. In hadrons containing a single heavy quark, as sketched in Fig.1.2, the typical momentum exchanged between the heavy and light constituents are of order Λ_{QCD}, and then the size of such systems, R_{had}, is about $1/\Lambda_{QCD}$. When the quark mass is much larger than the QCD scale, the Compton wave length, $1/m_Q$, of the heavy quark bound inside the hadron is much smaller than the typical hadronic distance of about 1 fm, then the heavy quark is like a static source of color. The strong interactions of such a system can be described by an effective theory, which is invariant under changes of the flavor and spin of the heavy quark in the heavy quark limit. Therefore in the limit of infinite heavy quark mass, QCD possesses heavy quark spin flavor
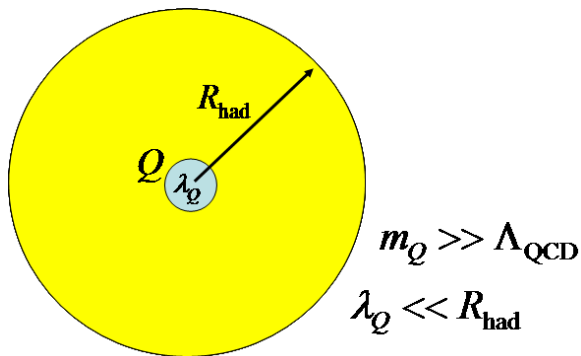
Figure 1.2: The hadrons with one single heavy quark in the heavy quark limit, where $R_{had} \sim \Lambda_{QCD}$ is the typical hadron size and $\lambda_Q \sim 1/m_Q$ is the Compton wave length.

symmetry. Because the interactions of the heavy quark with light degrees of freedom are spin independent to lowest order in $1/m_Q$, the angular momentum of the light degrees of freedom, j, is a good quantum number. Therefore in the heavy quark limit, hadrons containing a single heavy quark come in degenerate doublets of total angular momentum, $J = j \pm \frac{1}{2}$, where J is the total angular momentum of a heavy hadron.

The heavy quark fields are described in an effective field theory, heavy quark effective theory (HQET) [9, 6, 10]. The part of QCD Lagrangian involving the heavy quark field Q is

$$\mathcal{L} = \bar{Q}(i\slashed{D} - m_Q)Q \, , \tag{1.14}$$

where in this work the relevant heavy quarks are the charm and bottom quarks[1]. In

---

[1]This QCD symmetry cannot be applied to top quark, since top quark's lifetime is shorter than the hadronization time scale. However, the heavy quark limit is well defined for QCD if weak

the low energy regime, the heavy quark bound inside a hadron carries most of the energy and momentum of the system. In the low momentum regime it is appropriate to consider the limit of QCD where the heavy quark mass goes to infinity with its four velocity v^μ fixed. The four momentum of the heavy quark is decomposed as $p^\mu = m_Q v^\mu + k^\mu$ where $k^\mu \sim \Lambda_{QCD}$ is the residual momentum. The heavy quark is almost on-shell, its momentum fluctuates around the mass shell by an amount of order Λ_{QCD}. The velocity becomes a conserved quantity and is no longer a dynamical degree of freedom. The heavy quark field is rewritten in terms of fields with fixed velocity v^μ

$$Q = e^{-im_Q v \cdot x}(h_v + b_v) , \tag{1.15}$$

where

$$h_v = e^{im_Q v \cdot x}\frac{1 + \slashed{v}}{2}Q, \qquad b_v = e^{im_Q v \cdot x}\frac{1 - \slashed{v}}{2}Q. \tag{1.16}$$

The heavy quark is almost on-shell, $v \sim 1$, therefore the effects of b_v are suppressed by powers of $1/m_Q$ and can be neglected. After integrating out the b_v field, we obtain the effective Lagrangian

$$\mathcal{L}_v = \bar{h}_v iv \cdot D h_v + \frac{1}{2m_Q}\bar{h}_v[(iD_\perp)^2 - g_s\sigma_{\mu\nu}G^{A\mu\nu}T^A]h_v + O\left(\frac{1}{m_Q^2}\right) , \tag{1.17}$$

where $(D_\perp)_\mu = D_\mu - v_\mu v \cdot D$. The first term is the leading order effective heavy quark Lagrangian and has as its Feynman rules $i/(v \cdot k + i\epsilon)$ for the heavy quark propagator, and $-igT^A v_\mu$ for the vertex of gluon heavy quark interaction. There

interactions are turned off.

are no more gamma matrices in the effective theory, therefore the spin of the heavy quark is conserved. The second and third terms in the Lagrangian are of order $1/m_Q$ and are to be treated as perturbations. The third term breaks heavy quark spin symmetry.

Heavy hadron chiral perturbation theory (HHχPT) [11, 12, 13] is a low energy effective theory that incorporates chiral symmetry and heavy quark symmetry. It has heavy hadrons, Goldstone bosons, and photons as its elementary degrees of freedom and can be used to describe the low energy properties of heavy hadrons. Physical observables, such as the masses of the ground state heavy meson, are calculated in an expansion in light quark masses, m_q, and inverse heavy quark masses, $1/m_Q$. As we discussed before, in the heavy quark limit the hadrons containing a heavy quark come in degenerate doublets of the total angular momentum, $J = j \pm \frac{1}{2}$. For mesons with flavor $Q\bar{q}_a$, the ground state doublets with $j = \frac{1}{2}$ contain the pseudoscalar mesons, P_a, and the vector mesons, $P_a^{*\mu}$, where $a = 1, 2, 3$ denotes u, d, s respectively. The vector fields obey the constraint $v_\mu P_a^{*\mu} = 0$. These fields are combined into a composite field H_a in HHχPT,

$$H_a = \left(\frac{1 + \slashed{v}}{2} \right) (P_a^{*\mu} \gamma_\mu - \gamma_5 P_a) , \qquad (1.18)$$

which satisfies $\slashed{v} H_a = H_a = -H_a \slashed{v}$. The HH$\chi$PT effective Lagrangian that describes the low momentum behavior of the ground state heavy mesons which is invariant under chiral $SU(3)_L \times SU(3)_R$ symmetry, heavy quark symmetry, and parity is [14]

$$\mathcal{L} = -\text{Tr}[\bar{H}_a iv \cdot D_{ba} H_b] + g \text{Tr}[\bar{H}_a H_b \slashed{A}_{ba} \gamma_5] + \cdots , \qquad (1.19)$$

9

where $\bar{H}_a = \gamma^0 H_a^\dagger \gamma^0$ and the ellipsis denotes higher order terms. The chiral covariant derivative is defined by

$$D_{ab}^\mu \equiv \delta_{ab} \partial^\mu - V_{ab}^\mu = \delta_{ab} \partial^\mu - \frac{1}{2}(\xi^\dagger \partial^\mu \xi + \xi \partial^\mu \xi^\dagger)_{ab} . \qquad (1.20)$$

The axial vector field is

$$A_{ab}^\mu = \frac{i}{2}(\xi^\dagger \partial^\mu \xi - \xi \partial^\mu \xi^\dagger)_{ab} . \qquad (1.21)$$

Under heavy quark spin transformation H transforms as $H \to SH$ where S is the $SU(2)$ heavy quark spin rotation matrix. Under chiral symmetry, $H \to HU^\dagger$, $D_\mu H \to (D_\mu H)U^\dagger$ and $A^\mu \to UA_\mu U^\dagger$ where U is a unitary matrix that depends on spacetime. $\xi = e^{iM/f}$ transforms as $\xi \to L\xi U^\dagger = U\xi R^\dagger$ under $SU(3)_L \times SU(3)_R$. At leading order the Lagrangian of the ground state heavy meson and Goldstone bosons is Eq. (1.12) and Eq. (1.19).

At order $\sim m_q$, terms with light quark masses explicitly break the chiral symmetry

$$\delta\mathcal{L}^1 = \lambda_1 \text{Tr}[\bar{H}_b H_a (\xi m_q \xi + \xi^\dagger m_q \xi^\dagger)_{ab}] \qquad (1.22)$$

$$+ \lambda_1' \text{Tr}[\bar{H}_a H_a (\xi m_q \xi + \xi^\dagger m_q \xi^\dagger)_{bb}] .$$

These operators contribute to the leading order $SU(3)$ splittings. At order $\sim 1/m_Q$ the heavy quark spin symmetry breaking operator that gives the leading contribution to the hyperfine splittings is

$$\delta\mathcal{L}^2 = -\frac{\Delta_H}{8} \text{Tr}[\bar{H}_a \sigma^{\mu\nu} H_a \sigma_{\mu\nu}] , \qquad (1.23)$$

where Δ_H is the hyperfine splitting of heavy mesons.

10

This theory is a double expansion in Λ_{QCD}/m_Q and Q/Λ_χ where $Q \sim p \sim m_\pi \sim m_K$ and p is the typical momentum. The parameter Δ_H is treated as order Q. In loop diagrams, integrals scale as Q^4, the propagator of H as Q^{-1} and the propagators of Goldstone bosons as Q^{-2}. The couplings of pions and kaons to the heavy mesons are $\sim Q$. This theory for heavy mesons is well established [14] and an analogous theory for doubly heavy baryons has not been developed. This is the purpose of this thesis.

1.3   Non-Relativistic Quantum Chromodynamics

HQET is not the correct effective theory for hadrons containing two or more heavy quarks. This is because HQET only has two scales of energy, the heavy quark masses, m_Q and Λ_{QCD}, while a bound state containing two or more heavy quarks has two additional scales: $m_Q v$, the typical momentum of the heavy quarks within the bound state, and $m_Q v^2$, the typical kinetic energy of the heavy quarks. The appropriate theory is Non-Relativistic Quantum Chromodynamics (NRQCD) [15, 16]. In the NRQCD formalism, nonperturbative aspects of hadrons with two or more heavy quarks are organized in an expansion in powers of v. The typical velocity v of the heavy quark in the bound diquark decreases as the mass m_Q increases. If m_Q is large enough, v is proportional to the running coupling constant, $v \sim \alpha_s(m_Q v)$, which decreases asymptotically like $1/\ln(m_Q)$. NRQCD [15] assumes that the mass m_Q is large enough and the energy scales are well-separated: $m_Q \gg m_Q v \gg m_Q v^2$. This assumption is very good for doubly bottom hadrons because quark potential model

calculations and lattice QCD calculations indicate the average value of v^2 is about 0.1 for bottomonium, and reasonably good for doubly charm hadrons, for which $v^2 \sim 0.3$. Λ_{QCD} and $m_Q v^2$ are comparable for both charm and bottom.

The NRQCD Lagrangian is derived in Ref. [15, 16]:

$$\mathcal{L}_{NRQCD} = \mathcal{L}_{light} + \mathcal{L}_{heavy} + \delta\mathcal{L}. \tag{1.24}$$

The gluons and the n_f flavors of light quarks are described by the fully relativistic Lagrangian in Eq.(1.1). The heavy quark and antiquarks are described by

$$
\begin{aligned}
\mathcal{L}_{heavy} &= \sum_{\mathbf{p}} \psi_{\mathbf{p}}^{\dagger} \left(iD_0 - \frac{(\mathbf{p} - i\mathbf{D})^2}{2m_Q} \right) \psi_{\mathbf{p}} + \chi_{\mathbf{p}}^{\dagger} \left(iD_0 - \frac{(\mathbf{p} - i\mathbf{D})^2}{2m_Q} \right) \chi_{\mathbf{p}} \\
&+ \sum_{\mathbf{p},\mathbf{q}} \frac{4\pi\alpha_s}{(\mathbf{p} - \mathbf{q})^2} \psi_{\mathbf{q}}^{\dagger} T^A \psi_{\mathbf{p}} \chi_{-\mathbf{q}}^{\dagger} \bar{T}^A \chi_{-\mathbf{p}} + \cdots,
\end{aligned}
\tag{1.25}
$$

where $\psi_{\mathbf{p}}$ is the Pauli spinor field that annihilates a heavy quark and $\chi_{\mathbf{p}}$ is the Pauli spinor field that creates a heavy antiquark. Color and spin indices have been suppressed. The last term is the Coulomb interaction and is also leading order. The relativistic effects of full QCD are reproduced through the correction term $\delta\mathcal{L}$.

To examine the properties of baryons with two heavy quarks, an additional symmetry - heavy quark-diquark symmetry - is valuable. In the limit of $m_Q \to \infty$, the spatial extent of the diquark, $1/(m_Q v)$, is small compared to the size of the hadron, $1/\Lambda_{QCD}$, therefore the diquark can be treated as a pointlike object. The color representation of the anti-diquark decomposes as $\bar{3} \otimes \bar{3} = \bar{6} \oplus 3$ where $\bar{6}$ is symmetric color wavefunction and 3 is the antisymmetric wavefunction. The anti-diquark inside the baryon must be in the 3 representation in order to make the baryon color singlet.
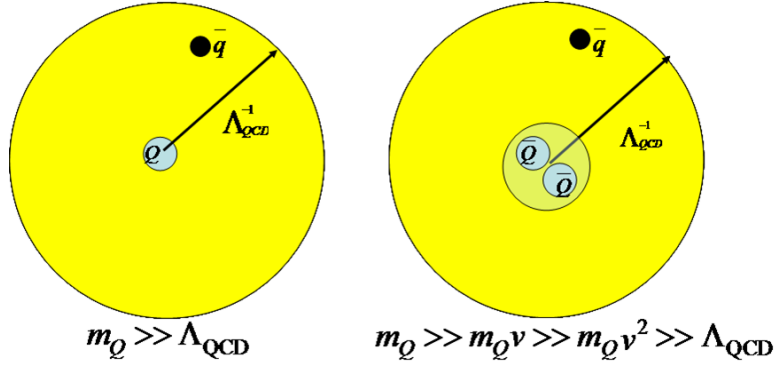
Figure 1.3: The properties of a heavy meson with one single heavy quark and those of a doubly heavy antibaryon with two heavy antiquarks are related by heavy quark-diquark symmetry, where $\sim \Lambda_{QCD}$ is the typical hadron size and $\sim 1/(m_Q v)$ is extend of the diquark.

Thus, bound anti-diquark inside the doubly heavy antibaryon gives rise to the same color triplet field as the heavy quark in the heavy meson. The heavy quark spin and flavor are irrelevant in the $m_Q \to \infty$ limit. Then the configuration of the light degrees of freedom will be the same in both hadrons. Therefore the properties of doubly heavy antibaryons with two heavy antiquarks can be related to those of the heavy mesons with a single heavy quark by this symmetry. Refs. [17, 18] derived effective Lagrangians for heavy diquarks within the framework of Non-Relativistic QCD (NRQCD) [15, 19, 16]. These papers obtain a prediction for the hyperfine splitting of the ground state doubly heavy baryons in terms of the ground state heavy meson hyperfine splitting[2].

---

[2]The formula for the hyperfine splittings in Ref. [20] differs from the correct formula in Refs. [17, 18] by a factor of 2.

In the next chapter, we construct a chiral Lagrangian for doubly heavy baryons and heavy mesons, which is invariant under heavy quark-diquark symmetry at leading order and includes the leading $O(1/m_Q)$ symmetry violating operators. Predictions for the strong and electromagnetic decays of the ground and excited states are made. Chiral corrections to the heavy quark-diquark symmetry predictions are explored. We provide numerical estimates for doubly charm baryons. In the third chapter, we extend the chiral Lagrangian for doubly heavy baryons to include semileptonic weak decays using χPT, heavy quark effective theory, and nonrelativistic QCD. Doubly heavy baryon zero-recoil semileptonic decay form factors are predicted from this theory with heavy quark-diquark symmetry. The theoretical predictions of masses and decays in these two chapters are very helpful for experimental searches for doubly charm baryons, doubly bottom baryons and charm bottom baryons in collider experiments like the LHC and the Tevatron. The EFT techniques with heavy quark-diquark symmetry for doubly heavy baryons can also be applied to doubly heavy systems simulated in lattice QCD calculations.We extend the chiral Lagrangian with heavy quark-diquark symmetry to the partially quenched theory. These theories can be used to derive formulae for the chiral extrapolation of zero recoil semileptonic decay of double heavy baryons in lattice QCD simulations.

1.4 Lattice QCD

Another useful tool to address the non-perturbative dynamics of quarks and gluons is lattice gauge theory. Lattice QCD can be employed to calculate QCD observables from first principles using non-perturbative numerical techniques. Lattice QCD is based on the lattice regularization which was introduced by Wilson in the 1970's [21]. The basic idea is to introduce lattice spacing a and discretize the theory on a lattice in a finite volume L^d, where d is the dimension. Expectation values of observables can be expressed as a path integral which can be directly evaluated using Monte-Carlo methods.

The lattice QCD calculations have a finite lattice spacing, a, a finite lattice size, L, and unphysical quark mass m_q. However relating the results of simulations to the real world requires extrapolation to zero lattice spacing, infinite lattice size and physical quark mass. Therefore actual lattice QCD calculations suffer from a number of systematic errors. Understanding and predicting these systematic errors are necessary for accurate determination of hadronic observables. For example, finite volume effects are important when $L \sim 1/m_\pi$. In recent lattice QCD simulations, this occurs when the lattice pion masses approach the physical pion masses. Another issue is quark masses. It is very computationally expensive to simulate virtual quarks with physical masses on the lattice. Sometimes the simulations omit the sea quark contributions alltogether, this is called quenching. This is equivalent to setting the sea quark masses to infinity. Other simulations have sea quark masses that are larger than the valence

quark masses, this is called partial quenching.

Effective field theory can be used to address these systematic errors and determine the quark mass dependence of the observables. We add two kinds of quarks to the theory, sea quarks with different masses than valence quarks and ghost quarks with the same masses as valence quark but with different statistics. Therefore $SU(3)$ is replaced by $SU(6|3)$. Ghost quarks are bosons which bring opposite sign to the loops and therefore cancel the valence quark contributions. Then only sea quark contributions are left and this is equivalent to the partially quenching artifact in lattice QCD simulations. If sea quark masses are set to infinity, the theory is then $SU(3|3)$ and is equivalent to the quenching artifact. This artifacts are considered in our doubly heavy baryon semileptonic decays.

In the last chapter we study the pion physics at finite volume L^3. We investigate the pion current matrix elements at finite volume using chiral perturbation theory. We determine the finite volume corrections to matrix element of the conserved pion electromagnetic currents. The Ward identities still work at finite volume. We also use chiral perturbation theory to study the extraction of pion electromagnetic polarizabilities from lattice QCD. We derive chiral extrapolation formulae for partially quenched and quenched QCD simulations and we calculate the finite volume corrections to the Compton scattering tensor of pions.

Chapter 2

Chiral Lagrangian with Heavy Quark-Diquark Symmetry

2.1   Introduction

Motivation[1] for this work comes from the SELEX experiment's recent observation of states which have been tentatively interpreted as doubly charm baryons [23, 24, 25], and also the COMPASS experiment, which in its second phase run in 2006 hopes to observe doubly charm baryons [26]. Many aspects of the SELEX states are difficult to understand. States observed by SELEX include the $\Xi_{cc}^{+}(3520)$, which decays weakly into $\Lambda_c^+ \pi^+ K^-$ [23] as well as $pD^+ K^-$ [25], the $\Xi_{cc}^{++}(3460)$, which decays weakly into $\Lambda_c^+ K^- \pi^+ \pi^+$ [24], and a broader state, $\Xi_{cc}^{++}(3780)$, also seen to decay into $\Lambda_c^+ K^- \pi^+ \pi^+$ [24]. The ground states of the Ξ_{cc}^+ and Ξ_{cc}^{++} are related by isospin symmetry and therefore should differ in mass by only a few MeV, so the observed difference of 60 MeV seems implausible. On the other hand, an unpublished talk [27] and conference proceedings [28] present evidence for additional states, $\Xi_{cc}^{+}(3443)$ and $\Xi_{cc}^{++}(3541)$. If these states exist the isospin splittings are closer to theoretical expectations, but still quite large. The difference between the mass of the $\Xi_{cc}^{+}(3520)$ and $\Xi_{cc}^{+}(3443)$ is 77 MeV, and the splitting between $\Xi_{cc}^{++}(3541)$ and $\Xi_{cc}^{++}(3460)$ is 81

---

[1]This chapter was previously published in Ref. [22] and was performed in collaboration with Prof. Mehen.

17

MeV. These splittings agree remarkably well with calculations of the doubly charm hyperfine splittings in quenched lattice QCD [29, 30, 31] and are within ~ 25 MeV of the heavy quark-diquark symmetry prediction obtained in Refs. [17, 18, 29, 32], an acceptable discrepancy given the expected corrections. However, interpretation of the $\Xi_{cc}^+(3520)$ as the $J = \frac{3}{2}$ member of the ground state doublet is impossible to reconcile with the fact that the $\Xi_{cc}^+(3520)$ is observed to decay weakly because if the $\Xi_{cc}^+(3520)$ is not the ground state of the ccd system it should decay electromagnetically. There are also discrepancies between the weak decay lifetimes predicted by HQET [33, 34, 35](~ 100 fs) and the observed lifetimes (< 33 fs) [23, 25]. Production cross sections are also poorly understood within perturbative QCD [36, 37]. However, the SELEX states are observed in the forward region, $\langle x_F \rangle \sim 0.3$, where nonperturbative production mechanisms such as intrinsic charm [38, 39, 40] or parton recombination [41, 42] may be important.

Even if there is difficulty interpreting the SELEX data, doubly charm baryons must exist and are expected to have masses of approximately 3.5 GeV [36, 43, 44, 45, 46, 47, 48], where the SELEX states are. In light of existing and future experimental efforts to observe doubly charm baryons, it is desirable to have model independent predictions for other properties besides the relation for the hyperfine splittings derived in Refs. [20, 17, 18]. Therefore it is important to develop theoretical tools for analyzing the properties of doubly heavy baryons systematically.

Heavy quark-diquark symmetry relates mesons with a single heavy quark to

antibaryons with two heavy antiquarks. Heavy hadron chiral perturbation theory (HHχPT) [11, 12, 13] is a useful tool for studying low energy strong and electromagnetic interactions of heavy hadrons. This theory has heavy hadrons, Goldstone bosons, and photons as its elementary degrees of freedom and incorporates the approximate chiral and heavy quark symmetries of QCD. In this chapter we derive a version of HHχPT that includes doubly heavy baryons and incorporates heavy quark-diquark symmetry. The theory is used to calculate chiral corrections to doubly heavy baryon masses and to obtain model-independent predictions for the electromagnetic decay of the $J = \frac{3}{2}$ member of the ground state doubly heavy baryon doublet. We also discuss the low lying excited doubly heavy baryons, show how these states can be included in the effective theory, and calculate their strong decay widths.

Our formalism works best in the limit $m_Q \gg m_Q v \gg m_Q v^2 \gtrsim \Lambda_{QCD}$. Such a separation of scales is only approximately realized in doubly charmed and doubly bottom baryons. The scale Λ_{QCD} should be identified with the hadronic matrix elements typical of heavy quark systems. Using the hyperfine splittings of heavy mesons, which are $O(\Lambda_{QCD}^2/m_Q)$, or the excitation energies of excited heavy mesons, which are $O(\Lambda_{QCD})$, one finds $\Lambda_{QCD} \sim 350-500$ MeV. Taking $m_b \sim 5$ GeV, $m_c \sim 1.5$ GeV, $v_b^2 \sim 0.1$ and $v_c^2 \sim 0.3$ [15] one finds $m_b v_b^2 \sim m_c v_c^2 \sim \Lambda_{QCD}$, while $m_b v_b \sim 1.5$ GeV and $m_c v_c \sim 800$ MeV. If one assumes that corrections to heavy quark-diquark symmetry scale as $\Lambda_{QCD}/(m_Q v)$ then these naive estimates lead to the expectation that heavy quark-diquark symmetry predictions should have $\sim 30\%$ errors for doubly

bottom baryons and $\sim 60\%$ errors for doubly charm baryons. Nevertheless, there is some empirical support for applying heavy quark-diquark symmetry to doubly charm baryons, since the leading heavy quark-diquark symmetry prediction for the hyperfine splitting of doubly charm baryons only differs from quenched lattice QCD calculations and preliminary experimental data by about 30% [17, 18, 29]. More data and theoretical predictions are needed to test whether heavy quark-diquark symmetry applies to doubly charm baryons, and an important goal of this chapter is to provide new predictions based on heavy quark-diquark symmetry for this purpose. Though doubly bottom baryons would make a better testing ground for the formalism of this chapter, no experimental observation of such states has been reported to date. Our formulas can be applied to doubly bottom baryons once they are discovered. In our numerical estimates, we will focus on doubly charmed baryons since there is some experimental evidence for the existence of these states [23, 24, 25].

The rest of this chapter is organized as follows. In Sec.2.2, we derive a chiral Lagrangian for the ground state doubly heavy baryons and heavy mesons with approximate heavy quark-diquark symmetry. In Sec.2.3, the electromagnetic decay widths of the $J = \frac{3}{2}$ members of the ground state doubly heavy baryon doublets are calculated. In Sec.2.4, we compute the chiral corrections to doubly heavy baryon masses. In Sec.2.5, we discuss the lowest lying excitations of the doubly heavy baryon, which turn out to be excitations of the diquark. The strong decay rates of these states are calculated. In Sec.2.6, a brief summary is given.

2.2   Derivation of the Chiral Lagrangian

Savage and Wise [20] wrote down a version of heavy quark effective theory (HQET) which includes diquarks as elementary degrees of freedom and derived a formula relating heavy meson and doubly heavy baryon hyperfine splittings. HQET only separates the scales Λ_{QCD} and m_Q, where m_Q is the heavy quark mass. The dynamics of a bound state of two heavy quarks is characterized by additional scales $m_Q v$ and $m_Q v^2$, where v is the typical velocity of the heavy quarks in the bound state. The correct effective theory for hadrons with two heavy quarks is Non-Relativistic QCD (NRQCD) [15], which properly accounts for the scales $m_Q v$ and $m_Q v^2$. Analysis of heavy diquarks within the framework of NRQCD was recently performed in Refs. [17, 18]. These papers derived Lagrangians for diquark fields starting from NRQCD and obtained the correct heavy quark symmetry prediction for the hyperfine splittings of the doubly heavy baryons. For simplicity, we will consider only one flavor of heavy quark. The lowest mass diquark will consist of two heavy antiquarks in an orbital S-wave in the **3** representation of color $SU(3)$. Then Fermi statistics demands that they have total spin one. In the rest frame of the heavy quark and lowest mass diquark, the Lagrangian to $O(1/m_Q)$ is [20, 18]

$$
\begin{aligned}
\mathcal{L} &= h^\dagger \left(iD_0 - \frac{\vec{D}^2}{2m_Q} \right) h + \vec{V}^\dagger \cdot \left(iD_0 + \delta - \frac{\vec{D}^2}{m_Q} \right) \vec{V} \\
&\quad + \frac{g_s}{2m_Q} h^\dagger \, \vec{\sigma} \cdot \vec{B}^a \frac{\lambda^a}{2} h + \frac{ig_s}{2m_Q} \vec{V}^\dagger \cdot \vec{B}^a \frac{\lambda^a}{2} \times \vec{V} .
\end{aligned}
\tag{2.1}
$$

Here h is the heavy quark field, $\vec{V}$ is the field for the diquarks, the $\lambda^a/2$ are the $SU(3)$ color generators, $\text{Tr}[\lambda^a \lambda^b] = 2\,\delta^{ab}$, D_0 and $\vec{D}$ are the time and spatial components of the gauge covariant derivative, respectively, $\vec{B}^a$ is the chromomagnetic field, and m_Q is the heavy quark mass. The term proportional to δ is the residual mass of the diquark. The heavy antiquarks in the diquark experience an attractive force and therefore the mass of the diquark is not $2m_Q$ but $2m_Q - \delta$, where δ is the binding energy. This residual mass can be removed by rephasing the diquark fields. Physically, this corresponds to measuring diquark energies relative to the mass of the diquark, rather than $2m_Q$. Once this is done the Lagrangian, at lowest order in $1/m_Q$, is invariant under a $U(5)$ symmetry which permutes the two spin states of the heavy quark and the three spin states of the heavy antiquarks. The $U(5)$ symmetry is broken by the $O(1/m_Q)$ kinetic energy and chromomagnetic couplings of the heavy quark and diquark. The latter terms are responsible for the hyperfine splittings.

The ground state doublet of heavy mesons is usually represented in HHχPT as a 4×4 matrix transforming covariantly under Lorentz transformations, and transforming as a doublet under $SU(2)$ heavy quark spin symmetry,

$$H_v = \left(\frac{1 + \slashed{v}}{2}\right) \left(P_v^{*\mu}\gamma_\mu - \gamma_5 P_v\right). \tag{2.2}$$

Here $P_v^{*\mu}$ is the $J^P = 1^-$ vector heavy meson field which obeys the constraint $v_\mu P_v^{*\mu} = 0$, where v^μ is the four-velocity of the heavy meson. P_v is the $J^P = 0^-$ pseudoscalar heavy meson field. The superfield H_v obeys the constraints $\slashed{v} H_v = -H_v \slashed{v} = H_v$, so H_v only has four independent degrees of freedom. These can be collected in a 2×2

22

matrix. For example, in the heavy meson rest frame where $v^\mu = (1, 0, 0, 0)$,

$$H_v = \begin{pmatrix} 0 & -\vec{P}_v^* \cdot \vec{\sigma} - P_v \\ 0 & 0 \end{pmatrix},$$ (2.3)

where we have used the Bjorken-Drell conventions for γ_μ and γ_5. For a process such as

the weak decay $B \to D\ell\nu$, in which the initial and final heavy hadrons have different

four-velocities, the covariant representation of fields is needed to determine heavy

quark symmetry constraints on heavy hadron form-factors. However, for studying

low energy strong and electromagnetic interactions in which the heavy meson four-

velocity is conserved (up to $O(\Lambda_{\rm QCD}/m_Q)$ corrections), it is also possible to work in

the heavy meson rest frame and use 2×2 matrix fields. This makes some calculations

simpler and we find it easiest to formulate the extension of HHχPT with $U(5)$ quark-

diquark symmetry in this frame. We define the heavy meson field in our theory to

be

$$H_a = \vec{P}_a^* \cdot \vec{\sigma} + P_a,$$ (2.4)

where a is an $SU(3)$ flavor anti-fundamental index and the $\vec{\sigma}$ are the Pauli matrices.

Since we have chosen to work in the heavy meson rest frame, Lorentz covariance is

lost and the symmetries of the theory are rotational invariance, $SU(2)$ heavy quark

spin symmetry, parity, time reversal and $SU_L(3) \times SU_R(3)$ chiral symmetry. Under

these symmetries the field H_a transforms as

$$\text{rotations} \quad H_a' = U H_a U^\dagger$$

$$\text{heavy quark spin} \quad H_a' = S H_a$$

$$\text{parity} \quad H_a' = -H_a$$

$$\text{time reversal} \quad H_a' = -\sigma_2 H_a^* \sigma_2$$

$$SU_L(3) \times SU_R(3) \quad H_a' = H_b V_{ba}^\dagger. \tag{2.5}$$

Here U and S are 2×2 rotation matrices and $V_{ba}^\dagger$ is an $SU(3)$ matrix which gives the standard nonlinear realization of $SU_L(3) \times SU_R(3)$ chiral symmetry. In the two component notation the HHχPT Lagrangian is:

$$\mathcal{L} = \text{Tr}[H_a^\dagger (iD_0)_{ba} H_b] - g\text{Tr}[H_a^\dagger H_b\, \vec{\sigma} \cdot \vec{A}_{ba}] + \frac{\Delta_H}{4}\text{Tr}[H_a^\dagger \sigma^i\, H_a\, \sigma^i]. \tag{2.6}$$

The last term breaks heavy quark spin symmetry and Δ_H is the hyperfine splitting of the heavy mesons. The time component of the covariant chiral derivative is $(D_0)_{ba}$, $\vec{A}_{ba}$ is the spatial part of the axial vector field, and g is the heavy meson axial coupling. Our definitions for the chiral covariant derivative, the axial current, and the Lagrangian for the Goldstone boson fields are the same as Ref. [14].

We are now ready to generalize the Lagrangian to incorporate the doubly heavy baryons and the $U(5)$ quark-diquark symmetry. The field H_a transforms like the tensor product of a heavy quark spinor and a light antiquark spinor. (This is how representations of heavy hadron fields were constructed in Ref. [10].) Writing the field with explicit indices, $(H_a)_{\alpha\beta}$, the index α corresponds to the spinor index of the

heavy quark and the index β is that of the light antiquark spinor. In the theory with quark-diquark symmetry, the heavy quark spinor is replaced with a five-component field, the first two components corresponding to the two heavy quark spin states and the last three components corresponding to the three spin states of the diquark:

$$\mathcal{Q}_\mu = \begin{pmatrix} h_\alpha \\ V_i \end{pmatrix}. \tag{2.7}$$

In terms of $\mathcal{Q}_\mu$ the kinetic terms of the Lagrangian in Eq.(2.1) are

$$\mathcal{L} = \mathcal{Q}_\mu^\dagger i D_0 \mathcal{Q}_\mu. \tag{2.8}$$

The fields in HHχPT with heavy quark-diquark symmetry transform as tensor products of the five component field $\mathcal{Q}_\mu$ and a two-component light antiquark spinor. Thus, the 2×2 matrix field H_a is promoted to a 5×2 matrix field

$$H_{a,\alpha\beta} \rightarrow \mathcal{H}_{a,\mu\beta} = H_{a,\alpha\beta} + T_{a,i\beta}. \tag{2.9}$$

Here the index μ takes on values between 1 and 5, $\alpha, \beta = 1$ or 2, and $i = 3, 4,$ or 5. The doubly heavy baryon fields are contained in $T_{a,i\beta}$. Under the symmetries of the theory $\mathcal{H}_a$ transforms as

$$
\begin{aligned}
\text{rotations} \quad & \mathcal{H}_a' = \mathcal{R}\mathcal{H}_a U^\dagger \\
\text{heavy quark spin} \quad & \mathcal{H}_a' = S\mathcal{H}_a \\
\text{parity} \quad & \mathcal{H}_a' = -\mathcal{H}_a \\
\text{time reversal} \quad & \mathcal{H}_a' = -\Sigma_2 \mathcal{H}_a^* \sigma_2 \\
SU_L(3) \times SU_R(3) \quad & \mathcal{H}_a' = \mathcal{H}_b V_{ba}^\dagger.
\end{aligned}
\tag{2.10}
$$

25

The matrix S is now an element of $U(5)$ and $\mathcal{R}$ is a 5×5 reducible rotation matrix

$$\mathcal{R}_{\mu\nu} = \begin{pmatrix} U_{\alpha\beta} & 0 \\ 0 & R_{ij} \end{pmatrix}, \tag{2.11}$$

where $U_{\alpha\beta}$ is an $SU(2)$ rotation matrix and R_{ij} is an orthogonal 3×3 rotation matrix related to U by $U^\dagger \sigma_i U = R_{ij} \sigma_j$. The 5×5 matrix appearing in the time reversal transformation is

$$(\Sigma_2)_{\mu\nu} = \begin{pmatrix} (\sigma_2)_{\alpha\beta} & 0 \\ 0 & \delta_{ij} \end{pmatrix}. \tag{2.12}$$

Under rotations the field $T_{a,\,i\beta}$ transforms as $T'_{a,\,i\beta} = R_{ij} \, T_{a,\,j\gamma} \, U^\dagger_{\gamma\beta}$. $T_{a,\,i\beta}$ can be further decomposed into its spin-$\frac{3}{2}$ and spin-$\frac{1}{2}$ components,

$$T_{a,\,i\beta} = \sqrt{2} \left(\Xi^*_{a,\,i\beta} + \frac{1}{\sqrt{3}} \Xi_{a,\,\gamma} \, \sigma^i_{\gamma\beta} \right), \tag{2.13}$$

where $\Xi^*_{a,\,i\beta}$ and $\Xi_{a,\,\gamma}$ are the spin-$\frac{3}{2}$ and spin-$\frac{1}{2}$ fields, respectively. The factor of $\sqrt{2}$ is a convention that ensures that the kinetic terms of the doubly heavy baryon fields have the same normalization as the heavy meson fields. The field $\Xi^*_{a,\,i\beta}$ obeys the constraint $\Xi^*_{a,\,i\beta} \, \sigma^i_{\beta\gamma} = 0$.

The $U(5)$ invariant generalizations of the first two terms of Eq. (2.6) are simply obtained by making the replacement $H_a \to \mathcal{H}_a$. To determine the proper generalization of the $U(5)$ breaking term we note that the chromomagnetic couplings in Eq. (2.1) can be written as

$$\frac{g_s}{2m_Q} \mathcal{Q}^\dagger_\mu \vec{\Sigma}_{\mu\nu} \cdot \vec{B}^a \frac{\lambda^a}{2} \mathcal{Q}_\nu, \tag{2.14}$$

where the $\vec{\Sigma}_{\mu\nu}$ are the 5×5 matrices

$$\vec{\Sigma}_{\mu\nu} = \begin{pmatrix} \vec{\sigma}_{\alpha\beta} & 0 \\ 0 & \vec{\mathcal{T}}_{jk} \end{pmatrix}, \tag{2.15}$$

and $(\mathcal{T}^i)_{jk} = -i\epsilon_{ijk}$. It is now obvious that the correct generalization of Eq. (2.6) is

$$\begin{aligned}
\mathcal{L} &= \mathrm{Tr}[\mathcal{H}_a^\dagger (iD_0)_{ba} \mathcal{H}_b] - g\,\mathrm{Tr}[\mathcal{H}_a^\dagger \mathcal{H}_b \, \vec{\sigma} \cdot \vec{A}_{ba}] + \frac{\Delta_H}{4} \mathrm{Tr}[\mathcal{H}_a^\dagger \Sigma^i \mathcal{H}_a \, \sigma^i] \\
&= \mathrm{Tr}[H_a^\dagger (iD_0)_{ba} H_b] - g\,\mathrm{Tr}[H_a^\dagger H_b \, \vec{\sigma} \cdot \vec{A}_{ba}] + \frac{\Delta_H}{4} \mathrm{Tr}[H_a^\dagger \sigma^i H_a \, \sigma^i] \\
&\quad + \mathrm{Tr}[T_a^\dagger (iD_0)_{ba} T_b] - g\,\mathrm{Tr}[T_a^\dagger T_b \, \vec{\sigma} \cdot \vec{A}_{ba}] + \frac{\Delta_H}{4} \mathrm{Tr}[T_a^\dagger \mathcal{T}^i T_a \, \sigma^i]. \tag{2.16}
\end{aligned}$$

The last line of Eq. (3.12) contains the terms relevant for doubly heavy baryons. Heavy quark-diquark symmetry relates the couplings in the doubly heavy baryon sector to the heavy meson sector. The propagator for the spin-$\frac{1}{2}$ doubly heavy baryon is

$$\frac{i\delta_{ab}\,\delta_{\alpha\beta}}{2(k_0 + \Delta_H/2 + i\epsilon)},$$

while the propagator for the spin-$\frac{3}{2}$ doubly heavy baryon is

$$\frac{i\delta_{ab}\,\mathcal{P}_{i\alpha,j\beta}}{2(k_0 - \Delta_H/4 + i\epsilon)} = \frac{i\delta_{ab}\,(\delta_{ij}\delta_{\alpha\beta} - \frac{1}{3}(\sigma^i\sigma^j)_{\alpha\beta})}{2(k_0 - \Delta_H/4 + i\epsilon)}.$$

The projection operator $\mathcal{P}_{i\alpha,j\beta}$ satisfies $\sigma_{\gamma\alpha}^i \mathcal{P}_{i\alpha,j\beta} = \mathcal{P}_{i\alpha,j\beta}\sigma_{\beta\gamma}^j = 0$. Comparison of the poles of the propagators shows that the hyperfine splitting for the doubly heavy baryons is $\frac{3}{4}\Delta_H$, reproducing the heavy quark-diquark symmetry prediction

$$m_{\Xi^*} - m_\Xi = \frac{3}{4}(m_{P^*} - m_P), \tag{2.17}$$

obtained in Refs. [17, 18].

2.3 Electromagnetic Decays

The decay $\Xi^* \to \Xi\gamma$ is related to the decay $P^* \to P\gamma$ by heavy quark-diquark symmetry and therefore is interesting to study in our formalism. For interpreting the SELEX states, it is useful to have estimates of the electromagnetic decay widths. Even with the substantial $O(\Lambda_{QCD}/(m_c v))$ corrections that could be present for doubly charm baryons, such estimates should be helpful for deciding whether an observed Ξ_{cc} is the $J = \frac{3}{2}$ member of the ground state doublet.

The Lagrangian for electromagnetic decays of the heavy mesons in the two-component notation is [49]

$$\mathcal{L} = \frac{e\beta}{2}\mathrm{Tr}[H_a^\dagger H_b \, \vec{\sigma} \cdot \vec{B} \, Q_{ab}] + \frac{e}{2m_Q}Q'\mathrm{Tr}[H_a^\dagger \vec{\sigma} \cdot \vec{B} H_a]\,, \qquad (2.18)$$

where $Q_{ab} = \mathrm{diag}(2/3, -1/3, -1/3)$ is the light quark charge matrix, β is the parameter introduced in Ref. [49], and Q' is the heavy quark charge. For charm, $Q' = 2/3$. The first term is the magnetic moment coupling of the light degrees of freedom and the second term is the magnetic moment coupling of the heavy quark. Both terms are needed to understand the observed electromagnetic branching fractions of the D^{*+} and D^{*0} [49]. The magnetic couplings of the heavy quark and diquark are

$$\begin{aligned}
\mathcal{L}_{em} &= \frac{e}{2m_Q}Q'h^\dagger \, \vec{\sigma} \cdot \vec{B} \, h - \frac{ie}{m_Q}Q' \, \vec{V}^\dagger \cdot \vec{B} \times \vec{V} \\
&= \frac{e}{2m_Q} Q' \, \mathcal{Q}_\mu^\dagger \, \vec{\Sigma}'_{\mu\nu} \cdot \vec{B}\mathcal{Q}_\nu\,,
\end{aligned} \qquad (2.19)$$

where the $\vec{\Sigma}'_{\mu\nu}$ are the 5×5 matrices

$$\vec{\Sigma}'_{\mu\nu} = \begin{pmatrix} \vec{\sigma}_{\alpha\beta} & 0 \\ 0 & -2\vec{T}_{jk} \end{pmatrix}. \tag{2.20}$$

The magnetic coupling of the diquark has the opposite sign as that of the heavy quark because it is composed of two heavy antiquarks. The coefficient of the chromomagnetic coupling of the diquark in Eqs. (2.1,2.14) is a factor of 2 smaller than the coefficient of the electromagnetic coupling of the diquark in Eq. (2.19) due to a color factor. The magnetic couplings in the HHχPT Lagrangian for heavy mesons and doubly heavy baryons are

$$\mathcal{L} = \frac{e\beta}{2}\mathrm{Tr}[\mathcal{H}_a^\dagger \mathcal{H}_b\, \vec{\sigma} \cdot \vec{B}\, Q_{ab}] + \frac{e}{2m_Q}Q'\mathrm{Tr}[\mathcal{H}_a^\dagger\, \vec{\Sigma}' \cdot \vec{B}\, \mathcal{H}_b]\,. \tag{2.21}$$

The part of this Lagrangian involving the doubly heavy baryon fields is

$$\mathcal{L} = \frac{e\beta}{2}\mathrm{Tr}[T_a^\dagger\, T_b\, \vec{\sigma} \cdot \vec{B}\, Q_{ab}] - \frac{e}{m_Q}Q'\mathrm{Tr}[T_a^\dagger\, \vec{\mathcal{T}} \cdot \vec{B}\, T_b]\,. \tag{2.22}$$

This can be used to obtain the following tree level predictions for the electromagnetic decay widths:

$$\begin{aligned}
\Gamma[P_a^* \to P_a\gamma] &= \frac{\alpha}{3}\left(\beta Q_{aa} + \frac{Q'}{m_Q}\right)^2 \frac{m_P}{m_{P^*}}E_\gamma^3 \\
\Gamma[\Xi_a^* \to \Xi_a\gamma] &= \frac{4\alpha}{9}\left(\beta Q_{aa} - \frac{Q'}{m_Q}\right)^2 \frac{m_\Xi}{m_{\Xi^*}}E_\gamma^3\,.
\end{aligned} \tag{2.23}$$

Here E_γ is the photon energy. These results could also be obtained in the quark model, with the parameter $\beta = 1/m_q$, where m_q is the light constituent quark mass. The effective theory allows one to improve upon this approximation by including

29

corrections from loops with light Goldstone bosons, which give $O(\sqrt{m_q})$ corrections to the decay rates [49]. If these loop corrections are evaluated in an approximation where heavy hadron mass differences are neglected, the correction to the above formulae can be incorporated by making the following replacements [49]

$$
\begin{aligned}
\beta Q_{11} &\rightarrow \frac{2}{3}\beta - \frac{g^2 m_K}{4\pi f_K^2} - \frac{g^2 m_\pi}{4\pi f_\pi^2} \\
\beta Q_{22} &\rightarrow -\frac{1}{3}\beta + \frac{g^2 m_\pi}{4\pi f_\pi^2} \\
\beta Q_{33} &\rightarrow -\frac{1}{3}\beta + \frac{g^2 m_K}{4\pi f_K^2} \,.
\end{aligned}
\tag{2.24}
$$

For charm mesons, hyperfine splittings are ≈ 140 MeV and the $SU(3)$ splitting is ≈ 100 MeV, while for bottom mesons the hyperfine splittings are ≈ 45 MeV and $SU(3)$ splitting is ≈ 90 MeV. The approximation of neglecting heavy hadron mass differences and keeping Goldstone boson masses is reasonable for kaon loops but not for loops with pions. However, the largest $O(\sqrt{m_q})$ corrections come from loops with kaons. When data on double heavy baryon electromagnetic decays is available, more accurate calculations along the lines of Ref. [14] should be performed. In this chapter, we will use Eqs. (2.23) and (2.24) to obtain estimates of doubly charm baryon electromagnetic decay widths.

Currently $\Gamma[D^{*+}]$ is measured to be 96 ± 22 keV, while there is only an upper limit for $\Gamma[D^{*0}]$. The branching ratios for the D^{*+} decays are $\mathrm{Br}[D^{*+} \rightarrow D^0 \pi^+] = (67.7 \pm 0.5)\%$, $\mathrm{Br}[D^{*+} \rightarrow D^+ \pi^0] = (30.7 \pm 0.5)\%$ and $\mathrm{Br}[D^{*+} \rightarrow D^+ \gamma] = (1.6 \pm 0.4)\%$. The branching ratios for D^{*0} decays are $\mathrm{Br}[D^{*0} \rightarrow D^0 \pi^0] = (61.9 \pm 2.9)\%$ and $\mathrm{Br}[D^{*0} \rightarrow D^0 \gamma] = (38.1 \pm 2.9)\%$. Isospin symmetry can be used to relate the strong partial

Fit	β^{-1}(MeV)	m_c(MeV)	$\Gamma[\Xi_{cc}^{*++}]$ (keV)	$\Gamma[\Xi_{cc}^{*+}]$ (keV)
QM 1	379	1863	$3.3 \left(\frac{E_\gamma}{80\,\mathrm{MeV}}\right)^3$	$2.6 \left(\frac{E_\gamma}{80\,\mathrm{MeV}}\right)^3$
QM 2	356	1500	$3.4 \left(\frac{E_\gamma}{80\,\mathrm{MeV}}\right)^3$	$3.2 \left(\frac{E_\gamma}{80\,\mathrm{MeV}}\right)^3$
χPT 1	272	1432	$2.3 \left(\frac{E_\gamma}{80\,\mathrm{MeV}}\right)^3$	$3.5 \left(\frac{E_\gamma}{80\,\mathrm{MeV}}\right)^3$
χPT 2	276	1500	$2.3 \left(\frac{E_\gamma}{80\,\mathrm{MeV}}\right)^3$	$3.3 \left(\frac{E_\gamma}{80\,\mathrm{MeV}}\right)^3$

Table 2.1: Predictions for the electromagnetic widths of the Ξ_{cc}^{*+} and Ξ_{cc}^{*++}. The fits are explained in the text.

width of the D^{*0} to the known strong partial width of the D^{*+}. Then the measured branching fractions of the D^{*0} can be used to obtain the partial electromagnetic width of the D^{*0}. We find

$$\Gamma[D^{*0} \to D^0\gamma] = 26.1 \pm 6.0\,\mathrm{keV}$$

$$\Gamma[D^{*+} \to D^+\gamma] = 1.54 \pm 0.35\,\mathrm{keV}\,, \tag{2.25}$$

where the error is dominated by the uncertainty in $\Gamma[D^{*+}]$. $\Gamma[D^{*+} \to D^+\gamma]$ is suppressed because of a partial cancellation between the magnetic moments of the light degrees of freedom and the charm quark. Using the partial widths in Eq. (2.25) and the formulae in Eqs. (2.23) and (2.24), we obtain predictions for doubly charm baryon electromagnetic decays in Table 2.1.

In our calculations of the doubly charm baryon decay widths the factor m_Ξ/m_{Ξ^*} in Eq. (2.23) has been set equal to one. For the expected masses and hyperfine splittings of the doubly charm baryons, this factor changes the predictions for the widths by

less than 3%. The fits are labeled in the left hand column of Table 2.1. In the fits labeled QM we have not included the $O(\sqrt{m_q})$ corrections in Eq. (2.24). Therefore, these predictions for the doubly charm baryon electromagnetic decays are the same as what would be obtained in the quark model. The values of the parameters β and m_c for each fit are shown along with the predictions for the electromagnetic decay widths. In QM 1, we have treated β and m_c as free parameters and fit these to the central values in Eq. (2.25). In QM 2 we have set $m_c = 1500$ MeV and performed a least squared fit to β. In the fits labeled χPT, we have included the leading $O(\sqrt{m_q})$ chiral corrections in Eq. (2.24). We have used $f_\pi = 130$ MeV, $f_K = 159$ MeV, and $g = 0.6$ which is extracted from a tree level fit to the D^{*+} width. In χPT 1, we fixed β and m_c to reproduce the central values in Eq. (2.25). In χPT 2, we set $m_c = 1500$ MeV and performed a least squares fit to β. There are several sources of error in the calculation. We expect 30% theoretical errors due to heavy quark symmetry breaking effects, 30% errors due to higher order $SU(3)$ breaking effects, and 25% uncertainty from the experimentally measured value of $\Gamma[D^{*+}]$ leading to at least 50% error in the predictions in Table 2.1.

Chiral perturbation theory and the nonrelativistic quark model give similar size estimates for the Ξ_{cc}^* electromagnetic decay widths which are expected to be $\sim$2-3 keV if the hyperfine splitting is 80 MeV. The electromagnetic decay should completely dominate any possible weak decay, even if the weak decay rates are an order of magnitude greater than calculated in Refs. [33, 34, 35]. The quark model predicts

32

$\Gamma[\Xi_{cc}^{*++}]$ slightly greater than $\Gamma[\Xi_{cc}^{*+}]$. This is in contrast with the charm meson sector where the magnetic moment of the light degrees of freedom and the magnetic moment of the charm quark add constructively to give a large $\Gamma[D^{*0} \to D^0\gamma]$ and destructively to give a small $\Gamma[D^{*+} \to D^+\gamma]$. In the doubly heavy baryon sector, the relative sign of the magnetic moments is reversed, and both decay rates are approximately the same. In fact from Eq. (2.23), we can see that for $\beta = 4/m_c$ the two rates are exactly equal in the quark model. Fits to the D^* electromagnetic decays yield values of β and m_c that are close to this point in parameter space. Including the $O(\sqrt{m_q})$ corrections from chiral perturbation theory, the most important effect is the kaon loop correction whose contribution to the Ξ_{cc}^{*++} decay has opposite sign as the contribution from β at tree level, therefore suppressing the Ξ_{cc}^{*++} decay relative to Ξ_{cc}^{*+}.

2.4   Mass Corrections

The theory can also be used to compute chiral corrections to doubly heavy baryon masses. The one loop corrections to the hadron masses are

$$
\begin{aligned}
\delta m_{\Xi_a^*} &= \sum_{i,b} \mathcal{C}_{ab}^i \frac{g^2}{16\pi^2 f_i^2} \left(\frac{5}{9} K(m_{\Xi_b^*} - m_{\Xi_a^*}, m_i, \mu) + \frac{4}{9} K(m_{\Xi_b} - m_{\Xi_a^*}, m_i, \mu) \right) \\
\delta m_{\Xi_a} &= \sum_{i,b} \mathcal{C}_{ab}^i \frac{g^2}{16\pi^2 f_i^2} \left(\frac{1}{9} K(m_{\Xi_b} - m_{\Xi_a}, m_i, \mu) + \frac{8}{9} K(m_{\Xi_b^*} - m_{\Xi_a}, m_i, \mu) \right) \\
\delta m_{H_a} &= \sum_{i,b} \mathcal{C}_{ab}^i \frac{g^2}{16\pi^2 f_i^2} K(m_{H_b^*} - m_{H_a}, m_i, \mu) \\
\delta m_{H_a^*} &= \sum_{i,b} \mathcal{C}_{ab}^i \frac{g^2}{16\pi^2 f_i^2} \left(\frac{1}{3} K(m_{H_b} - m_{H_a^*}, m_i, \mu) + \frac{2}{3} K(m_{H_b^*} - m_{H_a^*}, m_i, \mu) \right) \quad (2.26)
\end{aligned}
$$

Here m_i and f_i are the mass and decay constant of the Goldstone boson in the one loop diagram and $\mathcal{C}^i_{ab}$ is a factor which comes from $SU(3)$ Clebsch-Gordan coefficients in the couplings. For loops with charged pions we have $\mathcal{C}^{\pi^\pm}_{12} = \mathcal{C}^{\pi^\pm}_{21} = 1$, for loops with neutral pions $\mathcal{C}^{\pi^0}_{11} = \mathcal{C}^{\pi^0}_{22} = \frac{1}{2}$, for loops with kaons $\mathcal{C}^K_{3i} = \mathcal{C}^K_{i3} = 1$ ($i = 1$ or 2), and for loops with η mesons $C^\eta_{11} = C^\eta_{22} = \frac{1}{6}$ and $C^\eta_{33} = \frac{2}{3}$. The function $K(\delta, m, \mu)$ is related to the finite part of the integral

$$i \int \frac{d^D l}{(2\pi)^D} \frac{\vec{l}^2}{l^2 - m_\pi^2 + i\epsilon} \frac{1}{l_0 - \delta + i\epsilon} = \frac{1}{(4\pi)^2} K(\delta, m, \mu), \qquad (2.27)$$

evaluated using dimensional regularization in the $\overline{MS}$ scheme. We find

$$K(\delta, m, \mu) = (-2\delta^3 + 3m^2\delta) \ln\left(\frac{m^2}{\mu^2}\right) + 2\,\delta(\delta^2 - m^2)F\left(\frac{\delta}{m}\right) + 4\delta^3 - 5\delta m^2, \quad (2.28)$$

where

$$\begin{aligned}
F(x) &= 2\frac{\sqrt{1-x^2}}{x}\left[\frac{\pi}{2} - \mathrm{Tan}^{-1}\left(\frac{x}{\sqrt{1-x^2}}\right)\right] & |x| < 1 \\
&= -2\frac{\sqrt{x^2-1}}{x} \ln\left(x + \sqrt{x^2-1}\right) & |x| > 1,
\end{aligned}$$

and μ is the renormalization scale. The μ dependence in the one loop calculation is cancelled by counterterms that have not been included. Counterterms contributing to the self-energies of heavy mesons can be found in, e.g., Ref. [50]. Again there are many counterterms that contribute to the doubly heavy baryon self-energies, only some of which can be obtained from Ref. [50] by the substitution $H_a \to \mathcal{H}_a$. We focus on the nonanalytic dependence of the self-energies because they provide a rough estimate of the long distance corrections to the leading prediction for hyperfine splittings obtained earlier and because the nonanalytic dependence on the light quark

34

mass could be useful for chiral extrapolations in unquenched lattice QCD calculations of doubly heavy baryon masses.

We are interested in how the one loop corrections affect the leading order prediction for the hyperfine splittings. Unfortunately, it is impossible to give a reliable estimate without knowing the numerical value of the counterterms required to cancel the μ dependence in the nonanalytic contribution. Furthermore, to compute the contribution from kaon loops, one must know the masses of doubly charm strange baryons which have not been observed. We will assume that the ground state doubly charm strange baryons are 100 MeV higher in mass than their nonstrange counterparts, similar to the D meson system. This is consistent with theoretical estimate of the $SU(3)$ breaking in Refs. [36, 43, 44, 45, 47, 48]. We work in the isospin limit and use $g = 0.6$, $\Delta_H = 140$ MeV, $m_\pi = 137$ MeV, $m_K = 496$ MeV, $m_\eta = 548$ MeV and the experimental values of the pseudoscalar meson decay constants: $f_\pi = 130$ MeV, $f_K = 159$ MeV, and $f_\eta = 156$ MeV. The nonanalytic part of the one loop correction to the nonstrange doubly charm baryon hyperfine splitting is

$$\delta m_{\Xi_{cc}^*} - \delta m_{\Xi_{cc}} = \begin{cases} -7.0\,\text{MeV} & \mu = 500\,\text{MeV} \\ 8.1\,\text{MeV} & \mu = 1000\,\text{MeV} \\ 16.9\,\text{MeV} & \mu = 1500\,\text{MeV} \end{cases} , \qquad (2.29)$$

where we have shown our results for three values of μ. For these choices of μ the nonanalytic part of the chiral correction varies between -7 MeV and +17 MeV. The nonanalytic part of the chiral correction to the doubly charm baryon hyperfine splitting is quite sensitive to the choice of μ, and lies within 15% of the tree level prediction.

35

We also calculate the correction to the hyperfine splitting relationship of Eq. (2.17) and find for the masses in the nonstrange sector

$$\delta m_{\Xi_{cc}^*} - \delta m_{\Xi_{cc}} - \frac{3}{4}(\delta m_{D^*} - \delta m_D) = \begin{cases} 3.9\,\text{MeV} & \mu = 500\,\text{MeV} \\ 5.3\,\text{MeV} & \mu = 1000\,\text{MeV} \\ 6.1\,\text{MeV} & \mu = 1500\,\text{MeV} \end{cases} \quad (2.30)$$

The nonanalytic correction to the symmetry prediction is small (< 10 MeV) and relatively insensitive to the choice of μ. Chiral perturbation theory predicts the nonanalytic dependence of the doubly heavy baryon masses on the light quark masses, and generalized to include the effects of quenching as well as other lattice artifacts, formulae such as those in Eq. (2.26) should be useful for chiral extrapolations of doubly heavy baryon masses and hyperfine splittings in lattice simulations.

2.5 Excited States

In this section, we discuss excited doubly heavy baryons. There are two types of excitations in the doubly heavy baryon system: excitations of the light degrees of freedom and excitations of the diquark. Excitations of the first type are related to analogous excitations in the heavy meson sector by heavy quark-diquark symmetry. The lowest lying excited charm mesons are in a doublet of $J^P = 0^+$ and 1^+ mesons with masses approximately 425 MeV above the ground state in the nonstrange sector [51, 52, 53] and 350 MeV above the ground state in the strange sector [54, 55]. In the nonstrange sector these states decay via S-wave pion emission and have widths

in the range 250-350 MeV, while in the strange sector the strong decay is via π^0 emission which violates isospin, and therefore the states are very narrow with widths expected to be of order 10 keV [50]. These states have light degrees of freedom with angular momentum and parity $j^p = \frac{1}{2}^+$. The doubly charm baryons related to the even-parity excited charm mesons by quark-diquark symmetry are a doublet with $J^P = \frac{1}{2}^+$ and $J^P = \frac{3}{2}^+$. The excited charm mesons and doubly charm baryons can be incorporated into HHχPT with a 5×2 matrix field $\mathcal{S}_{\mu\beta}$ which is like the field $\mathcal{H}_{\mu\beta}$ except $\mathcal{S}_{\mu\beta}$ has opposite parity. The excitation energies and strong decay widths of these excited doubly charm baryons should be similar to their counterparts in the charm meson sector. Since the excited $\Xi_{cc}^{++}(3780)$ state observed by SELEX is only 320 MeV above the $\Xi_{cc}^{++}(3460)$, the lowest mass Ξ_{cc}^{++} candidate, and its width is considerably less than 300 MeV, it does not seem likely that this excited doubly charm baryon is related to the excited charm mesons by heavy quark-diquark symmetry.

This is not unexpected as the lowest lying excited doubly charm baryons are not excitations of the light degrees of freedom but rather states in which the diquark is excited. The lowest mass excited diquark is a P-wave excitation. Because of Fermi statistics the diquark is a heavy quark spin singlet. The diquark's orbital angular momentum couples with the angular momentum of the light degrees of freedom to form baryons with $J^P = \frac{1}{2}^+$ and $J^P = \frac{3}{2}^+$, which we will refer to as $\Xi_{cc}^{\mathcal{P}}$ and $\Xi_{cc}^{\mathcal{P}*}$, respectively. The next lowest lying states are doubly heavy baryons with a radially excited diquark, which form a heavy quark doublet with $J^P = \frac{1}{2}^-$ and $J^P = \frac{3}{2}^-$

baryons, which we will refer to as Ξ'_{cc} and Ξ'^{*}_{cc}, respectively. If the heavy antiquarks are sufficiently heavy that the force between them is approximately Coulombic, they interact via a potential which is $1/2$ as strong as the potential between the quark and antiquark in a quarkonium bound state. Therefore we expect the excitation energies of the charm diquarks to be significantly smaller than the analogous excitation energies in charmonium. Quark model calculations of excited doubly charm baryons predict that the $\Xi^{\mathcal{P}}_{cc}$ and $\Xi^{\mathcal{P}*}_{cc}$ states are about 225 MeV above the Ξ_{cc} and Ξ^{*}_{cc}, respectively, and that that the heavy quark doublet containing Ξ'_{cc} and Ξ'^{*}_{cc} is about 300 MeV above the ground state doublet [32, 56, 47, 57, 58]. These excitation energies are about $1/2$ the corresponding excitation energies in the charmonium system: $m_{h_c} - m_{J/\psi} = 430$ MeV and $m_{\psi'} - m_{J/\psi} = 590$ MeV. The charm diquark excitation energies are less than the expected excitation energy of the light degrees of freedom and therefore the lowest lying excited doubly charm baryons have excited diquarks. Excitation energies of a diquark made from two bottom quarks are similar to the excitation energies of a diquark made from charm, so the same conclusion holds for doubly bottom baryons.

Note that the excitation energies of the light degrees of freedom, which should scale as $\sim \Lambda_{QCD}$, are as much as 2 times larger than the excitations of the diquark, which should scale as $\sim m_Q v^2$. Since the difference is only a factor of 2, either power counting $m_Q v > \Lambda_{QCD} \sim m_Q v^2$ or $m_Q v \sim \Lambda_{QCD} > m_Q v^2$ seems plausible for excited doubly heavy baryons. Our calculations assume the first power counting,

but if the second power counting is more appropriate a formalism similar to strongly coupled pNRQCD needs to be developed instead [59]. It should be kept in mind that since excited diquarks will be less pointlike than the ground states, corrections to heavy quark-diquark symmetry could be larger for excited doubly heavy baryons. Our predictions for strong decays listed below could be used to test the validity of the assumption $m_Q v > \Lambda_{QCD} \sim m_Q v^2$ for excited doubly heavy baryons.

The doubly heavy baryons with P-wave excited diquarks decay to the ground state via S-wave pion emission. These decays violate heavy quark spin symmetry because the total spin of the diquark is changed in the transition. The Lagrangian for the excited $\Xi^{\mathcal{P}}$ and $\Xi^{\mathcal{P}*}$ states, including kinetic terms, residual mass terms and terms which mediate the S-wave decays, is

$$
\begin{aligned}
\mathcal{L} \;=\;& 2\,(\Xi_a^{\mathcal{P}})^\dagger \, (i\,(D_0)_{ba} - \delta_{\mathcal{P}}\,\delta_{ab})\,\Xi_b^{\mathcal{P}} + 2\,(\Xi_a^{\mathcal{P}*})^\dagger \, (i\,(D_0)_{ba} - \delta_{\mathcal{P}*}\,\delta_{ab})\,\Xi_b^{\mathcal{P}*} \\
&+ 2\,\lambda_{1/2}\,\left(\Xi_a^\dagger\,\Xi_b^{\mathcal{P}}\,A_{ba}^0 + h.c.\right) + 2\,\lambda_{3/2}\,\left(\Xi_a^{*\dagger}\,\Xi_b^{\mathcal{P}*}\,A_{ba}^0 + h.c.\right) .
\end{aligned}
\tag{2.31}
$$

The strong decay widths of the P-wave excited nonstrange doubly charm baryons are

$$
\begin{aligned}
\Gamma[\Xi_{cc}^{\mathcal{P}*} \to \Xi_{cc}^*\,\pi] \;&=\; \frac{\lambda_{3/2}^2}{2\pi f^2}\left(\frac{1}{2}E_{\pi^0}^2 p_{\pi^0} + E_{\pi^+}^2 p_{\pi^+}\right)\frac{m_{\Xi^*}}{m_{\Xi^{\mathcal{P}*}}} = \lambda_{3/2}^2\,111\,\mathrm{MeV} \\
\Gamma[\Xi_{cc}^{\mathcal{P}} \to \Xi_{cc}\,\pi] \;&=\; \frac{\lambda_{1/2}^2}{2\pi f^2}\left(\frac{1}{2}E_{\pi^0}^2 p_{\pi^0} + E_{\pi^+}^2 p_{\pi^+}\right)\frac{m_{\Xi}}{m_{\Xi^{\mathcal{P}}}} = \lambda_{1/2}^2\,111\,\mathrm{MeV} .
\end{aligned}
\tag{2.32}
$$

To obtain numerical estimates, we have assumed the masses $m_{\Xi_{cc}} = 3440$ MeV, $m_{\Xi_{cc}^*} = 3520$ MeV, $m_{\Xi_{cc}^{\mathcal{P}}} = 3665$ MeV and $m_{\Xi_{cc}^{\mathcal{P}*}} = 3745$ MeV, corresponding to a diquark excitation energy of 225 MeV. We sum over both charged and neutral pion decay modes. The coupling constants $\lambda_{1/2}$ and $\lambda_{3/2}$ are $O(\Lambda_{\mathrm{QCD}}/m_Q)$ so we should

expect this suppression makes $\lambda_{1/2}$ and $\lambda_{3/2} < 1$. Therefore these states could be quite narrow despite decaying via S-wave pion emission. The small widths are due to the small excitation energy which leaves little phase space for the decay. If the excitation energy is increased to 280 MeV, the widths are twice as large. Like the isospin violating decays of the D_s^* [60] and the even-parity excited D_s mesons [61, 50], the excited doubly heavy strange baryons below the kaon threshold decay through a virtual η which mixes into a π^0. Denoting the ground state doubly charm strange baryons as $\Omega_{cc}^{(*)}$ and the P-wave excited doubly charm strange baryons as $\Omega_{cc}^{\mathcal{P}(*)}$ we obtain the following formulae for the isospin violating strong decay widths

$$
\begin{aligned}
\Gamma[\Omega_{cc}^{\mathcal{P}*} \to \Omega_{cc}^* \, \pi^0] &= \frac{\lambda_{3/2}^2}{2\pi f^2} \frac{2}{3} \theta^2 \, E_{\pi^0}^2 p_{\pi^0} \\
\Gamma[\Omega_{cc}^{\mathcal{P}} \to \Omega_{cc} \, \pi^0] &= \frac{\lambda_{1/2}^2}{2\pi f^2} \frac{2}{3} \theta^2 \, E_{\pi^0}^2 p_{\pi^0} \, .
\end{aligned}
\tag{2.33}
$$

Here $\theta = 0.01$ is the $\pi^0 - \eta$ mixing angle. We expect these widths to be in the range 1-5 keV, but without knowing the masses of the $\Omega_{cc}^{(*)}$ and $\Omega_{cc}^{\mathcal{P}(*)}$ states or the couplings $\lambda_{1/2}$ and $\lambda_{3/2}$ we cannot make more precise predictions.

The $J^P = \frac{3}{2}^-$ and $J^P = \frac{1}{2}^-$ doubly heavy baryons with radially excited diquarks are members of a heavy quark doublet we will denote T_a' whose definition in terms of component fields is identical to Eq. (3.11). The Lagrangian describing this field, including terms which mediate its decay to the ground state, is

$$
\begin{aligned}
\mathcal{L} &= \text{Tr}[T_a'^\dagger((iD_0)_{ab} - \delta_{T'} \, \delta_{ab})T_b'] - g \, \text{Tr}[T_a'^\dagger \, T_b' \, \vec{\sigma} \cdot \vec{A}_{ba}] + \frac{\Delta_H}{4} \text{Tr}[T_a'^\dagger \, \mathcal{T}^i \, T_b' \, \sigma^i] \\
&\quad - \tilde{g} \left(\text{Tr}[T_a^\dagger \, T_b' \, \vec{\sigma} \cdot \vec{A}_{ba}] + \text{h.c.} \right) .
\end{aligned}
\tag{2.34}
$$

In the limit of infinite heavy quark mass, the light degrees of freedom in the radially excited doubly heavy baryons are in the same configuration as the ground state. Therefore, they are also related to the heavy meson ground state doublet by heavy quark-diquark symmetry. The axial coupling and hyperfine splitting of T'_a are the same as T_a, as long as the spatial extent of the excited diquark, which is of order $1/(m_Q v)$, is much smaller than $1/\Lambda_{\rm QCD}$. This is valid in the heavy quark limit, but could receive significant corrections in the charm sector. The last term in Eq. (2.34) mediates P-wave decays from the excited $J^P = \frac{3}{2}^-$ and $J^P = \frac{1}{2}^-$ doubly heavy baryons to the ground state. The partial decay widths are

$$\Gamma[\Xi'^*_a \to \Xi^*_b \pi] = \mathcal{C}_{ab} \frac{5}{9} \frac{\tilde{g}^2}{2\pi f^2} \frac{m_{\Xi^*}}{m_{\Xi'^*}} |p_\pi|^3 \qquad \Gamma[\Xi'^*_a \to \Xi_b \pi] = \mathcal{C}_{ab} \frac{4}{9} \frac{\tilde{g}^2}{2\pi f^2} \frac{m_{\Xi}}{m_{\Xi'^*}} |p_\pi|^3$$

$$\Gamma[\Xi'_a \to \Xi^*_b \pi] = \mathcal{C}_{ab} \frac{8}{9} \frac{\tilde{g}^2}{2\pi f^2} \frac{m_{\Xi^*}}{m_{\Xi'}} |p_\pi|^3 \qquad \Gamma[\Xi'_a \to \Xi_b \pi] = \mathcal{C}_{ab} \frac{1}{9} \frac{\tilde{g}^2}{2\pi f^2} \frac{m_{\Xi}}{m_{\Xi'}} |p_\pi|^3 \quad (2.35)$$

Here $\mathcal{C}_{ab}$ is an $SU(3)$ factor which is $1/2$ for decays involving π^0 and one for decays involving charged pions. The radially excited doubly heavy strange baryons should also be below the threshold for decays into kaons, and therefore should be quite narrow. The formulae in Eq. (2.35) can be used to obtain these decay widths as well. The isospin violating strong partial decay widths are obtained by using Eq. (2.35) with $C_{33} = \frac{2}{3}$ then multiplying by θ^2. The expected widths of these states are of order 10 keV, but more precise estimates cannot be made until the masses of the states and the coupling $\tilde{g}$ are known. For the nonstrange doubly heavy baryons, in the limit of infinite heavy quark mass, we obtain

$$\Gamma[\Xi'] = \Gamma[\Xi'^*] = \frac{3\tilde{g}^2}{4\pi f^2} p_\pi^3 = 55 \,\text{MeV} \left(\frac{\tilde{g}}{0.5}\right)^2 \left(\frac{p_\pi}{250 \,\text{MeV}}\right)^3 \qquad (2.36)$$

for the total widths, and for the branching fractions we find

$$\frac{\text{Br}[\Xi'^* \to \Xi^* \pi]}{\text{Br}[\Xi'^* \to \Xi \pi]} = \frac{5}{4} \qquad \frac{\text{Br}[\Xi' \to \Xi^* \pi]}{\text{Br}[\Xi' \to \Xi \pi]} = 8 \,. \tag{2.37}$$

These relations receive large corrections due to phase space effects. Once the hyperfine splittings are taken into account the factors of p_π^3 will differ greatly for the four decays. To get a feeling for these effects in the doubly charm sector we choose $m_{\Xi_{cc}} = 3440\,\text{MeV}$, $m_{\Xi_{cc}^*} = 3520\,\text{MeV}$, $m_{\Xi_{cc}'} = 3740\,\text{MeV}$, and $m_{\Xi_{cc}^{*\prime}} = 3820\,\text{MeV}$, which corresponds to a diquark excitation energy of 300 MeV and hyperfine splittings of 80 MeV. We then find

$$\Gamma[\Xi_{cc}'] = \tilde{g}^2\,336\,\text{MeV} \qquad\qquad \Gamma[\Xi_{cc}^{*\prime}] = \tilde{g}^2\,78\,\text{MeV}$$

$$\frac{\Gamma[\Xi_{cc}'^* \to \Xi_{cc}^* \pi]}{\Gamma[\Xi_{cc}'^* \to \Xi_{cc} \pi]} = 0.56 \qquad\qquad \frac{\Gamma[\Xi_{cc}' \to \Xi_{cc}^* \pi]}{\Gamma[\Xi_{cc}' \to \Xi_{cc} \pi]} = 2.3 \,. \tag{2.38}$$

Note that the Ξ_{cc}' unlike the $\Xi_{cc}'^*$ strongly prefers to decay to Ξ_{cc}^* relative to Ξ_{cc} despite the phase space suppression. This may be useful for distinguishing $\Xi_{cc}'^*$ and Ξ_{cc}' experimentally.

The SELEX $\Xi_{cc}^{++}(3780)$ is broad relative to the other SELEX doubly charm candidates. Since it is 260 MeV heavier than the $\Xi_{cc}^+(3520)$, it is a natural candidate for one of the low lying excited doubly charm baryons. Unfortunately, no measurement of the width exists and the pattern of decays is also hard to understand, since Ref. [24] states that 50% of the decays to $\Lambda_c^+ K^- \pi^+ \pi^+$ are through $\Xi_{cc}^+(3520)\,\pi^+$ while the other 50% are weak decays. More information on the quantum numbers of the

$\Xi_{cc}^{++}(3780)$ and the $\Xi_{cc}^{+}(3520)$ are needed before we can determine which of the excited doubly charm baryons should be identified with the $\Xi_{cc}^{++}(3780)$.

2.6 Summary

In this chapter we have developed a generalization of HHχPT which incorporates heavy quark-diquark symmetry and includes the leading symmetry breaking corrections from the chromomagnetic couplings of the heavy quark and diquark. We also included electromagnetic interactions in the Lagrangian, and obtained an estimate of the width of the $J = \frac{3}{2}$ member of the ground state doubly charm baryon doublet. The width of this state is completely dominated by electromagnetic decays. Our theory was used to calculate chiral corrections to doubly heavy baryon masses. The nonanalytic correction to the leading heavy quark-diquark symmetry prediction for the hyperfine splittings is small. Computations of chiral corrections to doubly heavy baryon masses which include effects of quenching and other lattice artifacts will be useful for chiral extrapolations in future lattice QCD calculations of doubly heavy baryon masses.

We showed how to include the lowest lying doubly charm baryons which are expected to be excitations of the doubly charm diquark rather than the light degrees of freedom. Strong decay widths of low lying excited states were calculated and the states are expected to be rather narrow because of limited phase space available for the decays. Of particular interest is the doubly charm strange sector where we expect

three pairs of excited baryons whose strong decay must violate isospin conservation because they are below the kaon decay threshold. These states will have narrow widths of 10 keV or less. Experimental efforts to observe the narrow doubly charm strange baryons would be of great interest.

Chapter 3

Doubly Heavy Baryon Zero-Recoil Semileptonic Decay with Heavy Quark-Diquark Symmetry

3.1 Introduction

Heavy quark-diquark symmetry relates heavy mesons to doubly heavy antibaryons. The heavy quark-diquark symmetry prediction for the doubly charm hyperfine splitting [17, 18, 29, 32] is within $25\% \sim 30\%$ of the quenched lattice QCD calculation. More observables are needed to see if heavy quark-diquark symmetry can be applied to charm and bottom. In the previous chapter, we derived an effective Lagrangian for doubly heavy baryons incorporating heavy quark-diquark symmetry and used this theory to study low energy strong and electromagnetic interactions of doubly heavy baryons. In this chapter, we will apply this theory to calculate leading chiral corrections to heavy quark-diquark symmetry predictions for zero-recoil doubly heavy baryon semileptonic decay form factors.

Lattice gauge theory is a useful tool for addressing the nonperturbative dynamics of quarks and gluons. Lattice calculation of decay matrix elements of heavy mesons and doubly heavy baryons can help determine the reliability of heavy quark-diquark symmetry for charm and bottom hadrons. HPQCD and MILC collaborations are

planning to calculate semileptonic decay form factors of heavy mesons in the near future. In lattice QCD, simulations are performed with unphysical sea quark masses which need to be extrapolated to the physical values. Chiral Lagrangians which include quenching and partially quenching effects are useful for the chiral extrapolations of lattice data. In this chapter, we will extend the chiral Lagrangian with heavy quark-diquark symmetry to include effects of quenching and partial quenching, and use it to derive formulae for the chiral extrapolation of zero-recoil semileptonic decay of double heavy baryons in lattice QCD simulations.

The rest of this chapter is organized as follows. In Sec. 3.2, we use NRQCD to derive couplings of heavy diquarks to weak currents that are consistent with heavy quark-diquark symmetry. In Sec. 3.3, we construct the chiral Lagrangian for doubly heavy baryons coupled to weak currents and calculate the doubly heavy baryon zero-recoil semileptonic decay matrix elements. We calculate the chiral corrections to doubly heavy baryon zero-recoil semileptonic decay using χPT. In the heavy quark-diquark symmetry limit the corrections vanish. In Sec. 3.4, we extend the chiral Lagrangian with heavy quark-diquark symmetry to the partially quenched theory and derive formulae for chiral extrapolation of doubly heavy baryon zero-recoil semileptonic decay form factors in lattice QCD simulations. We compare chiral corrections to the zero-recoil doubly heavy baryon semileptonic decay form factor in PQχPT with the corresponding corrections in χPT. In Sec. 3.5, a brief summary is given. Some useful formulae are collected in Appendix A.

3.2 Couplings of Heavy Diquark to Weak Currents from vNRQCD

NRQCD is the nonrelativistic effective theory that describes the dynamics of nonrelativistic heavy quarks. In NRQCD there are four important energy scales: the heavy quark mass, m_Q, the typical momentum of the heavy quarks within the bound state, $m_Q v$, the typical kinetic energy of the heavy quarks, $m_Q v^2$ and Λ_{QCD}. The total momentum of the heavy quark field is taken to be the sum of the label momentum $\mathbf{p}$ and the residual momentum $\mathbf{k}$: $\mathbf{p}_{total} = \mathbf{p}(\sim m_Q v) + \mathbf{k}(\sim m_Q v^2)$. vNRQCD [16] is an effective theory for NRQCD which has a consistent v expansion. The leading order vNRQCD Lagrangian to $O(v^5)$ for the $\bar{Q}\bar{Q}$ sector for $\bar{b}, \bar{c}$ antiquarks is

$$
\begin{aligned}
\mathcal{L} = {} & -\frac{1}{4} F^{\mu\nu} F_{\mu\nu} + \sum_{f=b,c} \sum_{\mathbf{p}} \chi_{\mathbf{p}}^{f\dagger} \left(iD_0 - \frac{(\mathbf{p} - i\mathbf{D})^2}{2m_{Q_f}} + \frac{g_s}{2m_{Q_f}} \boldsymbol{\sigma} \cdot \mathbf{B} \right) \chi_{\mathbf{p}}^{f} \qquad (3.1) \\
& - \frac{1}{2} \sum_{f=b,c} \sum_{\mathbf{p},\mathbf{q}} \frac{g_s^2}{(\mathbf{p} - \mathbf{q})^2} \chi_{\mathbf{q}}^{f\dagger} \bar{T}^A \chi_{\mathbf{p}}^{f} \chi_{-\mathbf{q}}^{f\dagger} \bar{T}^A \chi_{-\mathbf{p}}^{f} - \sum_{\mathbf{p},\mathbf{q}} \frac{g_s^2}{(\mathbf{p} - \mathbf{q})^2} \chi_{\mathbf{q}}^{b\dagger} \bar{T}^A \chi_{\mathbf{p}}^{b} \chi_{-\mathbf{q}}^{c\dagger} \bar{T}^A \chi_{-\mathbf{p}}^{c} + \cdots,
\end{aligned}
$$

where the ellipsis represents high order terms. $\chi_{\mathbf{p}}^{f}$ is a nonrelativistic antiquark field with flavor f which annihilates an antiquark. $\bar{T}^A$ is $SU(3)$ color generators for $\bar{3}$ representation, $\mathbf{B}$ is chromomagnetic field, and D_0 and $\mathbf{D}$ are the time and spatial components of the gauge covariant derivative. The kinetic energy, D_0, and momentum, $\mathbf{p}$, of the heavy quarks are $O(m_Q v^2)$ and $O(m_Q v)$, respectively. In order to derive an effective Lagrangian for diquarks we follow the methods of Ref. [18]. We

use the spin and color Fierz identities

$$\delta_{\alpha\delta}\delta_{\beta\gamma} = -\frac{1}{2}(\sigma^i \epsilon)_{\alpha\beta}(\epsilon\sigma^i)_{\gamma\delta} + \frac{1}{2}\epsilon_{\alpha\beta}\epsilon^T_{\gamma\delta}, \tag{3.2}$$

$$\bar{T}^A_{il}\bar{T}^A_{jk} = \frac{2}{3}\sum_m \frac{1}{2}\epsilon_{mij}\epsilon_{mkl} + \frac{1}{3}\sum_{(mn)} d^{(mn)}_{ij} d^{(mn)}_{kl}, \tag{3.3}$$

to project the potential onto the **3** and $\bar{\mathbf{6}}$ channels and to decompose the antiquark

bilinears such as $\chi^f_{\mathbf{p}}\chi^f_{-\mathbf{p}}$ into operators with spin 0 and spin 1. In Eq.(3.3) The Greek

letters denote spin indices, the σ^i denote the Pauli matrices and $\epsilon = i\sigma^2$. In Eq.(3.3),

the Roman letters denote the color indices and the matrices $d^{(mn)}_{ij}$ are symmetric

matrices in color space defined by

$$d^{(mn)}_{ij} = \begin{cases} (\delta^m_i \delta^n_j + \delta^n_i \delta^m_j)/\sqrt{2} & m \neq n \\ \\ \delta^m_i \delta^n_j & m = n \end{cases} . \tag{3.4}$$

For bb and cc, the diquark state must be in either$(\mathbf{3})_C(\mathbf{3})_S$ or $(\bar{\mathbf{6}})_C(\mathbf{1})_S$ by the Pauli

principle. However, there is no restriction on the color and spin for mixed flavor.

After a Fourier transform to obtain position space potentials, the Lagrangian can be

rewritten as

$$
\begin{aligned}
\mathcal{L} =\ & -\frac{1}{4}F^{\mu\nu}F_{\mu\nu} + \sum_{f=b,c}\sum_{\mathbf{p}} \chi^{f\dagger}_{\mathbf{p}}\left(iD_0 - \frac{(\mathbf{p}-i\mathbf{D})^2}{2m_{Q_f}} + \frac{g_s}{2m_{Q_f}}\boldsymbol{\sigma}\cdot\mathbf{B}\right)\chi^f_{\mathbf{p}} \\
& -\frac{1}{2}\sum_{f=b,c}\int d^3\mathbf{r}V^{(3)}(r)\left(\sum_{\mathbf{q}} e^{-i\mathbf{q}\cdot\mathbf{r}}\frac{\epsilon_{mij}}{2}(\chi^{f\dagger}_{\mathbf{q}})_i\boldsymbol{\sigma}\epsilon(\chi^{f\dagger}_{-\mathbf{q}})_j\right)\cdot\left(\sum_{\mathbf{p}} e^{i\mathbf{p}\cdot\mathbf{r}}\frac{\epsilon_{mkl}}{2}(\chi^f_{-\mathbf{p}})_k\epsilon\boldsymbol{\sigma}(\chi^f_{\mathbf{p}})_l\right) \\
& -\int d^3\mathbf{r}V^{(3)}(r)\left(\sum_{\mathbf{q}} e^{-i\mathbf{q}\cdot\mathbf{r}}\frac{\epsilon_{mij}}{2}(\chi^{b\dagger}_{\mathbf{q}})_i\boldsymbol{\sigma}\epsilon(\chi^{c\dagger}_{-\mathbf{q}})_j\right)\cdot\left(\sum_{\mathbf{p}} e^{i\mathbf{p}\cdot\mathbf{r}}\frac{\epsilon_{mkl}}{2}(\chi^c_{-\mathbf{p}})_k\epsilon\boldsymbol{\sigma}(\chi^b_{\mathbf{p}})_l\right) \\
& -\int d^3\mathbf{r}V^{(3)}(r)\left(-\sum_{\mathbf{q}} e^{-i\mathbf{q}\cdot\mathbf{r}}\frac{\epsilon_{mij}}{2}(\chi^{b\dagger}_{\mathbf{q}})_i\epsilon(\chi^{c\dagger}_{-\mathbf{q}})_j\right)\left(\sum_{\mathbf{p}} e^{i\mathbf{p}\cdot\mathbf{r}}\frac{\epsilon_{mkl}}{2}(\chi^c_{-\mathbf{p}})_k\epsilon^T(\chi^b_{\mathbf{p}})_l\right) \\
& + \cdots,
\end{aligned} \tag{3.5}
$$

where the ellipsis reflexes to terms in which the diquark is in the $\bar{6}$ of color, $V^{(3)}(r) = -\frac{2}{3}\frac{\alpha_s}{r}$ and $V^{(\bar{6})}(r) = \frac{1}{3}\frac{\alpha_s}{r}$. The first line includes the gauge boson fields, the kinetic terms for the antiquarks and the leading spin symmetry breaking interactions which generate hyperfine splittings. The next three lines are the quartic terms with diquark fields. In order to get the interaction for doubly heavy baryon semileptonic decay, we need the Lagrangian for diquarks of different flavor. The diquark fields for $\bar{c}\bar{c}$ and $\bar{b}\bar{b}$ can be introduced using the Hubbard-Strantonovich transformation as in Ref. [18]. We add to the Lagrangian:

$$
\begin{aligned}
\Delta\mathcal{L} = {} & \frac{1}{2}\sum_{f=b,c}\int d^3\mathbf{r}\, V^{(3)}(r)\left(\mathbf{T}_{\mathbf{r}}^{m\dagger} - \sum_{\mathbf{q}}e^{-i\mathbf{q}\cdot\mathbf{r}}\frac{\epsilon_{mij}}{2}(\chi_{\mathbf{q}}^{f\dagger})_i\boldsymbol{\sigma}\epsilon(\chi_{-\mathbf{q}}^{f\dagger})_j\right) \\
& \cdot\left(\mathbf{T}_{\mathbf{r}}^{m} - \sum_{\mathbf{p}}e^{i\mathbf{p}\cdot\mathbf{r}}\frac{\epsilon_{mkl}}{2}(\chi_{-\mathbf{p}}^{f})_k\epsilon\boldsymbol{\sigma}(\chi_{\mathbf{p}}^{f})_l\right) \\
& + \int d^3\mathbf{r}\, V^{(3)}(r)\left(\tilde{\mathbf{T}}_{\mathbf{r}}^{m\dagger} - \sum_{\mathbf{q}}e^{-i\mathbf{q}\cdot\mathbf{r}}\frac{\epsilon_{mij}}{2}(\chi_{\mathbf{q}}^{b\dagger})_i\boldsymbol{\sigma}\epsilon(\chi_{-\mathbf{q}}^{c\dagger})_j\right) \\
& \cdot\left(\tilde{\mathbf{T}}_{\mathbf{r}}^{m} - \sum_{\mathbf{p}}e^{i\mathbf{p}\cdot\mathbf{r}}\frac{\epsilon_{mkl}}{2}(\chi_{-\mathbf{p}}^{c})_k\epsilon\boldsymbol{\sigma}(\chi_{\mathbf{p}}^{b})_l\right) \\
& + \int d^3\mathbf{r}\, V^{(3)}(r)\left(T_{\mathbf{r}}^{\prime m\dagger} + \sum_{\mathbf{q}}e^{-i\mathbf{q}\cdot\mathbf{r}}\frac{\epsilon_{mij}}{2}(\chi_{\mathbf{q}}^{b\dagger})_i\epsilon(\chi_{-\mathbf{q}}^{c\dagger})_j\right) \\
& \times\left(T_{\mathbf{r}}^{\prime m} - \sum_{\mathbf{p}}e^{i\mathbf{p}\cdot\mathbf{r}}\frac{\epsilon_{mkl}}{2}(\chi_{-\mathbf{p}}^{c})_k\epsilon^T(\chi_{\mathbf{p}}^{b})_l\right),
\end{aligned}
\tag{3.6}
$$

where $m = 1, 2, 3$ is the color index. The $\mathbf{T}^m = \sum_{\mathbf{p}}e^{i\mathbf{p}\cdot\mathbf{r}}\frac{\epsilon_{mkl}}{2}(\chi_{-\mathbf{p}}^{f})_k\epsilon\boldsymbol{\sigma}(\chi_{\mathbf{p}}^{f})_l$ is the spin-1 $\bar{f}\bar{f}$ field, $\tilde{\mathbf{T}}^m = \sum_{\mathbf{p}}e^{i\mathbf{p}\cdot\mathbf{r}}\frac{\epsilon_{mkl}}{2}(\chi_{-\mathbf{p}}^{c})_k\epsilon\boldsymbol{\sigma}(\chi_{\mathbf{p}}^{b})_l$ is the spin-1 $\bar{b}\bar{c}$ field, and the $T^{\prime m} = \sum_{\mathbf{p}}e^{i\mathbf{p}\cdot\mathbf{r}}\frac{\epsilon_{mkl}}{2}(\chi_{-\mathbf{p}}^{c})_k\epsilon^T(\chi_{\mathbf{p}}^{b})_l$ is the spin-0 $\bar{b}\bar{c}$ field. The quartic terms of antiquark fields
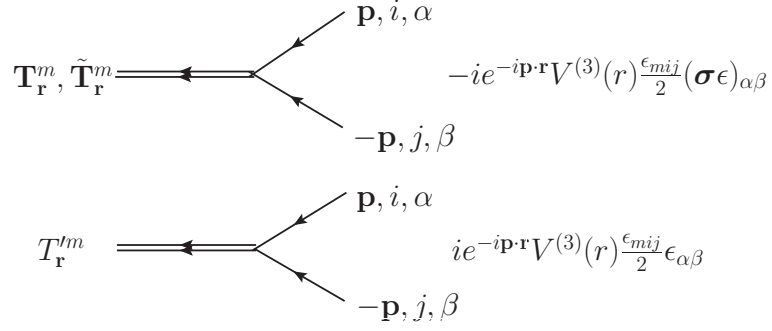
$\mathbf{T}_\mathbf{r}^m, \tilde{\mathbf{T}}_\mathbf{r}^m$ ⎯⎯⎯⟨ $\mathbf{p}, i, \alpha$; $-\mathbf{p}, j, \beta$ $\qquad -ie^{-i\mathbf{p}\cdot\mathbf{r}}V^{(3)}(r)\frac{\epsilon_{mij}}{2}(\boldsymbol{\sigma}\epsilon)_{\alpha\beta}$

$T_\mathbf{r}'^m$ ⎯⎯⎯⟨ $\mathbf{p}, i, \alpha$; $-\mathbf{p}, j, \beta$ $\qquad ie^{-i\mathbf{p}\cdot\mathbf{r}}V^{(3)}(r)\frac{\epsilon_{mij}}{2}\epsilon_{\alpha\beta}$

Figure 3.1: Feynman rules for the coupling of the diquarks $\mathbf{T}_\mathbf{r}^m, \tilde{\mathbf{T}}_\mathbf{r}^m$ and $T_\mathbf{r}'^m$ to antiquarks. The Greek letters denote spin indices and the Roman letters refer to the color indices.

cancel and we are left with the following action

$$\mathcal{L}=$$

$$\frac{1}{2}\sum_{f=b,c}\int d^3\mathbf{r}\,V^{(3)}(r)\left(\mathbf{T}_\mathbf{r}^{m\dagger}\mathbf{T}_\mathbf{r}^m-\mathbf{T}_\mathbf{r}^{m\dagger}\sum_\mathbf{p}e^{i\mathbf{p}\cdot\mathbf{r}}\frac{\epsilon_{mkl}}{2}(\chi_{-\mathbf{p}}^f)_k\epsilon\boldsymbol{\sigma}(\chi_\mathbf{p}^f)_l-\mathbf{T}_\mathbf{r}^m\sum_\mathbf{q}e^{-i\mathbf{q}\cdot\mathbf{r}}\frac{\epsilon_{mij}}{2}(\chi_\mathbf{q}^{f\dagger})_i\boldsymbol{\sigma}\epsilon(\chi_{-\mathbf{q}}^{f\dagger})_j\right)$$

$$+\int d^3\mathbf{r}\,V^{(3)}(r)\left(\tilde{\mathbf{T}}_\mathbf{r}^{m\dagger}\tilde{\mathbf{T}}_\mathbf{r}^m-\tilde{\mathbf{T}}_\mathbf{r}^{m\dagger}\sum_\mathbf{p}e^{i\mathbf{p}\cdot\mathbf{r}}\frac{\epsilon_{mkl}}{2}(\chi_{-\mathbf{p}}^c)_k\epsilon\boldsymbol{\sigma}(\chi_\mathbf{p}^b)_l-\tilde{\mathbf{T}}_\mathbf{r}^m\sum_\mathbf{q}e^{-i\mathbf{q}\cdot\mathbf{r}}\frac{\epsilon_{mij}}{2}(\chi_\mathbf{q}^{b\dagger})_i\boldsymbol{\sigma}\epsilon(\chi_{-\mathbf{q}}^{c\dagger})_j\right)$$

$$+\int d^3\mathbf{r}\,V^{(3)}(r)\left(T_\mathbf{r}'^{m\dagger}T_\mathbf{r}'^m-T_\mathbf{r}'^{m\dagger}\sum_\mathbf{p}e^{i\mathbf{p}\cdot\mathbf{r}}\frac{\epsilon_{mkl}}{2}(\chi_{-\mathbf{p}}^c)_k\epsilon^T(\chi_\mathbf{p}^b)_l+T_\mathbf{r}'^m\sum_\mathbf{q}e^{-i\mathbf{q}\cdot\mathbf{r}}\frac{\epsilon_{mij}}{2}(\chi_\mathbf{q}^{b\dagger})_i\epsilon(\chi_{-\mathbf{q}}^{c\dagger})_j\right).(3.7)$$

The Feynman rules for the couplings of the diquark fields to the pairs of antiquarks from the interaction terms in Eq.(3.7) are shown in Fig. 3.1. Integrating out the fields $\mathbf{T}_\mathbf{r}^m$, $\tilde{\mathbf{T}}_\mathbf{r}^m$ and $T_\mathbf{r}'^m$ will give us back the original NRQCD Lagrangian. Integrating out the antiquark fields $\chi_\mathbf{p}^b$ and $\chi_{-\mathbf{p}}^c$ will yield an effective action for the diquark fields $\mathbf{T}_\mathbf{r}^m$, $\tilde{\mathbf{T}}_\mathbf{r}^m$ and $T_\mathbf{r}'^m$. The $\bar{b}\bar{c}$ fields kinetic terms are the same as those of $\bar{c}\bar{c}$ fields in
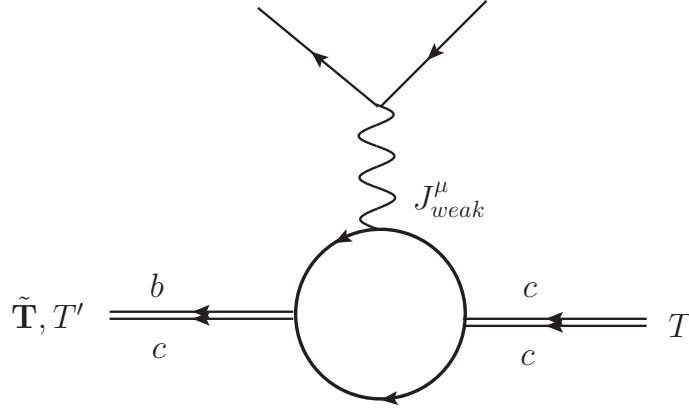
Figure 3.2: One loop diagram contributing to the coupling of composite anti-diquark fields and weak currents.

Ref. [18], with the exception that the diquark reduced mass is now

$$\frac{m_Q}{2} \to \mu_Q = \frac{m_b + m_c}{m_b m_c} .$$

(3.8)

The coupling of the diquarks to weak currents is obtained by evaluating graphs in Fig. 3.2. The flavor changing weak currents are given by $J^\mu_{QCD} = \bar{c}\gamma^\mu(1 - \gamma_5)b$. By matching onto NRQCD, the weak current is rewritten by $J^\mu_{NR} = \chi^{c\dagger}(\delta^{\mu 0} - \delta^{\mu i}\sigma^i)\chi^b +$ $\cdots$ where the ellipsis reflexes to higher order terms. For the lowest order diagram in Fig. 3.2 we find the couplings of diquark to weak currents. The Lagrangian for the weak interactions of diquarks is

$$
\begin{aligned}
\mathcal{L} &= J^\mu_{QQ}(J_W)_\mu \\
&= \int d^3\mathbf{r} \left(-\delta^{\mu 0}\mathbf{T}^{i\dagger}_\mathbf{r} \cdot \tilde{\mathbf{T}}^i_\mathbf{r} - i\delta^{\mu n}(\mathbf{T}^{i\dagger}_\mathbf{r} \times \tilde{\mathbf{T}}^i_\mathbf{r})^n - \delta^{\mu n}(T^{i\dagger}_\mathbf{r})^n T'^i_\mathbf{r} \right) (J_W)_\mu \\
&= \eta \left(-\delta^{\mu 0}\mathbf{T}^{i\dagger} \cdot \tilde{\mathbf{T}}^i - i\delta^{\mu n}(\mathbf{T}^{i\dagger} \times \tilde{\mathbf{T}}^i)^n - \delta^{\mu n}(T^{i\dagger})^n T'^i \right) (J_W)_\mu + \cdots ,
\end{aligned}
$$

(3.9)

where $(J_W)_\mu$ is the weak current and J^μ_{QQ} is the diquark current. In the last line we

51

expanded the diquark fields to the lowest order and wrote the Lagrangian in terms of local currents. The $\cdots$ denotes the excited diquark states contribution and the factor η can be interpreted as the spatial wavefunction overlap of the ground state initial diquark with the ground state final diquark system, which is not predicted by symmetry, i.e. $\eta = \int d^3\mathbf{r}\phi^*_{bc}(\mathbf{r})\phi_{cc}(\mathbf{r})$. Our results differ from Ref. [62] by a different relative sign of the coupling to the zeroth component of the weak current and that of the spatial component of the weak current.

3.3 Doubly Heavy Baryon Semileptonic Decay

In the heavy quark limit, the lowest mass states of the spin-0 heavy meson, P, and the spin-1 heavy meson, P^*, are degenerate, and therefore combined into a single field, H_a,

$$H_a = \vec{P}^*_a \cdot \vec{\sigma} + P_a \,, \tag{3.10}$$

where a is an $SU(3)$ flavor anti-fundamental index and the $\vec{\sigma}$ are the Pauli matrices. Similarly, the ground state degenerate doubly heavy baryon doublet, $T_{i\beta}$ [1], consists of a spin-$\frac{1}{2}$ doubly heavy baryon, $\Xi_{a,\gamma}$, and a spin-3/2 doubly heavy baryon, $\Xi^*_{a,i\beta}$,

$$T_{a,i\beta} = \sqrt{2}\left(\Xi^*_{a,i\beta} + \frac{1}{\sqrt{3}}\Xi_{a,\gamma}\,\sigma^i_{\gamma\beta}\right)\,, \tag{3.11}$$

---

[1]In this section, the T is the doubly heavy baryon field, although T is diquark field in the previous section.

where $\Xi^*_{a,i\beta}$ and $\Xi_{a,\gamma}$ are the spin-$\frac{3}{2}$ and spin-$\frac{1}{2}$ fields, respectively. The $i = 1, 2, 3$ are diquark spin indices and $\beta = 1, 2$ are light antiquark spin indices. The field $\Xi^*_{a,i\beta}$ obeys the constraint $\Xi^*_{a,i\beta}\,\sigma^i_{\beta\gamma} = 0$. Heavy quark-diquark symmetry relates the heavy mesons to doubly heavy antibaryons. The effective Lagrangian for doubly heavy baryon and heavy meson ground state doublets in the heavy hadron rest frame was constructed in Ref. [22],

$$\mathcal{L} = \mathrm{Tr}[\mathcal{H}^\dagger_a (iD_0)_{ba}\mathcal{H}_b] - g\,\mathrm{Tr}[\mathcal{H}^\dagger_a \mathcal{H}_b\,\vec{\sigma}\cdot\vec{A}_{ba}] + \frac{\Delta_H}{4}\mathrm{Tr}[\mathcal{H}^\dagger_a\,\Sigma^i\,\mathcal{H}_a\,\sigma^i]\,, \qquad (3.12)$$

where $\mathcal{H}_{a,\mu\beta} = H_{a,\alpha\beta} + T_{a,i\beta}$ is a 5×2 matrix field which transforms as tensor products of the five component field $\mathcal{Q}_\mu$ (which corresponding to the two heavy quark spin states and the three diquark spin states) and a two-component light antiquark spinor. Here the index μ takes on values between 1 and 5, $\alpha, \beta = 1$ or 2, and $i = 3, 4,$ or 5. The first term is the kinetic term, the second term is the coupling to the axial current and these two terms respect the $SU(5)$ heavy quark-diquark symmetry. The third term is the leading heavy quark symmetry breaking operator which is responsible to the hyperfine splitting. The $\vec{\Sigma}_{\mu\nu}$ are the 5×5 matrices

$$\vec{\Sigma}_{\mu\nu} = \begin{pmatrix} \vec{\sigma}_{\alpha\beta} & 0 \\ 0 & \vec{\mathcal{T}}_{jk} \end{pmatrix}, \qquad (3.13)$$

and $(\mathcal{T}^i)_{jk} = -i\epsilon_{ijk}$. Δ_H is the hyperfine splitting of the charmed mesons which is related to the hyperfine splitting of the doubly charm baryon by heavy quark-diquark symmetry. $\vec{A}_{ba}$ is the spatial part of the axial vector current.

The relevant terms of Eq. (3.12) for our calculation are

$$
\begin{aligned}
\mathcal{L} &= \tilde{T}^+_{\beta i} i D_0 \tilde{T}_{i\beta} - g \tilde{T}^+_{\beta i} \tilde{T}_{i\beta'} \vec{\sigma}_{\beta'\beta} \cdot \vec{A} + \frac{\Delta_H}{4} \tilde{T}^+_{\beta j} (-i\epsilon_{ijk}) \tilde{T}_{k\beta'} \sigma^i_{\beta'\beta} \\
&+ T^+_{\beta i} i D_0 T_{i\beta} - g T^+_{\beta i} T_{i\beta'} \vec{\sigma}_{\beta'\beta} \cdot \vec{A} + \left(\frac{m_c/2}{\mu_Q} \right) \frac{\Delta_H}{4} T^+_{\beta j} (-i\epsilon_{ijk}) T_{k\beta'} \sigma^i_{\beta'\beta} \\
&+ T'^+_\beta i D_0 T'_\beta - g' T'^+_\beta T'_{\beta'} \vec{\sigma}_{\beta'\beta} \cdot \vec{A}.
\end{aligned}
\tag{3.14}
$$

The composite fields are decomposed as

$$
\begin{aligned}
(T_{\bar{c}c\bar{q}})_{i\beta} &= \sqrt{2} \left(\Xi^*_{\bar{c}c\bar{q},i\beta} + \frac{1}{\sqrt{3}} \Xi_{\bar{c}c\bar{q},\alpha} \sigma^i_{\alpha\beta} \right), \\
(\tilde{T}_{\bar{b}c\bar{q}})_{i\beta} &= \sqrt{2} \left(\Xi^*_{\bar{b}c\bar{q},i\beta} + \frac{1}{\sqrt{3}} \Xi_{\bar{b}c\bar{q},\alpha} \sigma^i_{\alpha\beta} \right), \\
(T'_{\bar{b}c\bar{q}})_\beta &= \sqrt{2} \, \Xi'_{\bar{b}c\bar{q},\beta},
\end{aligned}
\tag{3.15}
$$

where $\Xi^*_{i\beta}$ and Ξ_α are the spin-$\frac{3}{2}$ and spin-$\frac{1}{2}$ fields, respectively. Here, we have suppressed the flavor indices. $T_{i\beta}$ and $\tilde{T}_{i\beta}$ are the ground state doublet of $\bar{c}c\bar{q}$ and $\bar{b}c\bar{q}$, respectively, and the diquarks have spin-1. T'_β is the spin-$\frac{1}{2}$ ground state of $\bar{b}c\bar{q}$ where the diquark has spin-0. The hyperfine splittings of the doubly heavy baryons are related to those of the charmed mesons by heavy quark-diquark symmetry, $m_{\Xi^*_{cc}} - m_{\Xi_{cc}} = \frac{3}{4}\Delta_H$ and $m_{\Xi^*_{bc}} - m_{\Xi_{bc}} = \left(\frac{m_c/2}{\mu_Q} \right) \frac{3}{4}\Delta_H$, where the μ_Q is the reduced mass of diquark bc.

Eq.(3.14) describes the low energy strong and electromagnetic interactions in the doubly heavy baryon rest frame in which the doubly heavy baryon four-velocity is conserved (up to $O(\Lambda_{QCD}/m_Q)$ corrections). For a process such as the weak decay, in which the initial and final baryons have different four-velocities, the covariant representation of baryon fields is needed. However, for studying the zero-recoil semileptonic

decay, in which the doubly heavy baryon four-velocity is conserved, it is possible to work in the baryon rest frame. Therefore we are allowed to match the weak current coupling of the diquark onto a current operator in the effective theory for doubly heavy baryons. The Lagrangian for semileptonic decays of doubly heavy baryon is

$$\mathcal{L} = i\eta \, T^+_{\beta i}\epsilon_{ijk}\tilde{T}_{k\beta}J^k_W - \eta \, T^+_{\beta i}\tilde{T}_{i\beta}J^0_W + i\eta \, T^+_{\beta i}T'_\beta J^i_W \,. \tag{3.16}$$

The couplings of the doubly heavy baryon to the weak currents is obtained by demanding that the diquark index on the doubly heavy baryons couple to the weak currents as in Eq.(3.9).

Expanding out Eq.(3.16) in terms of doubly heavy baryon fields, we find the following weak current matrix elements in terms of the initial and final spinor.

$$\langle \Xi_{\bar{c}\bar{c}\bar{q}}|J^\mu_W|\Xi_{\bar{b}\bar{c}\bar{q}}\rangle = \eta \, \bar{u}_{\alpha'}\left(-2i(1+\delta_1)\,\delta_{\alpha\alpha'}\delta^{\mu0} - \frac{4i}{3}(1+\delta_2)\,\sigma^j_{\alpha\alpha'}\delta^{\mu j}\right)u_\alpha \,, \tag{3.17}$$

$$\langle \Xi^*_{\bar{c}\bar{c}\bar{q}}|J^\mu_W|\Xi_{\bar{b}\bar{c}\bar{q}}\rangle = \eta \, \bar{u}_{i\beta}\left(\frac{2i}{\sqrt{3}}(1+\delta_3)\,\delta_{\alpha\beta}\delta^{\mu i}\right)u_\alpha \,, \tag{3.18}$$

$$\langle \Xi_{\bar{c}\bar{c}\bar{q}}|J^\mu_W|\Xi^*_{\bar{b}\bar{c}\bar{q}}\rangle = \eta \, \bar{u}_\alpha\left(\frac{2i}{\sqrt{3}}(1+\delta_4)\,\delta_{\alpha\beta}\delta^{\mu i}\right)u_{i\beta} \,, \tag{3.19}$$

$$\langle \Xi^*_{\bar{c}\bar{c}\bar{q}}|J^\mu_W|\Xi^*_{\bar{b}\bar{c}\bar{q}}\rangle = \eta \, \bar{u}_{k\beta}\left(-2i(1+\delta_5)\,\delta_{\alpha\beta}\delta_{ik}\delta^{\mu0} + 2i(1+\delta_6)\,\sigma^j_{\alpha\beta}\delta_{ik}\delta^{\mu j}\right)u_{i\alpha} \,, \tag{3.20}$$

$$\langle \Xi_{\bar{c}\bar{c}\bar{q}}|J^\mu_W|\Xi'_{\bar{b}\bar{c}\bar{q}}\rangle = \eta \, \bar{u}_{\alpha'}\left(-\frac{2}{\sqrt{3}}(1+\delta'_1)\,\sigma^j_{\alpha\alpha'}\delta^{\mu j}\right)u'_\alpha \,, \tag{3.21}$$

$$\langle \Xi^*_{\bar{c}\bar{c}\bar{q}}|J^\mu_W|\Xi'_{\bar{b}\bar{c}\bar{q}}\rangle = \eta \, \bar{u}_{i\beta}\left(-2(1+\delta'_2)\,\delta_{\alpha\beta}\delta^{\mu i}\right)u'_\alpha \,, \tag{3.22}$$

where $(u_\alpha, u'_\alpha, u_{i\beta})$ and $(\bar{u}_\alpha, \bar{u}_{i\beta}, \bar{u}'_\alpha)$ are nonrelativistic spinors for initial and final states, respectively. Up to an overall normalization, these form factors are predicted

by heavy quark-diquark symmetry. The tree level zero-recoil doubly heavy baryon semileptonic decay matrix elements agree with Ref. [63] up to an overall minus sign.[2] At tree level, the δ_i are zero and the δ_i vanish at any order in the heavy quark limit. They will receive corrections from heavy quark symmetry breaking effects. Obtaining those symmetry breaking corrections that come from chiral loop correction in Fig. 3.3 is the goal of this chapter. δ_1 to δ_6 involve the doubly heavy baryons which are related to the known heavy D mesons by heavy quark-diquark symmetry. Therefore the coupling constant g which appears in the chiral corrections is known. Chiral corrections as δ_1' and δ_2' depend on the coupling constant g' which is not known. We will only focuse on δ_1 to δ_6 for this thesis.

The pion-baryon vertex in Fig. 3.3 is generated from the pion-baryon interaction terms in Eq.(3.14) and the weak current vertex is from the weak current terms in Eq.(3.16). There are also loops for the wavefunction renormalization which are not shown here.

The chiral loop corrections to semileptonic decay form factors are given in Appendix A. Table 3.1 gives numerical results for δ_i for both $q = u, d$ and $q = s$. The PQχPT corrections will be discussed in the next section. Here we work in the isospin limit, so $m_u = m_d$. We take the the reduced mass of diquark bc to be $\mu_Q = \frac{m_b m_c}{m_b + m_c} \approx m_c$. We choose $g = 0.6$ [64] and we set $f_\pi = f_k = f_\eta = 130$ MeV. The

---

[2]They give results for Ξ_{bc} while we give the results for $\Xi_{\bar{b}\bar{c}}$. To obtain their result to the lowest order, we should use the decomposition of the ground state doublet as $T_{i\beta} = \sqrt{2}\left(\Xi^*_{i\beta} - \frac{1}{\sqrt{3}}\sigma^i_{\beta\gamma}\Xi_{a,\gamma}\right)$ and then we agree up to an overall sign.
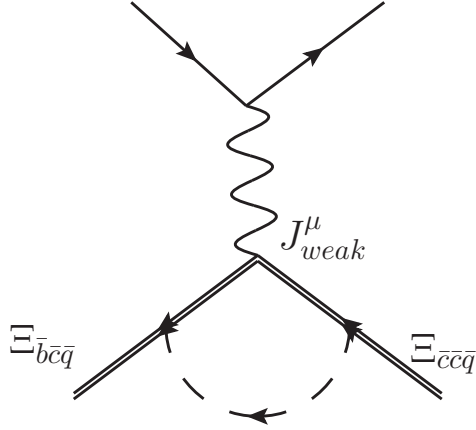
Figure 3.3: One-loop contributions to the doubly heavy baryon semileptonic decay.

	$\delta_1(u,d)$	$\delta_2(u,d)$	$\delta_3(u,d)$	$\delta_4(u,d)$	$\delta_5(u,d)$	$\delta_6(u,d)$
$\mu = 500$ MeV	0.25	0.25	0.07	0.15	-0.05	-0.05
$\mu = 1500$ MeV	0.32	0.32	0.10	0.19	-0.01	-0.02
	$\delta_1(s)$	$\delta_2(s)$	$\delta_3(s)$	$\delta_4(s)$	$\delta_5(s)$	$\delta_6(s)$
$\mu = 500$ MeV	-0.01	-0.01	-0.14	-0.14	-0.16	-0.16
$\mu = 1500$ MeV	-0.0002	-0.001	-0.13	-0.12	-0.13	-0.13

Table 3.1: Chiral corrections to doubly heavy baryon containing a u, d or s semilep-

tonic decay form factors for $\mu = 500$ MeV and $\mu = 1500$ MeV.

experimental value for Δ_H is 140 MeV. In the numerical calculations we use $m_\pi = 140$ MeV, $m_k = 500$ MeV, and $m_\eta = \sqrt{\frac{-m_\pi^2 + 4m_k^2}{3}}$. Then only one parameter can be varied, the renormalization scale, μ. Table 3.1 gives results for $\mu = 500$ MeV to $\mu = 1500$ MeV. In the chiral perturbation theory calculations the logarithmic μ-dependence from loops is cancelled by μ-dependent counterterms we have not included here. We vary μ from 500 MeV to 1500 MeV to obtain an estimate of uncertainty due to the unknown counterterm contributions. The μ dependence is pretty small. We find that, for the doubly heavy baryon containing anti-up or anti-down quark, δ_1 and δ_2 in the $\Xi_{bcq}^{1/2} \to \Xi_{ccq}^{1/2}$ transition get very big chiral corrections of order $25\% - 32\%$ and δ_5, δ_6 in the $\Xi_{bcq}^{3/2} \to \Xi_{ccq}^{3/2}$ transition get small correction of order 5%. The form factors for doubly heavy baryon containing antistrange quark obtain negative corrections and δ_1 and δ_2 are least sensitive to chiral corrections, with corrections of order 1%. It would be interesting to see if the observed deviations from heavy quark-diquark symmetry in either experiments or lattice simulations agree with the predictions form chiral perturbation theory. Disagreements with χPT predictions indicate the $1/m_Q$ heavy quark-diquark corrections are dominated by short distance effects.

3.4   PQχPT results

The EFT techniques with heavy quark-diquark symmetry for doubly heavy baryons can also be applied to doubly heavy systems simulated on the lattice. It is useful to extend the χPT results to include lattice artifacts such as quenching and partial

quenching. Here we will focus on partially quenched chiral corrections to the doubly heavy baryon zero-recoil semileptonic decay form factors, which provide the formulae needed for chiral extrapolations in lattice calculations. The major modification to the calculation in the previous section is that there is a modified propagator for the Goldstone mesons.

In a lattice calculation, the sea quark masses are often different from valence quark masses. In partially quenched QCD the sea quark masses are different from the valence quark masses, while in quenched QCD, the sea quark contributions are absent. To reproduce the lattice artifacts in field theory, fictitious ghost and quarks are added to the Lagrangian. Ghost quarks have same masses as valence quarks but are bosons, so the loops come with opposite sign and they cancel the valence contributions. Then we are left with the effects of the sea quarks. This is equivalent to the partial quenching artifact in lattice QCD simulations which use different masses for sea and valence quarks. In the limit of $m_{sea} = m_{valence}$, QCD is recovered. PQχPT is useful for lattice extrapolations to physical quark masses. The PQχPT and QχPT pseudoscalar meson sector is described by the Lagrangian [65, 66, 67, 68, 69, 70, 71, 72],

$$\mathcal{L} = \frac{f^2}{8}\text{str}\left(\partial^\mu\Sigma^\dagger\partial_\mu\Sigma\right) + \frac{\lambda}{4}\text{str}\left(m_q\Sigma^\dagger + m_q^\dagger\Sigma\right) + \alpha_\Phi\partial^\mu\Phi_0\partial_\mu\Phi_0 - \mu_0^2\Phi_0^2, \qquad (3.23)$$

where the field Σ is defined by

$$\Sigma = \exp\left(\frac{2i\Phi}{f}\right) = \xi^2, \qquad (3.24)$$

and the meson fields appear in the $U(6|3)$ matrix,

$$\Phi = \begin{pmatrix} M & \chi^\dagger \\ \chi & \tilde{M} \end{pmatrix}. \tag{3.25}$$

The operation str() in Eq. (3.23) is a supertrace over flavor indices, i.e., $\text{str}(A) = \sum_a \epsilon_a A_{aa}$, where $\epsilon_a = 1$ for $a = 1 - 6$ and $\epsilon_a = -1$ for $a = 7 - 9$. The M and $\tilde{M}$ matrices contain bosonic mesons, while the χ and $\chi^\dagger$ matrices contain fermionic mesons (one ghost quark with one sea/valence quark). The quark mass matrix is defined as [73]

$$m_q = diag(m_u, m_d, m_s, m_j, m_l, m_r, m_u, m_d, m_s). \tag{3.26}$$

We work in the isospin limit for both the valence and sea sectors, so $m_u = m_d$ and $m_l = m_j$. We take the strange sea quark to be same as the valence quark, $m_r = m_s$. From the lowest order PQχPT Lagrangian, the meson with quark content $q\bar{q}'$ has the mass of $m_{q\bar{q}'}^2 = \frac{\lambda}{f^2}(m_q + m_{q'})$. The PQ$\chi$PT propagators of the off-diagonal mesons have the usual Klein-Gordon form. The flavor neutral propagator can be conveniently written as [73]

$$\mathcal{G}_{ab}^{PQ} = \varepsilon_a \delta_{ab} P_a + \mathcal{P}_{ab}(P_a, P_b, P_X), \tag{3.27}$$

where

$$
\begin{aligned}
P_a &= \frac{i}{q^2 - m_{aa}^2 + i\varepsilon}, \quad P_b = \frac{i}{q^2 - m_{bb}^2 + i\varepsilon}, \quad P_X = \frac{i}{q^2 - m_X^2 + i\varepsilon}, \\
\mathcal{P}_{ab}(A, B, C) &= -\frac{1}{3}\left[\frac{(m_{aa}^2 - m_{jj}^2)(m_{aa}^2 - m_{rr}^2)}{(m_{aa}^2 - m_{bb}^2)(m_{aa}^2 - m_X^2)}A + \frac{(m_{bb}^2 - m_{jj}^2)(m_{bb}^2 - m_{rr}^2)}{(m_{bb}^2 - m_{aa}^2)(m_{bb}^2 - m_X^2)}B \right. \\
&\qquad \left. + \frac{(m_X^2 - m_{jj}^2)(m_X^2 - m_{rr}^2)}{(m_X^2 - m_{aa}^2)(m_X^2 - m_{bb}^2)}C \right].
\end{aligned} \tag{3.28}
$$

where $m_X^2 = \frac{1}{3}(m_{jj}^2 + 2m_{rr}^2)$.

In terms of the 5×2 field, the partially quenched Lagrangian for doubly heavy baryons and heavy mesons is [73],

$$
\begin{aligned}
\mathcal{L}^{PQ} &= \left(\mathcal{H}^\dagger(\mathcal{H}i\overleftarrow{D}_0)\right) - g\left(\mathcal{H}^\dagger \mathcal{H} \boldsymbol{A} \cdot \boldsymbol{\sigma}\right) \\
&+ \frac{\Delta_H}{4}\left(\mathcal{H}^\dagger \boldsymbol{\Sigma} \cdot \mathcal{H}\boldsymbol{\sigma}\right) + \sigma\left(\mathcal{H}^\dagger \mathcal{H}\mathcal{M}\right) + \sigma'\left(\mathcal{H}^\dagger \mathcal{H}\right)\mathrm{str}(\mathcal{M}),
\end{aligned}
\tag{3.29}
$$

where $\mathcal{M}$ is the mass operator defined by $\mathcal{M} = \frac{1}{2}\left(\xi m_q \xi + \xi^\dagger m_q \xi^\dagger\right)$ Therefore the baryon mass splittings in PQχPT are given by

$$
\begin{aligned}
\Delta_{ccqq'} &= m_{\Xi_{\bar{c}\bar{c}q'}} - m_{\Xi_{\bar{c}\bar{c}q}} = m_{\Xi^*_{\bar{c}\bar{c}q'}} - m_{\Xi^*_{\bar{c}\bar{c}q}} = -\sigma(m_{q'} - m_q)\,, \\
\Delta_{bcqq'} &= m_{\Xi_{bcq'}} - m_{\Xi_{bcq}} = m_{\Xi^*_{\bar{b}\bar{c}q'}} - m_{\Xi^*_{\bar{b}\bar{c}q}} = -\sigma(m_{q'} - m_q)\,, \\
\Delta^*_{ccqq'} &= m_{\Xi^*_{\bar{c}\bar{c}q'}} - m_{\Xi_{\bar{c}\bar{c}q}} = \frac{3}{4}\Delta_H - \sigma(m_{q'} - m_q)\,, \\
\Delta^*_{bcqq'} &= m_{\Xi^*_{\bar{b}\bar{c}q'}} - m_{\Xi_{\bar{b}\bar{c}q}} = \frac{1}{2}\left(\frac{3}{4}\Delta_H\right) - \sigma(m_{q'} - m_q)\,,
\end{aligned}
\tag{3.30}
$$

where we take the the reduced mass of diquark bc to be $\mu_Q = \frac{m_b m_c}{m_b + m_c} \approx m_c$, σ is the coupling constant in the mass operator in the Lagrangian in Eq.(3.29) . We choose $g = 0.6$ [64] and $f = 130$ MeV. The experiment value for Δ_H is 140 MeV. From the value of the $SU(3)$ splitting of the ground state D mesons, $m_{D_s} - m_D = -\sigma(m_s - m_u) \approx 100$ MeV, $m_\pi^2 = \frac{\lambda}{f^2}(m_u + m_d)$ and $m_k^2 = \frac{\lambda}{f^2}(m_s + m_d)$, we obtain $-\sigma = \frac{100}{m_k^2 - m_\pi^2}\frac{\lambda}{f^2}$. For the mass of η, we use the $SU(3)$ prediction $m_\eta = \sqrt{\frac{-m_\pi^2 + 4m_k^2}{3}}$. Then only three parameters can be varied, the valence pion mass $m_{\pi\,val} = m_{uu}$, the sea pion mass $m_{\pi\,sea} = m_{jj}$, and the renormalization scale μ. As in the previous section, we vary μ from 500 MeV to 1500 MeV to obtain an estimate of uncertainty

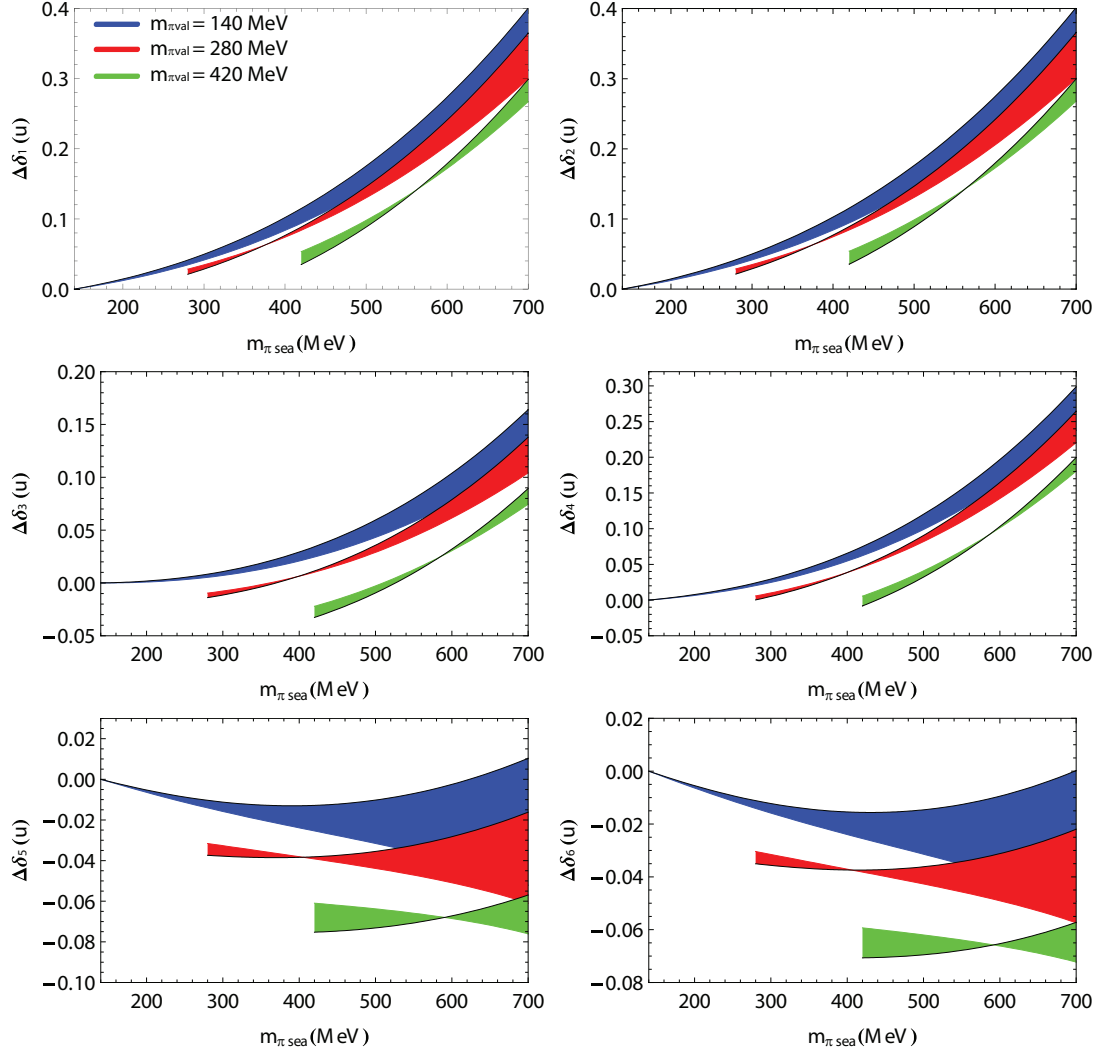**Figure 3.4**: $\Delta\delta_n$ $(q = u)$ as a function of $m_{\pi sea}$ for different values of $m_{\pi val}$. The width of the bands is the results of varying μ between 500 MeV and 1500 MeV.
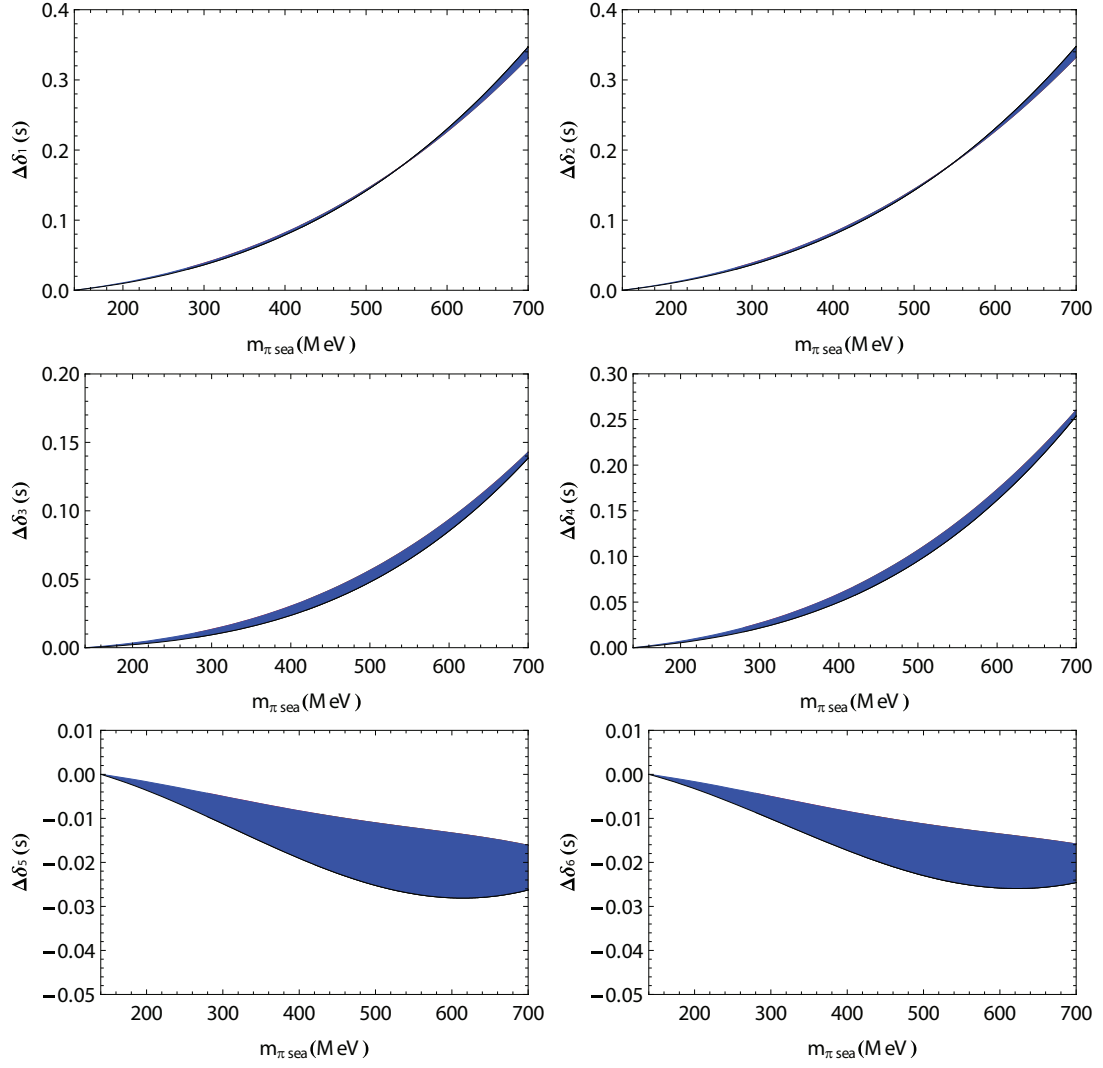
Figure 3.5: $\Delta\delta_n$ $(q = s)$ as a function of $m_{\pi sea}$ but independent of different values of $m_{\pi val}$. The width of the bands is the results of varying μ between 500 MeV and 1500 MeV.

due to higher order corrections. Calculating the PQχPT loop diagrams, such as Fig. 3.3, we find the corrections for the six form factors which we list in Appendix A.

In the Figs. 3.4 and 3.5 we plot the relevant corrections to the form factors $\Delta \delta_i = \delta_{iPQ} - \delta_{i\chi}$ in terms of $m_{\pi sea}$ for different values of $m_{\pi val}$ for $q = u$ and $q = s$. For each value of $m_{\pi val} = 140$ MeV, 280 MeV and 420 MeV, we let the $m_{\pi val}$ range from $m_{\pi val}$ up to the mass of eta-strange, $m_{\eta_s} = m_{ss} \approx 700$ MeV. The bands correspond to varying μ from 500 MeV to 1500 MeV, which is chosen to be the same for both χPT and PQχPT. From the plots, it is easy to see that the partially quenched chiral corrections reproduce the chiral corrections when the sea quark mass goes to the physical valence quark mass. As demonstrated by Figs. 3.4 and 3.5, the partially quenched chiral non-analytic corrections relevant to the chiral corrections are very insensitive to the choice of μ. The corrections to $\delta_1, \delta_2, \delta_3$ and δ_4 are affected most by sea quark masses and range from $10\% - 40\%$. Those corrections increase with increasing $m_{\pi sea}$ values. δ_5 and δ_6 are very insensitive to partial quenching effects, with corrections of order $1\% - 8\%$ small relevant corrections from partial quenching, and are insensitive to sea quark masses, while $\delta_1 - \delta_4$ are not. It would be interesting to test the the chiral predictions in a lattice simulation.

3.5 Summary

In this chapter we have used NRQCD to derive the couplings of heavy diquarks to weak currents with heavy quark-diquark symmetry. We constructed the chiral

Lagrangian for doubly heavy baryons coupled to weak currents and calculated the tree

level predictions for doubly heavy baryon semileptonic weak decay form factors. We

calculated the chiral corrections in both unquenched and partially quenched theory.

The partially quenched loop corrections to semileptonic decay form factors are given

in Appendix A. The formulae will be useful for chiral extrapolation of doubly heavy

baryon zero-recoil semileptonic decay form factors in lattice QCD simulations. It will

be interesting to test the calculations of this chapter with either experimental data

or lattice simulations.

Chapter 4

Pion Physics at Finite Volume

In addition to my work on doubly heavy baryons, I also coauthored two papers on the subject of finite volume corrections to pion electromagnetic current matrix elements and the pion Compton scattering tensor. These papers were written in collaboration with Dr. Brian Tiburzi and Dr. Fu-Jiun Jiang and the original papers are reprinted in Appendices B and C. Here I will give a concise summary of our work.

Our motivation comes from the discrepancy between experimental measurements of pion electromagnetic polarizabilities and the theoretical predictions. The physical meaning of the polarizability is the relative tendency of a charge distribution, like the electron cloud of an atom or molecule, to be distorted from its normal shape by an external electric field. This results in a shift in the ground state energy proportional to the field squared, $\Delta E_0 = -\frac{1}{2}\alpha_E \mathbf{E}^2$. The coefficient, α_E, is the electric polarizability. Similarly, the magnetic polarizability is defined in $\Delta E_0 = -\frac{1}{2}\beta_M \mathbf{B}^2$.

Pion polarizabilities have been measured indirectly in several experiments from radiative pion-nucleon scattering, pion photonproduction in photon nucleus scattering, and pion production seen in electron-positron Collisions. The most recent experimental results were given by MAMI at Mainz [74], which measured the the polarizabilities in the process $\gamma N \to \gamma \pi N$. They measured the difference of electric

and magnetic polarizabilities of the charged pion,

$$(\alpha_E - \beta_M)_{\pi^+} = (11.6 \pm 1.5_{st} \pm 3.0_{sys} \pm 0.5_{model}) \times 10^{-4} \text{fm}^3. \tag{4.1}$$

The theory used to calculate the polarizabilities is chiral perturbation theory. Pion electromagnetic polarizabilities are extracted from the energy expansion of the Compton scattering amplitude. At low energy the Compton scattering amplitude for a real photon to scatter off a pion is given by:

$$
\begin{aligned}
T_{\gamma\pi} &= 2m_\pi \left[\left(-\frac{e^2 Q_\pi^2}{m_\pi} + 4\pi\,\alpha_E\,\omega^2 \right) \boldsymbol{\varepsilon}'^* \cdot \boldsymbol{\varepsilon} + 4\pi\,\beta_M\,\omega^2 (\boldsymbol{\varepsilon}'^* \times \hat{\boldsymbol{k}}') \cdot (\boldsymbol{\varepsilon} \times \hat{\boldsymbol{k}}) \right] \\
&\quad + \frac{e^2 Q_\pi^2}{2m_\pi^2}\omega^2 (\boldsymbol{\varepsilon}'^* \cdot \hat{\boldsymbol{k}})(\boldsymbol{\varepsilon} \cdot \hat{\boldsymbol{k}}')(1 - \cos\theta) + \dots,
\end{aligned}
\tag{4.2}
$$

where the ellipsis denotes higher order in the photon energy. $k_\mu = (\omega, \omega\hat{\boldsymbol{k}})$ is the initial photon momenta in the center-of-momentum frame, while $k'_\mu = (\omega, \omega\hat{\boldsymbol{k}}')$ is the final photon momenta. The center-of-momentum scattering angle θ is given by $\cos\theta = \hat{\boldsymbol{k}}' \cdot \hat{\boldsymbol{k}}$. Q_π is the charge of the pion. In the expansion in ω/m_π, the coefficients of two of the second order terms are proportional to the electric and magnetic polarizabilities. Therefore from the Compton scattering amplitude, one can extract pion polarizabilities from the ω expansion. To one-loop order, the sum of the pion electromagnetic polarizabilities is zero for both neutral and charged pions. The difference to one-loop order is [75],

$$\alpha_E^{\pi^0} - \beta_M^{\pi^0} = -\frac{2\alpha Q_\pi^2}{3(4\pi f)^2 m_\pi} \tag{4.3}$$

$$\alpha_E^{\pi^\pm} - \beta_M^{\pi^\pm} = \frac{16\alpha(\alpha_9 + \alpha_{10})}{f^2 m_\pi}, \tag{4.4}$$

where α is the fine structure constant, $e^2/4\pi$. α_9 and α_{10} are low energy constants. The numerical value for charged pion is $\alpha_E^{\pi^+} - \beta_M^{\pi^+} = 5.4 \times 10^{-4} \text{fm}^3$. Even the two-loop chiral perturbation theory prediction, $\alpha_E^{\pi^+} - \beta_M^{\pi^+} = (5.7 \pm 1.0) \times 10^{-4} \text{fm}^3$ [76], does not agree with the experimental data very well.

Another theoretical approach to calculating the pion polarizabilities is lattice QCD. Calculation of the four-point function for pion Compton scattering,

$$T^{\mu\nu}(k', k) = \int_{x,y} e^{ik \cdot y - ik' \cdot x} \langle \pi | T\{J^\mu(x) J^\nu(y)\} | \pi \rangle , \qquad (4.5)$$

presently cannot be simulated on the lattice. But progress on extracting β_M^π has been made with background field methods. In background field methods a uniform external magnetic field is introduced on the lattice and the quadratic dependence of the hadrons mass shift on the external B field is measured to extract β_M^π. For example, Ref. [77] provided the pion magnetic polarizability for different pion masses. The goal of our work was to calculate the finite volume dependence of pion polarizabilities and other electromagnetic properties using finite volume chiral perturbation theory for the lattice.

In our calculations, we keep the temporal extent of the simulation box, T, infinite and the spatial extent, L, finite, to determine finite-size effects for the lattice QCD observables. The meson fields are in a box with periodic boundary conditions, which leads to quantized momenta, $\mathbf{p} = \frac{2\pi \mathbf{n}}{L}$. In the regime $m_\pi L > 1$, the power counting is $|p| < m_\pi \ll \Lambda_\chi$, which is the same as in the infinite volume chiral perturbation theory. Therefore the same Feynman diagrams contribute to the pion Compton tensor and

we only need to replace integrals over four momentum in χPT, with integrals over energy and sums over all spatial momentum modes permitted by periodicity:

$$\int d^4q \rightarrow \sum_{\mathbf{q}} \int_{-\infty}^{\infty} dq^0 .$$ (4.6)

This leads to modifications of the infinite volume results. The volume dependence of pion Compton scattering tensor is derived in Ref. [78] (appendix C).

In Refs. [79], we work at zero photon energy and to the order $O(p^2)$ in pion momentum, and calculated the finite volume corrections to matrix element of electromagnetic current. In the infinite volume case, the charge current matrix element is normalized to be proportional to the pion charge and pion momentum as

$$\langle \pi^{\pm}(p)|J^{\mu}|\pi^{\pm}(p)\rangle = \pm 2ep^{\mu}.$$ (4.7)

This is an exact result to all orders in chiral perturbation theory. This follows from the infinite volume Ward identity,

$$-i\Gamma^{\mu}(P,P) = Qe \frac{\partial}{\partial P_{\mu}} G(P)^{-1}.$$ (4.8)

Here $\Gamma^{\mu}(P,P)$ is the charged pion photon vertex function at zero recoil and $G(P)$ is the pion propagator. At finite volume, the spatial part of the current obtains additional corrections as,

$$\langle \pi^{\pm}|\mathbf{J}|\pi^{\pm}\rangle = \pm 2e\mathbf{p}(1 + \Delta J(L)).$$ (4.9)

as was shown in Ref. [79](Appendix B). At first sight this might seem surprising in

Figure 4.1: The Ward-Takahashi Identity is still valid at Finite Volume.

light of Eq.(4.8). However, we showed that the correct form of the Ward-Takahashi identity at finite volume is

$$-ik_\mu \Gamma^\mu(P+k, P) = Qe\left[G(P+k)^{-1} - G(P)^{-1}\right].$$ (4.10)

The infinite volume identity in Eq.(4.8) follows from Eq.(4.10) by taking $k^\mu \to 0$. Such a limit is not possible in finite volume because of the discretization of momentum. We checked that our results are consistent with the Ward-Takahashi identity in Eq.(4.10).

In order to address the finite volume effect in the electromagnetic polarizability predictions obtained from the lattice background field method, We calculated the finite volume corrections to the pion Compton scattering tensor and showed the results for both neutral and charged pion in Ref. [78](Appendix C). If the two-current two pion correlation functions are performable on lattice, our results can be used directly to isolate the finite volume physics. However, this simulation presently cannot be performed on lattice. All terms in our results are form factors in ωL. Because of the momentum quantization, these form factors cannot be expanded in ωL for the smallest modes. Therefore the connections from the Compton scattering tensor to finite volume corrections to polarizabilities from background field theory

70

methods are lacking.

Appendix A

One-loop χPT and PQχPT corrections to zero-recoil semileptonic decay.

Here we give the detailed one-loop χPT and PQχPT corrections to zero-recoil semileptonic decay. In the calculation we use $\bar{M}S$ scheme and have not included the counterterms. In the chiral corrections to the six form factors f is pion decay constant, m_i is the mass of the Goldstone boson in the one-loop diagram and C_{ab}^i is a factor which comes from $SU(3)$ Clebsch-Gordan coefficients in the couplings. For loops with charged pions we have $C_{12}^{\pi^\pm} = C_{21}^{\pi^\pm} = 1$, for loops with neutral pions $C_{11}^{\pi^0} = C_{22}^{\pi^0} = \frac{1}{2}$, for loops with kaons $C_{3i}^K = C_{i3}^K = 1$ (i =1 or 2), and for loops with η mesons $C_{11}^\eta = C_{22}^\eta = \frac{1}{6}$ and $C_{33}^\eta = \frac{2}{3}$.

$$\delta_{1\chi}(q) = \sum_{i,q'} C_{qq'}^i \frac{g^2}{(4\pi f)^2} \left(-\frac{1}{9} I(\Delta_{bcqq'}, \Delta_{ccqq'}, m_i, \mu) - \frac{8}{9} I(\Delta_{bcqq'}^*, \Delta_{ccqq'}^*, m_i, \mu) \right),$$

$$\delta_{2\chi}(q) = \sum_{i,q'} C_{qq'}^i \frac{g^2}{(4\pi f)^2} (\frac{1}{27} I(\Delta_{bcqq'}, \Delta_{ccqq'}, m_i, \mu) - \frac{4}{27} I(\Delta_{bcqq'}, \Delta_{ccqq'}^*, m_i, \mu)$$
$$- \frac{4}{27} I(\Delta_{bcqq'}^*, \Delta_{ccqq'}, m_i, \mu) - \frac{20}{27} I(\Delta_{bcqq'}^*, \Delta_{ccqq'}^*, m_i, \mu)),$$

$$\delta_{3\chi}(q) = \sum_{i,q'} C_{qq'}^i \frac{g^2}{(4\pi f)^2} (-\frac{8}{27} I(\Delta_{bcqq'}, -\Delta_{ccqq'}^*, m_i, \mu) + \frac{5}{27} I(\Delta_{bcqq'}, \Delta_{ccqq'}, m_i, \mu)$$
$$- \frac{4}{27} I(\Delta_{bcqq'}^*, -\Delta_{ccqq'}^*, m_i, \mu) - \frac{20}{27} I(\Delta_{bcqq'}^*, \Delta_{ccqq'}, m_i, \mu)),$$

$$\delta_{4\chi}(q) = \sum_{i,q'} C_{qq'}^i \frac{g^2}{(4\pi f)^2} (-\frac{8}{27} I(-\Delta_{bcqq'}^*, \Delta_{ccqq'}, m_i, \mu) + \frac{5}{27} I(-\Delta_{bcqq'}^*, \Delta_{ccqq'}^*, m_i, \mu)$$
$$- \frac{4}{27} I(\Delta_{bcqq'}, \Delta_{ccqq'}, m_i, \mu) - \frac{20}{27} I(\Delta_{bcqq'}, \Delta_{ccqq'}^*, m_i, \mu)),$$

$$\delta_{5\chi}(q) = \sum_{i,q'} C^i_{qq'} \frac{g^2}{(4\pi f)^2} \left(-\frac{4}{9} I(-\Delta^*_{bcqq'}, -\Delta^*_{ccqq'}, m_i, \mu) - \frac{5}{9} I(\Delta_{bcqq'}, \Delta_{ccqq'}, m_i, \mu) \right),$$

$$\delta_{6\chi}(q) = \sum_{i,q'} C^i_{qq'} \frac{g^2}{(4\pi f)^2} \left(-\frac{8}{27} I(-\Delta^*_{bcqq'}, -\Delta^*_{ccqq'}, m_i, \mu) - \frac{4}{27} I(-\Delta^*_{bcqq'}, \Delta_{ccqq'}, m_i, \mu) \right.$$
$$\left. - \frac{4}{27} I(\Delta_{bcqq'}, -\Delta^*_{ccqq'}, m_i, \mu) - \frac{11}{27} I(\Delta_{bcqq'}, \Delta_{ccqq'}, m_i, \mu) \right). \tag{A.1}$$

The formulae for χPT corrections to doubly heavy baryon semileptonic decay form factors are given in terms of the following functions,

$$I(0, 0, m, \mu) = 0,$$

$$I(\Delta, \Delta, m, \mu) = -6\Delta^2 \ln\left(\frac{\mu^2}{m^2}\right) + 4\left(m^2 - 3\Delta^2\right) + 8m\Delta F\left(\frac{\Delta}{m}\right) + 4\left(\Delta^2 - m^2\right) F'\left(\frac{\Delta}{m}\right),$$

$$I(\Delta_1, \Delta_2, m, \mu) = -2\left(\Delta_1^2 + \Delta_1\Delta_2 + \Delta_2^2\right) \ln\left(\frac{\mu^2}{m^2}\right) + 4\left(m^2 - \Delta_1^2 - \Delta_1\Delta_2 - \Delta_2^2\right)$$
$$+ \frac{4}{\Delta_2 - \Delta_1} \left((\Delta_2^2 - m^2)F\left(\frac{\Delta_2}{m}\right) m - (\Delta_1^2 - m^2)F\left(\frac{\Delta_1}{m}\right) m \right), \tag{A.2}$$

where

$$F(x) = \begin{cases} -\sqrt{1 - x^2} \left(\frac{\pi}{2} - tan^{-1}\left(\frac{x}{\sqrt{1-x^2}}\right)\right), & |x| < 1 \\ \sqrt{x^2 - 1} \ln\left(x + \sqrt{x^2 - 1}\right), & |x| \geq 1 \end{cases}, \tag{A.3}$$

and $F'(x)$ is the first derivative of x.

Next we give the same corrections for the partially quenched case.

$$\delta_{1PQ}(q) = \sum_{q'=j,l,r} \frac{g^2}{(4\pi f)^2} \left(-\frac{1}{9} I(\Delta_{bcqq'}, \Delta_{ccqq'}, m_{qq'}, \mu) - \frac{8}{9} I(\Delta^*_{bcqq'}, \Delta^*_{ccqq'}, m_{qq'}, \mu) \right)$$
$$+ \frac{g^2}{(4\pi f)^2} \left(-\frac{1}{9} K(\Delta_{bcqq}, \Delta_{ccqq}, m_{qq}, m_{qq}, \mu) - \frac{8}{9} K(\Delta^*_{bcqq}, \Delta^*_{ccqq}, m_{qq}, m_{qq}, \mu) \right),$$

$$\delta_{2PQ}(q) = \sum_{q'=j,l,r} \frac{g^2}{(4\pi f)^2}\Big(\frac{1}{27}I(\Delta_{bcqq'},\Delta_{ccqq'},m_{qq'},\mu) - \frac{4}{27}I(\Delta_{bcqq'},\Delta^*_{ccqq'},m_{qq'},\mu)$$

$$- \frac{4}{27}I(\Delta^*_{bcqq'},\Delta_{ccqq'},m_{qq'},\mu) - \frac{20}{27}I(\Delta^*_{bcqq'},\Delta^*_{ccqq'},m_{qq'},\mu)\Big)$$

$$+ \frac{g^2}{(4\pi f)^2}\Big(\frac{1}{27}K(\Delta_{bcqq},\Delta_{ccqq},m_{qq},m_{qq},\mu) - \frac{4}{27}K(\Delta_{bcqq},\Delta^*_{ccqq},m_{qq},m_{qq},\mu)$$

$$- \frac{4}{27}K(\Delta^*_{bcqq},\Delta_{ccqq},m_{qq},m_{qq},\mu) - \frac{20}{27}K(\Delta^*_{bcqq},\Delta^*_{ccqq},m_{qq},m_{qq},\mu)\Big)\,,$$

$$\delta_{3PQ}(q) = \sum_{q'=j,l,r} \frac{g^2}{(4\pi f)^2}\Big(-\frac{8}{27}I(\Delta_{bcqq'},-\Delta^*_{ccqq'},m_{qq'},\mu) + \frac{5}{27}I(\Delta_{bcqq'},\Delta_{ccqq'},m_{qq'},\mu)$$

$$- \frac{4}{27}I(\Delta^*_{bcqq'},-\Delta^*_{ccqq'},m_{qq'},\mu) - \frac{20}{27}I(\Delta^*_{bcqq'},\Delta_{ccqq'},m_{qq'},\mu)\Big)$$

$$+ \frac{g^2}{(4\pi f)^2}\Big(-\frac{8}{27}K(\Delta_{bcqq},-\Delta^*_{ccqq},m_{qq},m_{qq},\mu) + \frac{5}{27}K(\Delta_{bcqq},\Delta_{ccqq},m_{qq},m_{qq},\mu)$$

$$- \frac{4}{27}K(\Delta^*_{bcqq},-\Delta^*_{ccqq},m_{qq},m_{qq},\mu) - \frac{20}{27}K(\Delta^*_{bcqq},\Delta_{ccqq},m_{qq},m_{qq},\mu)\Big)\,,$$

$$\delta_{4PQ}(q) = \sum_{q'=j,l,r} \frac{g^2}{(4\pi f)^2}\Big(-\frac{8}{27}I(-\Delta^*_{bcqq'},\Delta_{ccqq'},m_{qq'},\mu) + \frac{5}{27}I(-\Delta^*_{bcqq'},\Delta^*_{ccqq'},m_{qq'},\mu)$$

$$- \frac{4}{27}I(\Delta_{bcqq'},\Delta_{ccqq'},m_{qq'},\mu) - \frac{20}{27}I(\Delta_{bcqq'},\Delta^*_{ccqq'},m_{qq'},\mu)\Big)$$

$$+ \frac{g^2}{(4\pi f)^2}\Big(-\frac{8}{27}K(-\Delta^*_{bcqq},\Delta_{ccqq},m_{qq},m_{qq},\mu) + \frac{5}{27}K(-\Delta^*_{bcqq},\Delta^*_{ccqq},m_{qq},m_{qq},\mu)$$

$$- \frac{4}{27}K(\Delta_{bcqq},\Delta_{ccqq},m_{qq},m_{qq},\mu) - \frac{20}{27}K(\Delta_{bcqq},\Delta^*_{ccqq},m_{qq},m_{qq},\mu)\Big)\,,$$

$$\delta_{5PQ}(q) = \sum_{q'=j,l,r} \frac{g^2}{(4\pi f)^2}\left(-\frac{4}{9}I(-\Delta^*_{bcqq'},-\Delta^*_{ccqq'},m_{qq'},\mu) - \frac{5}{9}I(\Delta_{bcqq'},\Delta_{ccqq'},m_{qq'},\mu)\right)$$

$$+ \frac{g^2}{(4\pi f)^2}\left(-\frac{4}{9}K(-\Delta^*_{bcqq},-\Delta^*_{ccqq},m_{qq},m_{qq},\mu) - \frac{5}{9}k(\Delta_{bcqq},\Delta_{ccqq},m_{qq},m_{qq},\mu)\right)\,,$$

$$\delta_{6PQ}(q) = \sum_{q'=j,l,r} \frac{g^2}{(4\pi f)^2}\Big(-\frac{8}{27}I(-\Delta^*_{bcqq'},-\Delta^*_{ccqq'},m_{qq'},\mu) - \frac{4}{27}I(-\Delta^*_{bcqq'},\Delta_{ccqq'},m_{qq'},\mu)$$

$$- \frac{4}{27}I(\Delta_{bcqq'},-\Delta^*_{ccqq'},m_{qq'},\mu) - \frac{11}{27}I(\Delta_{bcqq'},\Delta_{ccqq'},m_{qq'},\mu)\Big)$$

$$+ \frac{g^2}{(4\pi f)^2}\Big(-\frac{8}{27}K(-\Delta^*_{bcqq},-\Delta^*_{ccqq},m_{qq},m_{qq},\mu) - \frac{4}{27}K(-\Delta^*_{bcqq},\Delta_{ccqq},m_{qq},m_{qq},\mu)$$

$$- \frac{4}{27}K(\Delta_{bcqq},-\Delta^*_{ccqq},m_{qq},m_{qq},\mu) - \frac{11}{27}K(\Delta_{bcqq},\Delta_{ccqq},m_{qq},m_{qq},\mu)\Big)\,, \qquad (A.4)$$

74

where the function $K(\Delta_1, \Delta_2, m, m, \mu)$ which arises from the hairpins is given by

$$K(\Delta_1, \Delta_2, m_a, m_b, \mu) = \mathcal{P}_{ab}\left(I(\Delta_1, \Delta_2, m_a, \mu), I(\Delta_1, \Delta_2, m_b, \mu), I(\Delta_1, \Delta_2, m_X, \mu)\right) .$$

Appendix B

Current Renormalization in Finite Volume

B.1   Introduction

Since Wilson's pioneering work [21], there has been considerable activity to solve field theories non-perturbatively by numerical simulation on Euclidean spacetime lattices. Today lattice gauge theory is a mature field, and current state-of-the-art lattice QCD calculations are beginning to confront the challenges provided by the hadron spectrum. For an overview of lattice methods, see [80]. One aspect to these numerical simulations is the finite-size scaling of observables. The finite spacetime volume employed on the lattice is a source of systematic error in the numerical determination of observables. Thus the study of field theories in finite volume, while a theoretical curiosity, is also of practical utility.

Recent work [81] suggests that electromagnetically gauge invariant amplitudes at finite volume may differ from their infinite volume form. Specifically investigated was the finite-size scaling of nucleon electromagnetic and spin polarizabilities that arise in nucleon Compton scattering (see, e.g., [82, 83]). A goal in [81] was to address systematic errors in the extraction of polarizabilities from classical background field methods employed in lattice simulations [84, 85, 86, 87, 88, 89, 90, 91, 92, 77, 93]. An

analysis of the finite volume behavior of nucleon polarizabilities was presented, as was an oddity relating to the zero-frequency scattering amplitude. In infinite volume, the zero-frequency Compton amplitude is fixed by gauge invariance to be proportional to the total charge squared. Finite volume modifications, however, were found for nucleon Compton scattering at zero frequencies [81]. These results suggest a finite volume renormalization of the basic interaction between the photon and the hadron's charge. In this work, we show that gauge invariance in finite volume allows for such modifications to zero-frequency photon couplings. In essence, conserved currents are not protected from additive renormalization as they are in infinite volume. For definiteness, we focus on the chiral dynamics of pions coupled to photons [94], but could just as well choose any interacting field theory coupled to gauge fields.[1]

Our presentation is organized as follows. First in Sec. B.2, we analyze the electromagnetic interactions of pions in finite volume. We demonstrate the infrared running of electromagnetic current matrix elements by explicit one-loop calculations in chiral perturbation theory (χPT). In Sec. B.3, consequences of gauge invariance on a torus are detailed. Gauge invariant zero-mode interactions allow for infrared renormalization of electromagnetic couplings. We write down gauge invariant, zero-frequency effective field theories for pions that reproduce our one-loop finite volume χPT re-

---

[1]An instructive alternate example is the QED electron. Straightforward evaluation shows that the electron vertex function at zero frequency is modified by volume effects. This modification, however, is infrared divergent and we have chosen to avoid such difficulties by using a theory that is infrared finite.

sults. Understanding such volume effects is necessary in practice for the extraction of infinite volume physics from lattice QCD simulations. We show how our results are consistent with Ward identities and low-energy theorems in Sec. B.4. A conclusion in Sec. B.5 summarizes our findings, while a glossary of finite volume functions is provided in AppendixB.6.

B.2 Pions in Finite Volume

The chiral Lagrangian is written in terms of a coset field $\Sigma = \exp(2i\Phi/f)$ which parametrizes the Goldstone manifold arising from spontaneous chiral symmetry breaking: $SU(2)_L \otimes SU(2)_R \to SU(2)_V$. The pions are contained in the matrix Φ, explicitly as

$$\Phi = \begin{pmatrix} \frac{1}{\sqrt{2}}\pi^0 & \pi^+ \\ \pi^- & -\frac{1}{\sqrt{2}}\pi^0 \end{pmatrix}. \tag{B.1}$$

In our conventions, the dimensionful parameter $f = 132$ MeV. The chiral Lagrangian provides an effective theory of low-energy QCD. At leading-order in an expansion in momentum, p^2, and quark mass, m_q, there are two terms in this Lagrangian

$$\mathcal{L} = \frac{f^2}{8}\operatorname{tr}\left(D_\mu\Sigma D^\mu\Sigma^\dagger\right) + \frac{f^2}{4}\lambda\operatorname{tr}\left(\Sigma m_q + \Sigma^\dagger m_q\right), \tag{B.2}$$

where m_q is the quark mass matrix, $m_q = \operatorname{diag}(m_u, m_d)$. We shall work exclusively in the isospin limit, $m_u = m_d \equiv m$. The kinetic term of the chiral Lagrangian includes a $U(1)$ gauge covariant derivative that couples pions to photons, $D_\mu\Sigma = \partial_\mu\Sigma + ieA_\mu[Q,\Sigma]$, where the quark electric charge matrix, Q, is given by

$Q = \text{diag}(2/3, -1/3)$.

Expanding the Lagrangian in Eq. (C.4) to tree level, one sees that the pions are correctly normalized and their mass, m_π, is given by $m_\pi^2 = 2\lambda m$. The couplings of pions to zero-momentum photons at tree level can be read off from Eq. (C.4), from which we find their canonical charges. We now investigate whether loop corrections in a finite spatial volume modify these couplings.

B.2.1   Charged pion current

To consider the one-loop corrections to the electromagnetic current of charged pions, we accordingly expand the χPT Lagrangian in Eq. (C.4) to second order to generate vertices for one-loop graphs. Furthermore local terms at higher-order can then contribute at tree-level, but these are absent for zero-frequency photons. Thus we need to determine only the diagrams depicted in Fig. B.1.

In the limit of zero frequency and infinite volume, the current matrix element between charged pion states is required by gauge and Lorentz invariance to be

$$\langle \pi^\pm(P)|J_\mu|\pi^\pm(P)\rangle = \pm 2eP_\mu, \tag{B.3}$$

where the overall sign reflects the charge of the pion. It is a straightforward exercise to verify the above form at one-loop order in infinite volume. At an intermediate step, we reach the result

$$\langle \pi^\pm(P)|J_\mu|\pi^\pm(P)\rangle = \pm 2e\left\{P_\mu - \frac{2i}{f^2}\int \frac{d^4q}{(2\pi)^4}\frac{(q^2 - m_\pi^2)P_\mu - 2(q\cdot P)q_\mu}{[q^2 - m_\pi^2]^2}\right\}, \tag{B.4}$$
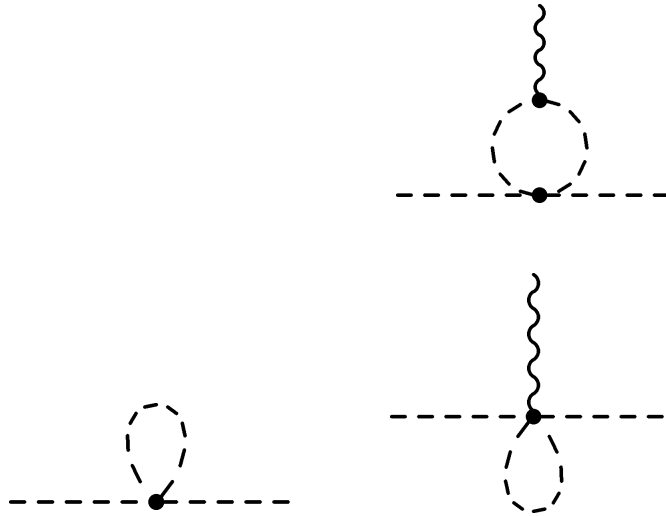
Figure B.1: One-loop graphs required to evaluate the pion electromagnetic current. On the left appears the wavefunction correction; while, on the right, diagrams contributing to the pion form factor. Vertices shown are generated from the leading-order χPT Lagrangian, Eq. (C.4).

from which we see the wavefunction correction to the tree-level vertex is exactly canceled by the loop contributions to the form factor at zero frequency [95]. In this way, the matter fields do not contribute to the running of the coupling and Eq. (B.3) is preserved.

In finite volume, we repeat the calculation of the pion current to one-loop order. We consider each of the three spatial directions of finite length L, and the quark fields subjected to boundary conditions that maintain discrete translational invariance. For definiteness, we assume periodic boundary conditions.[2] As the pions are point-like objects in the effective theory, they satisfy the same boundary conditions as the point-like interpolating field $\Phi(x) \sim \bar{q}(x)\gamma_5 q(x)$. Pions are hence also periodic with quantized spatial momentum modes of the form

$$q = \frac{2\pi}{L}n, \qquad (B.5)$$

where n is a triplet of integers. To keep matters simple, we keep the temporal extent infinite as is commonly done to determine finite-size effects for lattice QCD observables.[3] To evaluate the pion current, we use the finite volume theory defined by Eq. (C.4). The loop diagrams shown in Fig. B.1 are again generated. The only

[2]Similar results for anti-periodic boundary conditions, for example, can be derived easily using a modified momentum quantization condition for the quark fields. As pions remain periodic, the expressions we derive also hold for anti-periodic quarks.

[3]We implicitly choose $m_\pi L \gtrsim 1$ so that pion zero modes do not become strongly coupled [96, 97]. With this assumption, the ordinary χPT power counting in infinite volume can be carried over to finite volume [98].

difference compared to infinite volume is that the spatial momenta of real and virtual states are quantized. The finite and infinite volume theories share exactly the same ultraviolet divergences, so we can calculate the finite volume effect by matching the two theories in the infrared. For an observable X calculated in both finite, $X(L)$, and infinite, $X(\infty)$, volumes, we have

$$X(L) = X(\infty) + \Delta X(L), \tag{B.6}$$

where the matching term, $\Delta X(L)$, is free from ultraviolet divergences and gives the finite volume effect.

Returning to Eq. (B.4), we can carry out the finite volume matching, Eq. (B.6), for the pion current. We find

$$\langle \pi^\pm(P)|J_\mu|\pi^\pm(P)\rangle = \pm 2eP_\mu \left\{ 1 - \frac{\delta_{\mu j}}{3f^2} \left[2\, I_{1/2}(m_\pi^2, L) + m_\pi^2 I_{3/2}(m_\pi^2, L) \right] \right\}, \tag{B.7}$$

where $I_\beta(m^2, L)$ is defined in Appendixap:current. Results are consistent with charge conjugation invariance and the current is only modified in the spatially finite directions. Specifically the virtual pion cloud in finite volume screens the current of the infinite volume pion. In Fig. B.2, we plot the finite volume modification to the pion current. Here the relative difference in the current matrix element at finite volume versus infinite volume, ΔJ_{π^+}, given by

$$\Delta J_{\pi^+} = \frac{\langle \pi^+(P)|\hat{e} \cdot \boldsymbol{J}|\pi^+(P)\rangle_L - \langle \pi^+(P)|\hat{e} \cdot \boldsymbol{J}|\pi^+(P)\rangle_\infty}{\langle \pi^+(P)|\hat{e} \cdot \boldsymbol{J}|\pi^+(P)\rangle_\infty}, \tag{B.8}$$

is plotted as a function of the length L of the spatial dimension.
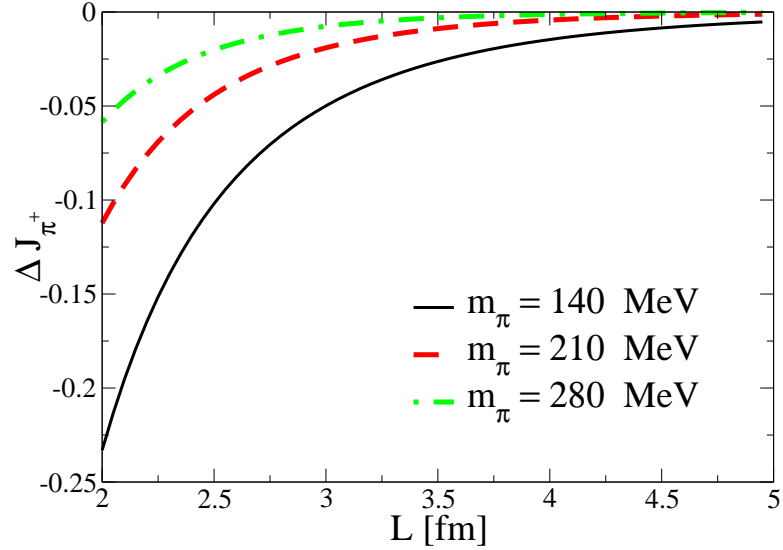
Figure B.2: Finite volume screening of the pion current. The relative difference in pion current $\Delta J_{\pi+}$ is plotted as a function of the box size L, for a few values of the pion mass.

We have used a unit vector $\hat{\boldsymbol{e}}$ to project onto the spatial part of the current. Accordingly the pion cannot be at rest, $\boldsymbol{P} \neq \boldsymbol{0}$. Subscripts on matrix elements denote the box size, with infinity corresponding to infinite volume. The finite volume effect is exponentially suppressed in asymptotic ($m_\pi L \gg 1$) volumes. Consequently taking the infrared cutoff, $1/L$, to zero, the additive current renormalization vanishes and infinite volume limit is maintained.

B.2.2 Neutral pion current matrix elements

Charge conjugation invariance demands the identical vanishing of single current matrix elements between neutral pion states. Indeed whether the calculation of the

neutral pion current is carried out in infinite or finite volume, we find zero for the matrix element. The $SU(2)$ flavor structure of the form factor diagrams shown in Fig. B.1 ensures this vanishing and consistency with charge conjugation.

Neutral pion matrix elements of an even number of electromagnetic currents, however, are not restricted to vanish by charge conjugation invariance. Indeed, it is well known that the neutral pion has electric and magnetic polarizabilities that can be predicted at one-loop order in χPT solely in terms of f and m_π [75]. Such polarizabilities arise at second order in the low-frequency expansion of the matrix element of two currents (the so-called Compton scattering tensor). The Compton tensor also has a term at zeroth order in the photon frequencies

$$T_{\mu\nu}(\omega = \omega' = 0) = 2(Qe)^2 g_{\mu\nu}, \tag{B.9}$$

which is sensitive only to the longest ranged electromagnetic interaction. This term in the Compton tensor, when combined with relevant phase space factors, yields the classical Thomson scattering cross section, $\sigma = 8\pi(Qe)^4/3m_\pi^2$. For the neutral pion, the total charge is zero and the longest ranged interaction vanishes.

Using the χPT Lagrangian defined in Eq. (C.4), we can determine the Compton amplitude for pions. We restrict our attention to the zero-frequency amplitude. Due to charge neutrality, there are no tree-level couplings to the neutral pion. At one-loop order, evaluation of the diagrams shown in Fig. B.3 is required to determine the Compton amplitude. At an intermediate step in the calculation, contributions from
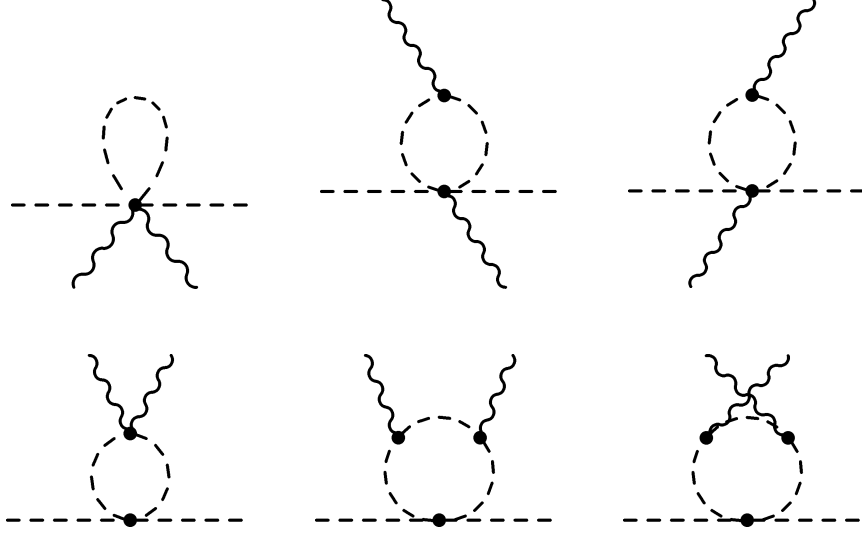
Figure B.3: One-loop contributions to neutral pion Compton scattering in χPT. Vertices shown are generated from the leading-order Lagrangian.

all six diagrams can be simplified to

$$T_{\mu\nu}(\omega = \omega' = 0) = \frac{4ie^2 m_\pi^2}{f^2} \int \frac{d^4 q}{(2\pi)^4} \frac{(q^2 - m_\pi^2)g_{\mu\nu} - 4q_\mu q_\nu}{[q^2 - m_\pi^2]^3}, \qquad (B.10)$$

which vanishes. Hence in infinite volume, a delicate cancellation between all diagrams maintains the vanishing of the Compton amplitude at zero frequency [99, **?**]. On the other hand, the same is not true in finite volume. Carrying out the one-loop matching between finite and infinite volume theories, Eq. (B.6), for the Compton amplitude in Eq. (B.10), we find

$$T_{\mu\nu}(\omega = \omega' = 0) = e^2(\delta_{\mu 0}\delta_{\nu 0} - g_{\mu\nu})\frac{m_\pi^4}{f^2} I_{5/2}(m_\pi^2, L). \qquad (B.11)$$

Thus when one considers the purely spatial components of the Compton tensor, the neutral pion has an effective charge-squared, *cf.* Eq. (B.9). In transverse gauge,
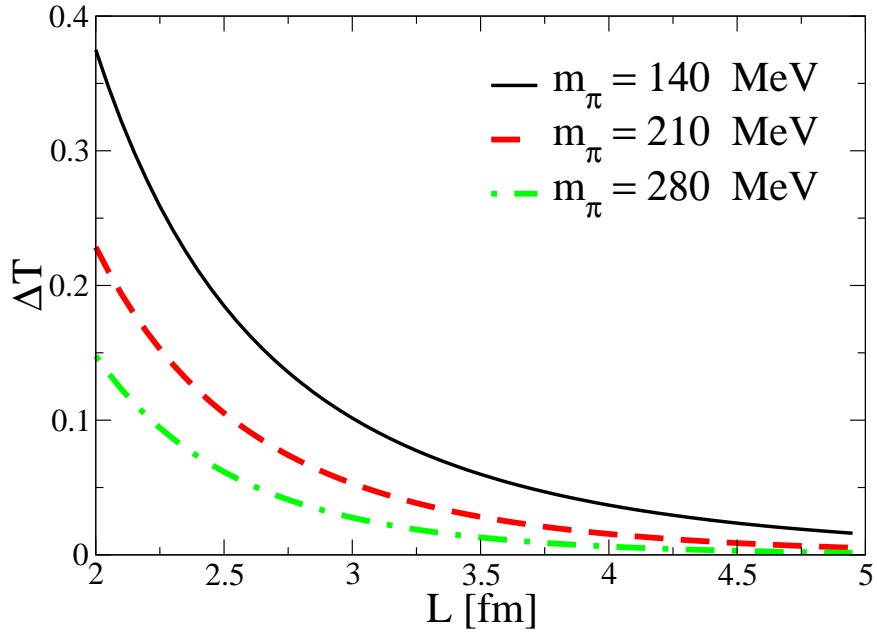
Figure B.4: Zero frequency Compton amplitude for the neutral pion. The finite volume amplitude ΔT is plotted as a function of the box size L, for a few values of the pion mass. In infinite volume, this amplitude is identically zero.

the above expression gives the amplitude to scatter zero-frequency photons off the neutral pion. There is a non-vanishing contribution to this scattering amplitude when the pion is confined to a periodic box with size on the order of the pion Compton wavelength. When the box size becomes large compared to this scale, the amplitude is exponentially suppressed and infinite volume results are recovered. We demonstrate this in Fig. B.4, where we plot the finite volume amplitude ΔT defined by

$$\Delta T = -\frac{1}{3e^2}g^{\mu\nu}T_{\mu\nu}(\omega = \omega' = 0). \tag{B.12}$$

B.3 Gauge invariance on a torus

To explain our above results, we investigate electromagnetism in finite volume. The analogous finite temperature case is well known and described, e.g., in [100]. Because our applications are with classical background fields, or equivalently current operator insertion methods in lattice field theory, there are no quantum corrections to the photon field itself.[4]

B.3.1 Spatial Torus

Let us consider a classical electromagnetic field defined on a finite spatial torus with infinite time extent. On the gauge field $A_\mu(\boldsymbol{x}, t)$, we impose periodic boundary con-

---

[4]Dynamical photons in QED cause additional complications as the vector current is renormalized in infinite volume [101]. With classical background fields, penguin graphs are absent and such renormalization does not occur.

ditions and expand $A_\mu(\boldsymbol{x}, t)$ in Fourier modes

$$A_\mu(\boldsymbol{x}, t) = \sum_{\boldsymbol{n}} \tilde{A}_\mu(\boldsymbol{n}, t) \, e^{2\pi i \boldsymbol{n} \cdot \boldsymbol{x}/L}, \tag{B.13}$$

where $\boldsymbol{n} = (n_x, n_y, n_z) \in \mathbb{Z}^3$. It is convenient to separate out the zero-mode contribution, so we write

$$A_\mu(\boldsymbol{x}, t) = \mathcal{A}_\mu(t) + \overline{A}_\mu(\boldsymbol{x}, t), \tag{B.14}$$

where the zero mode $\mathcal{A}_\mu(t) \equiv \tilde{A}_\mu(\boldsymbol{0}, t)$.

Under a gauge transformation, the photon field transforms in the familiar way, $A_\mu(\boldsymbol{x}, t) \longrightarrow A_\mu(\boldsymbol{x}, t) + \partial_\mu \alpha(\boldsymbol{x}, t)$, and observables are invariant. Requiring the gauge transformed field to be single valued mandates that $\partial_\mu \alpha(\boldsymbol{x}, t)$ is periodic. Thus we can decompose the gauge function $\alpha(\boldsymbol{x}, t)$ into the sum of two terms, $\alpha(\boldsymbol{x}, t) = \alpha_0(\boldsymbol{x}, t) + \overline{\alpha}(\boldsymbol{x}, t)$, where

$$\alpha_0(\boldsymbol{x}, t) = \alpha_0(t) + \boldsymbol{\alpha} \cdot \boldsymbol{x}, \tag{B.15}$$

and

$$\overline{\alpha}(\boldsymbol{x}, t) = \sum_{\boldsymbol{m} \neq \boldsymbol{0}} \tilde{\overline{\alpha}}(\boldsymbol{m}, t) \, e^{2\pi i \boldsymbol{m} \cdot \boldsymbol{x}/L}. \tag{B.16}$$

Here we have dropped all overall irrelevant constants, and the vector $\boldsymbol{\alpha}$ is a constant vector. Using this decomposition for the gauge function, the gauge field transforms as

$$\begin{cases} \mathcal{A}_\mu(t) & \longrightarrow \mathcal{A}_\mu(t) + \partial_\mu \alpha_0(\boldsymbol{x}, t) \\[2mm] \overline{A}_\mu(\boldsymbol{x}, t) & \longrightarrow \overline{A}_\mu(\boldsymbol{x}, t) + \partial_\mu \overline{\alpha}(\boldsymbol{x}, t) \end{cases}. \tag{B.17}$$

In particular, the photon zero-mode transforms as

$$
\mathcal{A}_\mu(t) \longrightarrow \mathcal{A}_\mu(t) + \begin{cases} \partial_0 \alpha_0(t), & \mu = 0 \\ \\ \alpha_i, & \mu = i \end{cases}. \tag{B.18}
$$

The time-component of the zero mode is absent from the field strength tensor. The remaining three components of the zero mode field are translated by a constant under the gauge transformation. In the gauge invariant free theory, each spatial component of the zero mode is thus a massless one-dimensional scalar.

B.3.2   Coupling to Matter

For a generic matter field $\varphi(\boldsymbol{x}, t)$ of unit charge, the effects of a gauge transformation show up as a local phase factor

$$
\varphi(\boldsymbol{x}, t) \longrightarrow \varphi'(\boldsymbol{x}, t) = e^{-i\alpha(\boldsymbol{x},t)} \varphi(\boldsymbol{x}, t). \tag{B.19}
$$

Now we assume that the matter field $\varphi(\boldsymbol{x}, t)$ is subject to periodic boundary conditions. We again split the gauge function into zero mode and non-zero mode pieces, $\alpha(\boldsymbol{x}, t) = \alpha_0(\boldsymbol{x}, t) + \overline{\alpha}(\boldsymbol{x}, t)$. With the form given in Eq. (B.16), we see that the non-zero modes will maintain the periodicity of the matter field under the transformation in Eq. (B.19). The same is not in general true of the zero modes given the form of $\alpha_0(\boldsymbol{x}, t)$ in Eq. (B.15). If the gauge transformed matter field is to remain periodic under translations by L, then we must have the quantization condition

$$
\boldsymbol{\alpha} = \frac{2\pi}{L} \boldsymbol{n}, \tag{B.20}
$$

on the spatial zero mode part of the gauge function. This quantization condition reduces the continuous translational invariance of the spatial zero modes to discrete translations. As gauge transformations are now less general compared to infinite volume, more gauge invariant operators can be built.

Imagine that we start with some microscopic theory with electromagnetic interactions. Take the scalar field $\varphi(\boldsymbol{x}, t)$ as some composite low-energy degree of freedom of this theory. Further we assume that the energies of interest are ultra-low in the sense that any interactions of $\varphi(\boldsymbol{x}, t)$ with itself or other fields have been integrated out. In the absence of electromagnetism, e.g., we have a simple single particle effective theory[5]

$$\mathcal{L} = |\partial_\mu \varphi|^2 - m(L)^2 |\varphi|^2, \tag{B.21}$$

where $m(L)$ is a running mass that depends on the infrared cutoff $1/L$ (and parametrically depends on the other couplings, masses, etc. that have been integrated out of the theory). Running the cutoff to zero completes the infrared sector of the theory and produces infinite volume physics.

Now we include electromagnetism in this single particle effective theory by adding all possible gauge invariant operators. The minimal coupling prescription, $\partial_\mu \rightarrow D_\mu = \partial_\mu + iA_\mu$, renders the kinetic term of Eq. (B.21) gauge invariant. Because we imagine φ is a composite particle, there can be non-minimal couplings that respect

---

[5]We have written only $SO(4)$ symmetric terms in Eq. (B.21). Strictly speaking volume corrections will reduce the dispersion relation down to only cubic symmetry. For pions in finite volume the first $SO(4)$ breaking effects occur at two-loop order in the chiral expansion.

gauge invariance, e.g., the $\boldsymbol{E}^2$ and $\boldsymbol{B}^2$ terms for the particle's polarizabilities. Further terms in this ultra low-energy theory are allowed, however, because $SO(4)$ is not respected, and the gauge invariance of the zero mode has a special nature. As we will show, these further terms are responsible for current renormalization. To simplify the discussion, we will restrict ourselves to the effective theory operators for zero frequency photons.

Using gauge symmetry, we can write down the general form of the ultra low-energy effective theory for a single φ field coupled to zero frequency photons. We choose to construct this theory using Wilson lines. By cycling once over the i-th compact dimension, we can form gauge invariant Wilson lines $\mathcal{W}_i$ of the form,

$$\mathcal{W}_i = \exp\left(i \oint dx_i \, A_i\right). \tag{B.22}$$

Notice that there is no sum over repeated indices in this definition. Due to the periodicity of the gauge field in the i-th direction, the loop integral

$$\int_0^L dx_i \, A_i(\boldsymbol{x}, t) = L\mathcal{A}_i(t) + L \sum_{n_{j \neq i},\, n_i = 0} \tilde{A}_i(\boldsymbol{n}, t)e^{2\pi i \boldsymbol{n} \cdot \boldsymbol{x}/L}, \tag{B.23}$$

produces just the $n_i = 0$ modes of the gauge field. Indeed the gauge transformation of the zero and non-zero modes, Eq. (B.17), demonstrates that the Wilson line $\mathcal{W}_i$ is gauge invariant. For our purpose, we wish to isolate completely the gauge field zero-mode and accordingly form modified Wilson lines W_i given by

$$W_i = \mathcal{P}_{\boldsymbol{0}} \mathcal{W}_i \mathcal{P}_{\boldsymbol{0}}^{\dagger}, \tag{B.24}$$

where $\mathcal{P}_{\boldsymbol{0}}$ is an operator that projects onto the zero-mode of the gauge field. A

practical way to implement the action of $\mathcal{P}_0$ is to change the loop integration

$$\oint dx_i \longrightarrow \frac{1}{L^2} \oint \prod_{j=1}^{3} dx_j \equiv \frac{1}{L^2} \oint d\boldsymbol{x} \tag{B.25}$$

so that

$$W_i = \exp\left(i \oint d\boldsymbol{x} \, A_i/L^2 \right). \tag{B.26}$$

Furthermore it is useful to define Hermitian combinations of modified Wilson lines that transform simply under parity and charge conjugation,

$$W_i^{(+)} = \frac{1}{2}\left(W_i + W_i^\dagger \right) \tag{B.27}$$

$$W_i^{(-)} = \frac{1}{2i}\left(W_i - W_i^\dagger \right). \tag{B.28}$$

Notice that because $W_i^{(+)} = \sqrt{1 - [W_i^{(-)}]^2}$, any operator involving $W_i^{(+)}$ can be traded in for a tower of operators involving $W_i^{(-)}$. Hence we can build our theory solely in terms of $W_i^{(-)}$ operators.

In addition to gauge, C, P, and T invariance, the theory on a torus has S_4 cubic invariance. Writing down operators consistent with these symmetries, we arrive at the following ultra low-energy effective Lagrangian for a single φ field

$$
\begin{aligned}
\mathcal{L} &= |D_\mu \varphi|^2 - m(L)^2 |\varphi|^2 + \mathcal{Q}_1(L)\boldsymbol{W}^{(-)} \cdot \boldsymbol{J} + \mathcal{Q}_2(L)\left(\boldsymbol{W}^{(-)} \cdot \boldsymbol{W}^{(-)}\right)|\varphi|^2 \\
&+ \mathcal{Q}_3(L)\left(\boldsymbol{W}^{(-)} \cdot \boldsymbol{D}\varphi^*\right)\left(\boldsymbol{W}^{(-)} \cdot \boldsymbol{D}\varphi\right) + \mathcal{Q}_4(L)\sum_i W_i^{(-)}W_i^{(-)}D_i\varphi^* D_i\varphi \\
&+ \mathcal{Q}_5(L)\left(\boldsymbol{W}^{(-)} \cdot \boldsymbol{W}^{(-)}\right)\left(\boldsymbol{W}^{(-)} \cdot \boldsymbol{J}\right) + \mathcal{Q}_6(L)\sum_i W_i^{(-)}W_i^{(-)}W_i^{(-)}J_i + \dots \tag{B.29}
\end{aligned}
$$

Above we have employed the current operator $\boldsymbol{J}$, given by $\boldsymbol{J} = i\left[(\boldsymbol{D}\varphi^*)\varphi - \varphi^*(\boldsymbol{D}\varphi)\right]$. A number of things about Eq. (B.29) must be clarified. The ... denotes that we have

not finished writing the general Lagrangian allowed by symmetries. The most general Lagrangian contains a tower of terms with n insertions of $W_i^{(-)}$ operators. Writing down all such terms consistent with S_4 for a given n is arbitrarily complicated. Fortunately the series expansion of $W_i^{(-)}$ in terms of the gauge field starts out at a single zero-frequency photon. Thus operators with n insertions of $W_i^{(-)}$ contribute to processes with at least n zero-frequency photons. In Eq. (B.29), we have written down all operators with at most three insertions of $W_i^{(-)}$. Thus the Lagrangian generates all possible couplings to *at most* three zero-frequency photons. We have also restricted the dynamics to ultra-low energies, so have only kept terms with at most two derivatives, D, acting on φ. Finally while a term of the form, $\left(\boldsymbol{W}^{(-)} \cdot \boldsymbol{W}^{(-)} \right) |D_\mu \varphi|^2$, is allowed by symmetries, it has been removed by a field redefinition.

The coefficients $\mathcal{Q}_j(L)$ in Eq. (B.29) must be determined from matching, and thus in general require the calculation of loop graphs with an arbitrary number of photons in the microscopic theory. It is possible that certain additional symmetries of the underlying theory constrain some coefficients to vanish. Because this is the zero-frequency sector of an effective theory for a stable particle, no multi-particle production thresholds can be attained in loop graphs that determine the matching coefficients. Thus in asymptotically large volumes, the new coupling constants $\mathcal{Q}_j(L)$ will be exponentially small [102, 103, 104]. Consequently $SO(4)$ will be restored in large volumes.

B.3.3 Zero frequency effective theories

Using the general analysis from above, it is straightforward to construct single particle effective theories that reproduce the zero-frequency results derived in Sec. B.2. There is one difference, however. The underlying theory, QCD, has quark fields with fractional charges. Maintaining periodicity of both quark fields under zero-mode gauge transformations requires a slightly modified quantization condition, namely

$$\boldsymbol{\alpha} = \frac{6\pi}{eL}\boldsymbol{n}. \tag{B.30}$$

This modification reflects that both quark charges are quantized in units of $e/3$. The Wilson lines $\mathcal{W}_i$ are now given by

$$\mathcal{W}_i = \exp\left(\frac{ie}{3}\oint dx_i\, A_i\right), \tag{B.31}$$

and similarly for the W_i. Thus for charged and neutral pions,[6] we require the effective Lagrangian

$$
\begin{aligned}
\mathcal{L} &= \frac{1}{2}\mathrm{tr}(D_\mu\Phi D^\mu\Phi) - \frac{1}{2}m_\pi(L)^2\mathrm{tr}(\Phi^2) + i\mathcal{Q}(L)\,\boldsymbol{W}^{(-)}\cdot\mathrm{tr}\left[Q(\boldsymbol{D}\Phi)\Phi - Q\Phi(\boldsymbol{D}\Phi)\right] \\
&\quad + \overline{\mathcal{Q}}(L)^2\,\boldsymbol{W}^{(-)}\cdot\boldsymbol{W}^{(-)}\,\mathrm{tr}\left[(Q\Phi)^2 + \frac{4}{5}Q^2\Phi^2\right] - \tilde{\mathcal{Q}}(L)^2\,\boldsymbol{W}^{(-)}\cdot\boldsymbol{W}^{(-)}\,\mathrm{tr}\left[(Q\Phi)^2 - Q^2\Phi^2\right],
\end{aligned}
\tag{B.32}
$$

---

[6]Because electromagnetism explicitly breaks isospin symmetry, we should formulate the low-energy theories for charged and neutral pions separately. Although we utilize traces over $SU(2)$ pion fields $\Phi(\boldsymbol{x}, t)$, there are no interactions between pions in Eq. (B.32).

where $m_\pi(L)$ includes the infrared running of the pion mass (not calculated here), and the new coupling constants $\mathcal{Q}(L)$, $\overline{\mathcal{Q}}(L)$, and $\tilde{\mathcal{Q}}(L)$ are given by

$$\mathcal{Q}(L) = -\frac{1}{f^2 L} \left[2I_{1/2}(m_\pi^2, L) + m_\pi^2 I_{3/2}(m_\pi^2, L) \right] \tag{B.33}$$

$$\overline{\mathcal{Q}}(L)^2 = \frac{9}{2f^2 L^2} m_\pi^4 I_{5/2}(m_\pi^2, L) \tag{B.34}$$

$$\tilde{\mathcal{Q}}(L) = 0. \tag{B.35}$$

For the charged pions, we have also calculated all two-photon graphs to one-loop order using Eq. (C.4) (this includes the one-pion irreducible contributions shown in Fig. B.3, and additionally the set of one-pion reducible diagrams which are not depicted) and do not find the need for an extra two-photon coupling to charged pions in Eq. (B.32). For this reason, the coupling constant $\tilde{\mathcal{Q}}(L)$ vanishes. The term with coefficient $\overline{\mathcal{Q}}(L)$ only couples zero-frequency photons to neutral pions.

The single particle effective theory described by Eq. (B.32) correctly reproduces the infrared running of one- and two-photon processes for both charged and neutral pions at zero frequency. This theory is gauge invariant in finite volume because of the allowance for new operators which are Wilson lines that cycle the compact dimensions. These operators, moreover, lead to violation of $SO(4)$ invariance. Consider a charged pion at rest, $\boldsymbol{P} = \boldsymbol{0}$. The current in Eq. (B.3) is

$$\langle \pi^\pm(\boldsymbol{0})|J_\mu|\pi^\pm(\boldsymbol{0})\rangle = 2m_\pi \left(\pm e \right) g_{\mu 0}, \tag{B.36}$$

where $2m_\pi$ is a relativistic normalization factor. Boosting to a frame where $\boldsymbol{P} \neq \boldsymbol{0}$,

generates a current

$$\langle\pi^{\pm}(\boldsymbol{P})|\boldsymbol{J}|\pi^{\pm}(\boldsymbol{P})\rangle = 2\sqrt{\boldsymbol{P}^2 + m_{\pi}^2}\,(\pm e)[1 - \mathcal{Q}(L)]\,\boldsymbol{V}, \tag{B.37}$$

where $\boldsymbol{V} = \boldsymbol{P}/\sqrt{\boldsymbol{P}^2 + m_{\pi}^2}$ is the relativistic velocity. Because of $SO(4)$ breaking, the current in this frame is not simply the charge times the velocity, $\boldsymbol{J} \neq (\pm e)\boldsymbol{V}$. Instead, the current is screened by finite volume effects, $\boldsymbol{J} = (\pm e)[1 - \mathcal{Q}(L)]\boldsymbol{V}$.

B.4 Field Theory Identities

Above we have derived finite volume modifications to the current of the charged pions and the zero-frequency scattering tensor for the neutral pions. While we have accounted for these findings using gauge invariant single particle effective theories, here we show that our results are completely consistent with field theoretic identities valid in finite volume.

B.4.1 Electromagnetic Vertex

The zero-frequency part of the electromagnetic vertex is constrained by gauge invariance via the Ward identity [105]. Let $\Gamma^{\mu}(P, P)$ denote the zero-frequency electromagnetic vertex function of the charged pions. The Ward identity requires

$$-i\Gamma^{\mu}(P, P) = Qe\,\frac{\partial}{\partial P_{\mu}}G(P)^{-1}, \tag{B.38}$$

where $G(P)$ is the pion propagator. In finite volume, we found that the wave function correction did not exactly cancel the forward part of the vertex function. This lead

to the new coupling $\mathcal{Q}(L)$ in Eq. (B.33). Thus at finite volume, the differential form of the Ward identity shown in Eq. (B.38) is violated. Quite simply, however, the steps used to derive Eq. (B.38) are not valid in a fixed finite volume.

On the other hand, starting from the Ward-Takahashi identity [106, 107] we have

$$-ik_\mu \Gamma^\mu(P+k, P) = Qe \left[G(P+k)^{-1} - G(P)^{-1} \right]. \tag{B.39}$$

This identity is valid in finite volume. We can demonstrate this explicitly using the charged pion vertex function, $\Gamma^\mu(P+k, P) = \langle \pi^\pm(P+k)|J^\mu|\pi^\pm(P)\rangle$. To one-loop order, we evaluate the diagrams in Fig. B.1 and contract with the momentum transfer, k_μ. We find

$$-ik_\mu \langle \pi^\pm(P+k)|J^\mu|\pi^\pm(P)\rangle$$
$$= \mp ie \left\{ (2P+k)\cdot k - \frac{2i}{f^2} \sum_q \left[\frac{(2P+k)\cdot k}{q^2 - m_\pi^2} - \frac{(2P+k)\cdot q\,(2q+k)\cdot k}{[q^2 - m_\pi^2][(q+k)^2 - m_\pi^2]} \right] \right\} \tag{B.40}$$

where we have abbreviated

$$\sum_q \equiv \frac{1}{L^3} \sum_{q=2\pi n/L} \int \frac{dq^0}{2\pi}, \tag{B.41}$$

and implicitly regulate ultraviolet divergences using dimensional regularization. We then write

$$(2q+k)\cdot k = (q+k)^2 - m_\pi^2 - [q^2 - m_\pi^2],$$

in order to reduce factors in the numerator of the last term. To arrive at the Ward-Takahashi identity from Eq. (B.40), we must show that the terms in the $\sum$ vanish. This follows immediately by using discrete translational invariance to re-index the

sum. If $\boldsymbol{k} \neq 2\pi\boldsymbol{m}/L$, then the summation over spatial momentum modes cannot be re-indexed in this manner. Consequently the validity of the Ward-Takahashi identity, Eq. (B.39), in finite volume hinges on quantized photon momentum.

Having established that the Ward-Takahashi identity holds in finite volume, there must be a flaw in the subsequent derivation of the Ward identity. To arrive at the differential form of the identity, Eq. (B.38), from Eq. (B.39) a limiting process $k_\mu \to 0$ is required. At fixed volume, the spatial momentum quantization condition invalidates this procedure. Contrary to Eq. (B.38), there is no condition imposed on $\Gamma^\mu(P, P)$ in a compact space. In finite volume with infinite time extent, only the spatial part of the differential form of the Ward identity does not hold. One can take the limiting procedure with respect to the zeroth component of momentum transfer, $k^0 \to 0$. Consequently the time component of Eq. (B.38) remains valid. Our results are indeed consistent with this fact, *cf.* Eq. (B.7).[7]

B.4.2   Compton Tensor

The classical Thomson cross section arises in the zero-frequency limit of electromagnetic waves scattering off charged particles. According to low-energy theorems [110, 111], any sensible gauge invariant field theory of charged particles will reproduce the Thomson cross section. In terms of the off-shell Compton scattering amplitude for a

---

[7] χPT studies of the volume effects for form factors of pseudoscalar mesons [108, 109] have utilized only the time-component of the current, and considered the extent of the time direction as infinite. In this framework, no modification to meson charges was found, consistent with Eq. (B.38).

scalar particle, the zero-frequency part is required to be of the form

$$T_{\mu\nu}(\omega = \omega' = 0) = 2(Qe)^2 \left(g_{\mu\nu} - \frac{4P_\mu P_\nu}{P^2 - m^2} \right), \tag{B.42}$$

where P_μ is the particle's four momentum. Upon squaring and multiplying with phase space factors, the first term produces the Thomson cross section, while the second term is the Born contribution (which survives when we take the zero frequency limit *before* going on-shell). For the neutral pion, Eq. (B.42) mandates that the Compton tensor vanishes, contrary to our results in finite volume, Eq. (B.11).

The Thomson limit of the Compton tensor can be derived rigorously in field theory from generalized Ward identities, specifically for a scalar particle we have

$$iT_{\mu\nu}(\omega = \omega' = 0) = (Qe)^2 G(P)^{-1} \left[\frac{\partial^2}{\partial P^\mu \partial P^\nu} G(P) \right] G(P)^{-1}, \tag{B.43}$$

which reproduces both the Thomson and Born terms. This generalized Ward identity for the two-photon amplitude is not valid in finite volume; because, as with its counterpart in Eq. (B.38), its derivation relies on a limiting procedure.

Returning to the step in the derivation of Eq. (B.43) before the limiting procedure, we have a version of the Ward-Takahashi identity that is valid in finite volume. Let the initial particle (photon) momentum be denoted by P (k), and the final particle (photon) momentum by P' (k'). Then we have

$$k'^\nu k^\mu G(P') iT_{\mu\nu}(P', k'; k, P) G(P) = (Qe)^2 \Big[G(P+k) - G(P') - G(P) + G(P - k') \Big]. \tag{B.44}$$

Using the analytic expression for the one-loop diagrams in Fig. B.3 for the neutral pion, one can verify explicitly that Eq. (B.44) holds in finite volume provided that the

photon momenta, $\boldsymbol{k}$ and $\boldsymbol{k}'$, are quantized. The validity of Ward-Takahashi identities requires discrete translational invariance.

Now by taking the limit $k' \to k$, followed by $k \to 0$ in Eq. (B.44), we accordingly recover the differential form of the identity in Eq. (B.43). Quite simply then, the zero frequency part of the Compton tensor is not constrained in finite volume as the limit $k \to 0$ cannot be taken. Gauge symmetry constrains only the frequency dependent combination appearing in Eq. (B.44). Because we have kept the time direction infinite, a limiting procedure does exist for the time-time component of the scattering tensor. Consequently Eq. (B.43) must apply to $T_{00}(\omega = \omega' = 0)$, as is indeed the case for our one-loop results for the neutral pion, Eq. (B.11).[8]

B.5   Conclusion

Above we have considered infrared effects on currents in finite volume field theories. Using the chiral Lagrangian as an example, we showed that matter fields can additively renormalize electric current in finite volume. Such effects do not violate

---

[8]By taking the limit $k^0 \to 0$ in the singly contracted identity

$$k^\mu G(P')iT_{\mu\nu}G(P) = Qe\left[G(P')i\Gamma_\nu(P', P+k)G(P+k) - G(P'-k)i\Gamma_\nu(P'-k, P)G(P)\right],$$

(B.45)

we additionally see that $T_{0\nu}(\omega = \omega' = 0) = 0$ for the neutral pion in finite volume with infinite time extent. Similarly the other singly contracted identity yields $T_{\mu 0}(\omega = \omega' = 0) = 0$ upon taking the limit k'^0 to zero. Both of these conditions are satisfied by our one-loop results, Eq. (B.11).

gauge invariance; on the contrary, new couplings are allowed because of periodicity constraints on zero-mode gauge field transformations. Consequently gauge invariant single particle effective theories can be formulated that reproduce the infrared behavior of the interacting theory. These theories are written in terms of Wilson lines that cycle over the compact dimensions. As $SO(4)$ is explicitly broken in these theories, boosting a charged particle from its rest frame to a frame moving with velocity $\boldsymbol{V}$ does not result in a current $\boldsymbol{J} = Qe\boldsymbol{V}$. There are no contradictions with Ward-Takahashi identities, or low-energy theorems. Differential forms of Ward identities are inapplicable in finite volume.

Conserved currents are not protected from infrared renormalization in finite spaces with discrete translational invariance. As non-perturbative field theories, such as QCD, are numerically simulated in a finite Euclidean space, it is important to understand the infrared running of current couplings. As a practical application of our work, the single particle effective theory derived here can be extended to describe volume effects for properties of hadrons determined from lattice QCD.

B.6 Appendix: Finite Volume Functions

For processes without momentum insertion, all finite volume matching terms, $\Delta X(L)$, in Eq. (B.6) can be cast in terms of the basic building block

$$
\begin{aligned}
I_\beta(m^2, L) &= \frac{1}{L^3} \sum_{\boldsymbol{q}} \frac{1}{[\boldsymbol{q}^2 + m^2]^\beta} - \int \frac{d\boldsymbol{q}}{(2\pi)^3} \frac{1}{[\boldsymbol{q}^2 + m^2]^\beta} \qquad \text{(B.46)} \\
&= \frac{(m^2)^{3/2-\beta}}{(4\pi)^{3/2}\Gamma(\beta)} \int_0^\infty d\tau \tau^{\beta-5/2} e^{-\tau} \left[\vartheta_3(0, e^{-m^2 L^2/4\tau})^3 - 1 \right], \quad \text{(B.47)}
\end{aligned}
$$

where $\vartheta_3(z, q)$ is a Jacobi theta function. To see that all other required finite volume functions can be written in terms of $I_\beta(m^2, L)$, we first define

$$
I_\beta^{i_1 \ldots i_n}(m^2, L) = \frac{1}{L^3} \sum_{\boldsymbol{q}} \frac{q^{i_1} \cdots q^{i_n}}{[\boldsymbol{q}^2 + m^2]^\beta} - \int \frac{d\boldsymbol{q}}{(2\pi)^3} \frac{q^{i_1} \cdots q^{i_n}}{[\boldsymbol{q}^2 + m^2]^\beta}. \qquad \text{(B.48)}
$$

As a consequence of cubic invariance in the sums, we have $I_\beta^{i_1 \ldots i_n}(m^2, L) = 0$, for n odd. For even values, we find

$$
I_\beta^{i_1 \ldots i_{2n}}(m^2, L) = \frac{1}{2n+1} \delta^{\{i_1 i_2} \cdots \delta^{i_{2n-1} i_{2n}\}} \sum_{j=0}^n \binom{n}{j} (-m^2)^j I_{\beta+j-n}(m^2, L) \qquad \text{(B.49)}
$$

The bracketed indices denote complete symmetrization in the usual way, e.g., $\{AB\} = \frac{1}{2!}(AB + BA)$.

Appendix C

Pion Polarizabilities and Volume Effectes in Lattice QCD

C.1   Introduction

Electromagnetic[1] polarizabilities encode fundamental properties of bound states. The electric polarizability of the ground state hydrogen atom, for example, $\alpha_E^H = \alpha_{fs}N/m_e E_0^2$, represents the ease at which the atomic electron cloud deforms in an applied electric field. Here $\alpha_{fs} = e^2/4\pi$ is the fine structure constant, m_e is the electron mass, E_0 is the ground state energy, and N is a pure number, which turns out to be 9/8. Atomic polarizability data are well described by theoretical calculations using atomic wave-functions of the weakly bound electrons. Hadronic polarizabilities, on the other hand, involve non-perturbative physics. The electrically charged quarks inside hadrons respond to applied electromagnetic fields but against the strong chromo-electromagnetic forces that confine them into bound states. If the pion were a weakly bound system of quarks with mass m_q, we might expect its electric polarizability to be of the form, $\alpha_E^\pi \sim \alpha_{fs}N/m_q m_\pi^2$. The actual behavior is considerably different, $\alpha_E^\pi = \alpha_{fs}N/m_\pi \Lambda_\chi^2$, where Λ_χ is the chiral symmetry breaking scale. It thus appears that the pion cloud of the pion is what deforms in the applied field, and that

---

[1]The results in this chapter were first published in Ref. [78].

the relevant energy scale is Λ_χ, which is an order of magnitude greater than the pion mass. Compared to the weakly bound scenario, the electric polarizability is a few orders of magnitude smaller, which indicates stiffness of quarks inside hadrons.

Chiral peturbation theory (χPT) [94] provides a low-energy effective theory of QCD from which the pion polarizabilities can be calculated in terms of a few low-energy constants [75]. At leading order in the chiral power counting, calculated values for the pure number N are $N^{\pi^0} = -1/3$ for the neutral pion, and $N^{\pi^\pm} \approx 1/6$ for the charged pions. Comparing these polarizability predictions to experimental data is unlike the situation with atomic polarizabilities. Without stable targets, experimental determination is considerably challenging at best. Pion polarizabilities, however, have been probed indirectly in several experiments. Three reactions are used: radiative pion-nucleon scattering ($\pi N \to \pi N \gamma$), pion photoproduction in photon nucleus scattering ($\gamma A \to \gamma A \pi$), and pion production seen in electron-positron collisions ($\gamma^* \gamma \to \pi\pi$). Neutral pion polarizabilities have been accessed only by the last reaction by the Crystal Ball Collaboration [112]. The most recent experimental effort has been by MAMI at Mainz [74] in measuring the difference of electric and magnetic polarizabilities of the charged pion through radiative pion-nucleon scattering, and by Compass at CERN [113] to measure charged pion polarizabilities using photoproduction off lead. In the latter experiment, final data are being taken, and soon will be analyzed. After the 12 GeV upgrade, Jefferson Lab has plans to measure pion polarizabilities in the future.

Experiments to determine pion polarizabilities have one feature in common: disagreement with predictions from chiral perturbation theory. Considerable effort has been expended to determine polarizabilities to two-loop order in χPT [114, 115, 116, 76], but discrepancy with experiment remains. Because these experiments are indirect, the challenge is removing the hadronic background to isolate the signal. This is a largely model-dependent process with uncontrolled systematic error. Recent dispersion relation calculations, however, appear consistent with experimental values for the polarizabilities [117, 118]. Thus it remains unclear whether disagreement between theory and experiment has its roots in the experimental analysis, or in the behavior of the chiral expansion.

As a first principles method, lattice QCD [80] can be employed to determine pion polarizabilities. Currently and foreseeably this is itself a considerable challenge, but progress has been made with background field methods [84, 85, 86, 87, 90, 91, 92, 77, 81, 119]. Such calculations suffer a number of systematic errors, such as: quenching or partial quenching, quenching of sea quark charges, and volume effects. While predictions of physical polarizabilities are not currently possible from lattice QCD alone, forthcoming lattice QCD data on polarizabilities can be used as a diagnostic for χPT. The predictions of χPT can be tested against lattice QCD data. To this end, we perform a one-loop analysis of the quenching and partial quenching effects, as well as the volume dependence of pion Compton scattering. As polarizabilities are the coefficients at second order in an expansion in photon momentum ω, one would

naively expect that finite volume corrections to polarizabilities can be determined from momentum expanding the finite volume Compton tensor. We find this is not the case. There are many terms in the finite volume Compton tensor not anticipated by infinite volume gauge invariance. All terms, moreover, are form factors in ωL, where L is the spatial size of the lattice. Because of momentum quantization, these form factors cannot be expanded in ωL. Thus the infinite volume connection between the frequency expansion and the polarizabilities is lost. As polarizabilities are typically calculated in lattice QCD using background field methods, this means we cannot use the finite volume Compton tensor to deduce finite volume corrections to polarizabilities extracted from background field correlation functions. The same problem exists for electromagnetic moments. Their volume effects cannot be deduced from series expanding finite volume electromagnetic form factors about zero momentum transfer.

Our work has the following organization. First in Section C.2.1, we detail our conventions for Compton scattering and the electromagnetic polarizabilities of the pion. In Section C.2.2, we review the low-energy effective theories of QCD, and partially quenched QCD. Quenched QCD is discussed in Appendix C.5. These theories are then utilized in Section C.2.3 to compute the pion electromagnetic polarizabilities in infinite volume. Next in Section C.3, we consider the modifications to polarizabilities in finite volume. These modifications are complicated by both $SO(4)$ breaking and photon zero-mode interactions. We determine the finite volume modifications to

106

pion Compton scattering. Here we argue, however, that these modifications cannot be straightforwardly utilized to ascertain finite volume effects for background field calculations of polarizabilities in lattice QCD. Section C.4 summarizes our work, and Appendix C.6 collects the finite volume functions employed in the main text.

C.2   Pion Compton Scattering

C.2.1   Compton Scattering Amplitude

For Compton scattering in infinite volume, the amplitude for a real photon to scatter off a pion can be parametrized as

$$
\begin{aligned}
T_{\gamma\pi} &= 2m_\pi \left[\left(-\frac{e^2 Q_\pi^2}{m_\pi} + 4\pi\,\alpha_E\,\omega^2 \right) \boldsymbol{\varepsilon}'^* \cdot \boldsymbol{\varepsilon} + 4\pi\,\beta_M\,\omega^2 (\boldsymbol{\varepsilon}'^* \times \hat{\boldsymbol{k}}') \cdot (\boldsymbol{\varepsilon} \times \hat{\boldsymbol{k}}) \right] \\
&\quad + \frac{e^2 Q_\pi^2}{2m_\pi^2}\omega^2 (\boldsymbol{\varepsilon}'^* \cdot \hat{\boldsymbol{k}})(\boldsymbol{\varepsilon} \cdot \hat{\boldsymbol{k}}')(1 - \cos\theta) + \dots,
\end{aligned}
\tag{C.1}
$$

where in the center-of-momentum frame the photon momenta are $k_\mu = (\omega, \omega\hat{\boldsymbol{k}})$ for the initial state, and $k'_\mu = (\omega, \omega\hat{\boldsymbol{k}}')$ for the final state. Terms denoted by ... are higher order in the photon energy. The frame-dependent scattering angle θ is given by $\cos\theta = \hat{\boldsymbol{k}}' \cdot \hat{\boldsymbol{k}}$. In the above expression, Q_π is the charge of the pion in units of $e > 0$. In writing the physical amplitude, we have made use of Coulomb gauge in which the initial and final polarization vectors, ε_μ and ε'^*_ν, satisfy $\varepsilon_0 = \varepsilon'^*_0 = 0$. The Compton amplitude appearing above, moreover, includes the one-particle reducible and irreducible pieces, as we have retained the Born terms.

The frequency independent term proportional to Q_π^2 reproduces the Thomson

cross-section for low-energy scattering of charged particles when the amplitude squared is combined with appropriate phase-space factors. This term is exactly fixed by the total charge of the system in accordance with the Gell-Mann–Golberger–Low low energy theorems [110, 111]. The induced E1-E1 interaction strength α_E is the electric polarizability, while the induced M1-M1 interaction strength β_M is the magnetic polarizability. In order to identify these as polarizabilities one must pull out a factor of twice the target mass from the Compton amplitude, as we have in Eq. (C.1). The electric and magnetic polarizabilities are the first structure dependent terms in the low-energy expansion of the Compton scattering amplitude. These polarizabilities can be determined from first principles using lattice QCD techniques. In order to make the connection between lattice data and real world QCD, extrapolations in quark mass and lattice volume are required. To perform these requisite extrapolations, we turn to the low-energy effective theory of QCD, χPT.

C.2.2   PQχPT for Pion Compton Scattering

In current lattice calculations, valence and sea quarks are often treated differently. In the rather extreme approximation known as quenched QCD, the sea quarks are completely absent. Less extreme is partially quenched QCD, where sea quarks are retained but have different masses than their valence counterparts. While both approximations are certainly contrary to nature, the latter retains QCD as a limit. Observables computed in partially quenched QCD can be connected to their real

world values by utilizing partially quenched χPT (PQχPT) to derive formulae for the required extrapolation in sea quark mass. Because χPT is contained as a limiting case of PQχPT, we focus our discussion on PQχPT. Peculiarities of quenched χPT (QχPT) will be noted where relevant and the general conventions appear in Appendix C.5. For further details on QχPT and PQχPT, see [65, 66, 67, 69, 70, 71, 72].

To determine pion observables, we imagine that the strange quark mass is fixed at the physical value so that no extrapolations are needed in the valence strange or sea strange quark masses. To this end, we consider a partially quenched theory of valence u and d quarks, paired with degenerate ghost quarks $\tilde{u}$ and $\tilde{d}$, and two additional sea quarks j and l. The quark masses are given in a matrix

$$m_Q = \mathrm{diag}\left(m_u, m_d, m_j, m_l, m_u, m_d\right), \qquad (C.2)$$

where the last two entries are ghost quark masses that are degenerate with their valence counterparts. For simplicity below, we work in the isospin limit of the valence and sea sectors, so that $m_u = m_d$ and $m_j = m_l$. PQχPT describes the low-energy dynamics of partially quenched QCD and is written in terms of the mesons Φ that appear in the coset field Σ as[2]

$$\Sigma = \exp\left(\frac{2i\Phi}{f}\right). \qquad (C.3)$$

These mesons are the pseudo-Goldstone modes appearing from spontaneous chiral symmetry breaking: $SU(4|2)_L \otimes SU(4|2)_R \to SU(4|2)_V$. The dynamics of these

[2]In our conventions, the pion decay constant $f \approx 132\,\mathrm{MeV}$.

modes is described at leading-order by the PQχPT Lagrangian

$$\mathcal{L} = \frac{f^2}{8}\text{str}\left(D_\mu\Sigma^\dagger D^\mu\Sigma\right) + \lambda\frac{f^2}{4}\text{str}\left(m_Q^\dagger\Sigma + \Sigma^\dagger m_Q\right) - m_0^2\Phi_0^2. \qquad \text{(C.4)}$$

Here $\Phi_0 = \text{str}(\Phi)/\sqrt{2}$ is the flavor singlet field which has been included as a device to obtain the flavor neutral propagators in PQχPT. Expanding the Lagrangian to tree-level, one finds that mesons composed of a quark Q_i and antiquark $\overline{Q}_j$ have masses given by

$$m_{Q_iQ_j}^2 = \lambda\left[(m_Q)_{ii} + (m_Q)_{jj}\right]. \qquad \text{(C.5)}$$

The flavor singlet field additionally acquires a mass m_0^2. In PQχPT (as well as in χPT), the strong $U(1)_A$ anomaly generates a mass for the flavor singlet field and hence m_0 can be taken on the order of the chiral symmetry breaking scale, $m_0 \sim \Lambda_\chi \approx 4\pi f$. The flavor singlet field can thus be integrated out. Flavor neutral propagators in PQχPT, however, cannot be diagonalized into simple single pole forms [72]. This fact notwithstanding, the results of our calculations will not require the explicit form of these flavor neutral propagators.

In writing the above theory of mesons, we have added the effects of electromagnetism in the leading-order Lagrangian. The $U(1)$ gauge field, A_μ, appears in the action of the covariant derivative, D_μ, namely

$$D_\mu\Sigma = \partial_\mu\Sigma + ieA_\mu\left[\mathcal{Q}, \Sigma\right], \qquad \text{(C.6)}$$

where $\mathcal{Q}$ is the quark electric charge matrix. To completely specify how electromagnetism is coupled, we must extend the quark charges to the partially quenched theory.

The choice

$$\mathcal{Q} = \text{diag}\,(q_u, q_d, q_j, q_l, q_u, q_d)\,, \tag{C.7}$$

with $q_j + q_l \neq 0$, is particularly useful because it retains sensitivity to all electromagnetic couplings in the theory as well as maintains the cancellation of disconnected operator insertions between the valence and ghost sectors [120, 121]. Other choices are possible but can be computationally cumbersome in actual lattice simulations.

C.2.3 Pion Polarizabilities in Infinite Volume

To determine the pion polarizabilities, we calculate the Compton scattering amplitude for the process $\gamma\pi \to \gamma\pi$ using PQχPT. Contributions to the amplitude are of three types: tree-level, wavefunction renormalization corrections, and one-loop contributions. The first contributions arise from tree-level graphs generated from local electromagnetic vertices in the effective theory. The relevant diagrams have been depicted in Figure C.1, and are only non-vanishing for the charged pion. The first diagram represents the local coupling of two photons to the pion. This diagram arises from both the charge-squared operator contained in the leading-order Lagrangian, as well as from terms in the next-to-leading order Lagrangian. Specifically in the notation of [122], the local two-photon, two-pion interactions are contained in the next-to-leading order terms[3]

---

[3]Although we use the $SU(3)$ notation for these terms, final results depend on the scale-independent combination $\alpha_9 + \alpha_{10}$, which has the same value in $SU(2)$ as it does in $SU(3)$.

Figure C.1: Tree-level contributions to the Compton scattering amplitude. The dashed lines represent mesons, while the wiggly lines represent photons. Vertices are generated from the leading and next-to-leading order Lagrangian.

$$\mathcal{L} = i\, e\, \alpha_9\, F_{\mu\nu}\, \text{str}\left(\mathcal{Q}D^\mu\Sigma D^\nu\Sigma^\dagger + \mathcal{Q}D^\mu\Sigma^\dagger D^\nu\Sigma\right) + e^2\alpha_{10}\, F^2 \text{str}\left(\mathcal{Q}\Sigma\mathcal{Q}\Sigma^\dagger\right), \qquad \text{(C.8)}$$

where $F_{\mu\nu} = \partial_\mu A_\nu - \partial_\nu A_\mu$ is the electromagnetic field-strength tensor. In PQχPT, the low-energy constants α_9 and α_{10} have the same numerical values as in χPT, which can be demonstrated by matching. The remaining two diagrams in Figure C.1 are Born terms that do not contribute to the one-pion irreducible Compton amplitude.

The next contributions are those that arise from the pion wavefunction renormalization. The leading self-energy diagrams are depicted in Figure C.2. The leading-order diagrams involving the photon coupling to the pion charge must be multiplied by the wavefunction renormalization to obtain contributions to the Compton amplitude at next-to-leading order. Thus we require only the wavefunction renormalization of the the charged pion. Due to fortuitous cancellation in both PQχPT and QχPT, the hairpin diagram, which arises from the double pole structure of the flavor-neutral propagator, vanishes.

The remaining contributions to the Compton amplitude arise from one-loop diagrams. In Figure C.3, we display the diagrams for the one-pion irreducible scattering amplitude. Contributions from such diagrams lead to chiral corrections to the elec-

112

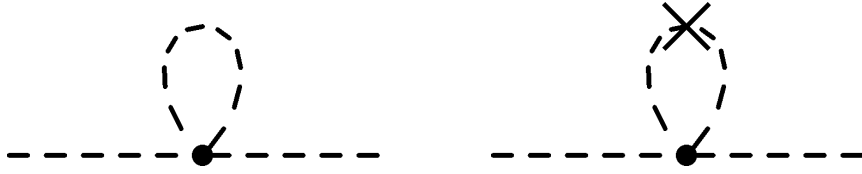**Figure C.2**: Wavefunction renormalization in PQχPT. Diagram elements are the sames as in Figure C.1, and the cross denotes the partially quenched hairpin. The vertex is generated by the leading-order Lagrangian.
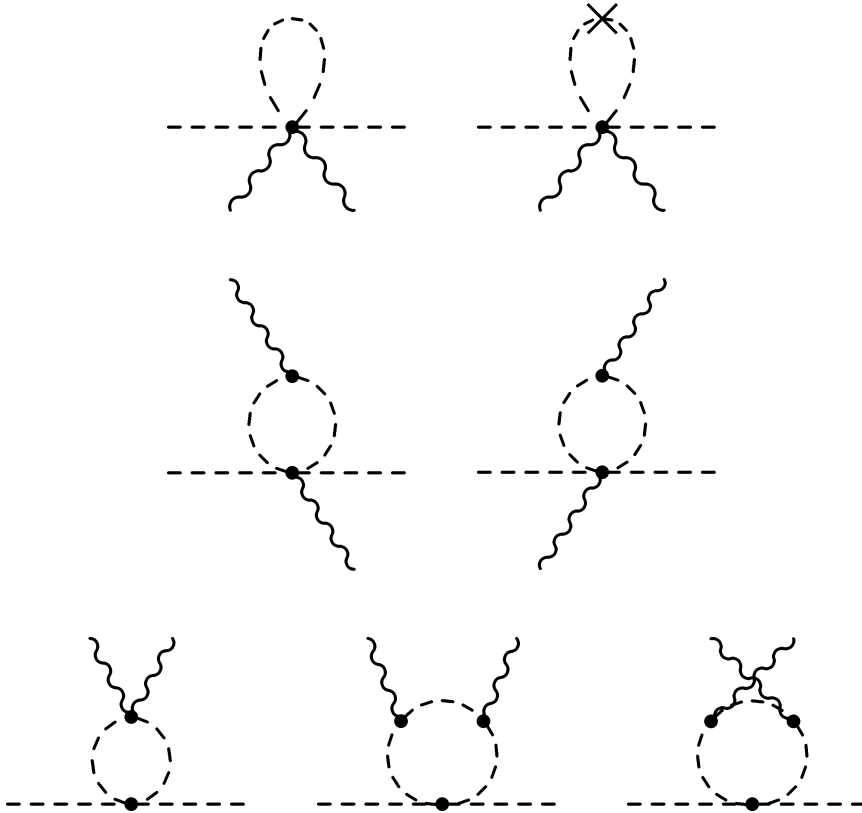

Figure C.3: One-loop contributions to the Compton scattering amplitude in PQχPT. Vertices shown are generated from the leading-order Lagrangian, and diagrams depicted are all one-pion irreducible.

tromagnetic polarizabilities. For the charged pion, there are additional one-pion reducible pieces in PQχPT. These diagrams are displayed in Figure C.4. The effects of such diagrams in infinite volume, however, are to renormalize the mass of the intermediate state pion, and to provide the necessary cancellations which preserve the charge interaction of the leading Born terms. The latter cancellations were first worked out explicitly for the case of the pion charge radius in PQχPT in [123, 108]. Assembling the results of Figures C.1–C.4, we can extract the pion polarizabilities using Eq. (C.1) by utilizing Coulomb gauge in the center-of-momentum frame.

At one-loop order, it is well known that $\alpha_E + \beta_M = 0$ for both charged and neutral pions [99, 124, 75]. We find this remains true to one-loop order in PQχPT, as well as QχPT. This is expected because extending the flavor algebra from $SU(2)$ to graded Lie algebras cannot alter the helicity structure of the Compton amplitude. As for the orthogonal combination of polarizabilities, $\alpha_E - \beta_M$, we arrive at

$$\alpha_E^{\pi^0} - \beta_M^{\pi^0} = -\frac{2\alpha_{fs}Q_\pi^2}{3(4\pi f)^2 m_\pi} \tag{C.9}$$

$$\alpha_E^{\pi^\pm} - \beta_M^{\pi^\pm} = \frac{16\alpha_{fs}Q_\pi^2(\alpha_9 + \alpha_{10})}{f^2 m_\pi}, \tag{C.10}$$

with $Q_\pi = q_u - q_d$. These results are the same in χPT, PQχPT, and QχPT, with the exception that in QχPT the low-energy constants $\alpha_9 + \alpha_{10}$, and f have different numerical values. Furthermore our χPT result agrees with the literature, see [75] (being careful to note $f = \sqrt{2}f_\pi$). In deriving the above result, we remark that the delicate cancellation between pion loops in the zero frequency limit present in χPT remains in PQχPT, and QχPT. This cancellation is required by the infinite volume
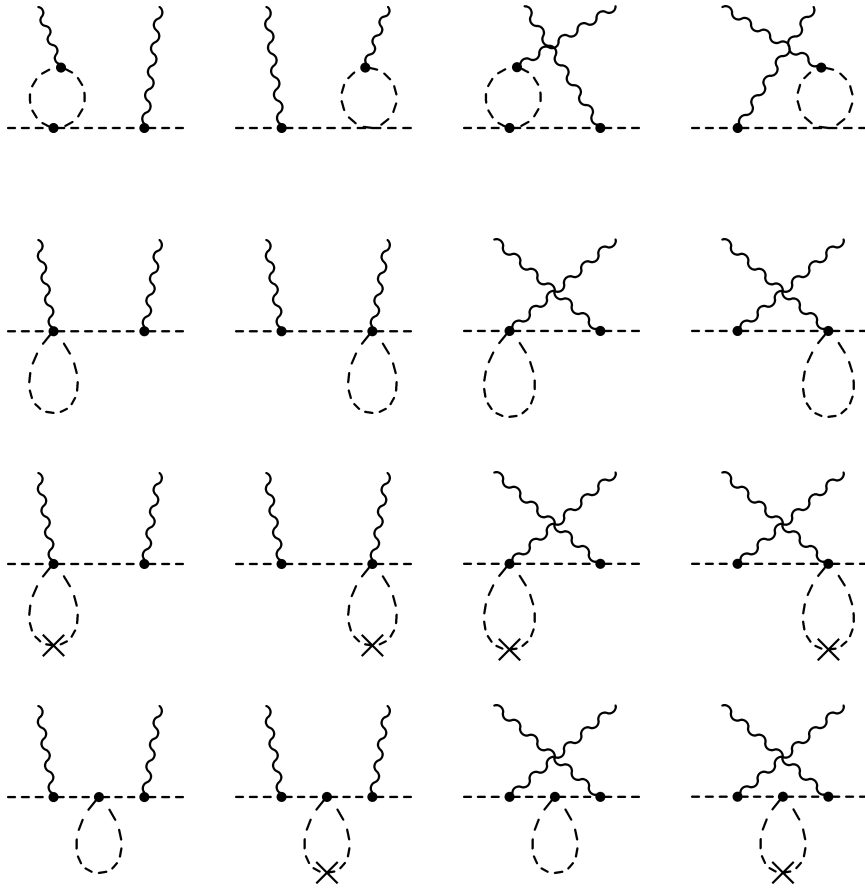
Figure C.4: One-pion reducible contributions to the Compton scattering amplitude at one-loop order in PQχPT.

gauge invariance of the amplitude and reflects that the longest-range coupling to the pion is only to the total charge. In this way the Thomson scattering cross section is produced in these three theories when the zero frequency limit is taken.

In each theory, there are no local electromagnetic interaction terms for the neutral pion in the next-to-leading order Lagrangian. Thus there can be no divergences in the polarizabilities of the neutral pion, as we found explicitly at one-loop. While chiral logarithms are absent for the neutral pion, there are finite terms from the loop graphs. In fact, the entire pion cloud contribution to the neutral pion polarizabilities manages to survive quenching. This is rather surprising, but can be understood by considering the quark-line topologies generated at one-loop order.

The five topologies arising from the four-pion vertex generated from Eq. (C.4) are depicted in Figure C.5. The topologies in the second row are only possible for flavor neutral external states, such as the neutral pion. Let us investigate which topologies can make non-vanishing contributions to the neutral pion polarizabilities. Diagram A contains a sea quark loop and thus associated contributions are proportional to

$$\Delta Q^2 = (q_u - q_j)^2 + (q_u - q_l)^2 + (q_d - q_j)^2 + (q_d - q_l)^2, \qquad \text{(C.11)}$$

which sums the charge-squared couplings from all possible valence-sea loop mesons. In the isospin limit of $SU(4|2)$ all such mesons are degenerate with mass m_{ju}. The net contribution from topology A, however, vanishes because contributions from the four-meson vertex with two derivatives exactly cancel contributions from the four-meson vertex with quark mass insertion. Terms from all of the meson loop diagrams in

116
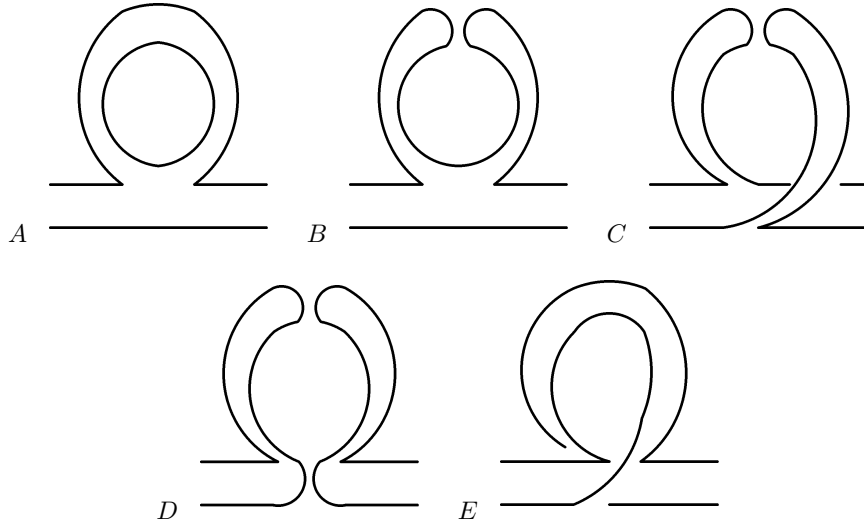
Figure C.5: Quark-line topologies generated at one-loop order. Diagrams in the second row contribute only when the external states are flavor neutral.

Figure C.3 are required for this delicate cancellation. As a result, the characteristic factor of ΔQ^2 is absent from Eq. (C.9). Next, each of the quark line topologies B, C, and D, require flavor disconnected contributions from flavor-neutral meson propagators. As flavor neutral mesons are also electrically neutral, coupling to the photon eliminates such contributions. Indeed looking at Figure C.3, there is only one possible diagram with a hairpin vertex. Direct evaluation shows that this contribution vanishes, ruling out the B, C, and D topologies. Therefore the loop contributions to neutral pion polarizabilities in Eq. (C.9) stem entirely from topology E. As this topology is quark-line connected, the contribution has the same form regardless of quenching.

Let us examine topology E closer by writing the pion field in terms of quark basis

mesons, η_u and η_d,

$$\pi^0 = \frac{1}{\sqrt{2}} \left(\eta_n - \eta_d \right).$$
(C.12)

The diagonal contractions, η_u-η_u and η_d-η_d, for topology E result in an electrically neutral loop meson. Only the first diagram of Figure C.3 could yield the diagonal contractions of topology E. Close inspection of the Lagrangian shows, however, that the four-meson, two-photon vertex with four electrically neutral mesons is identically zero. Thus neutral pion polarizabilities stem entirely from topology E's non-diagonal flavor contractions: η_u-η_d, and η_d-η_u. To one-loop order, the neutral pion polarizabilities arise entirely from annihilation contractions of lattice QCD correlation functions.

Returning to Eq. (C.10) for the charged pion polarizabilities, the quark-line picture helps to show why Eq. (C.10) has no loop contributions. In Figure C.5, the quark-line topologies in the second row are no longer relevant because the external states are charged. Furthermore topologies B and C require hairpins, but the hairpin graphs in Figures C.2 and C.3 vanish. Loop contributions to charged pion polarizabilities can only arise from topology A. Cancellation of divergent loop contributions from this topology must occur in χPT, PQχPT, and QχPT because the combination $\alpha_9 + \alpha_{10}$ is renormalization scale independent. This independence disallows chiral logarithms from loop contributions in χPT, and QχPT. While one can imagine scale invariant combinations of the form $\log(m_{ju}^2/m_{lu}^2)$, say, away from the isospin limit of $SU(4|2)$, charge-squared couplings do not allow for loop contributions to alternate in sign, see Eq. (C.11). Thus such logarithms are absent. While logarithms are not

allowed, finite contributions can be present. As with the neutral pions for topology A, however, the contributions from the four-meson vertex with two derivatives exactly cancel contributions from the four-meson vertex with quark mass insertion. The characteristic factor of ΔQ^2 is consequently absent from from the charged pion polarizabilities, Eq. (C.10). Thus the accidental cancellation of finite terms in χPT also occurs in PQχPT, and QχPT.

As a final comment on the inifinite volume results in Eqs. (C.9) and (C.10), the only pion mass dependence in both charged and neutral pion polarizabilities arises from the target mass m_π. The target mass depends on the valence quark mass. Both of these statements hold only to one-loop order in the chiral expansion.

C.3 Compton Tensor in Finite Volume

In finite volume, the pion is already deformed. Thus its ability to polarize in an applied electric or magnetic field will differ from that in infinite volume. As finite volume modifications to hadron properties are long distance in nature, they can be quite generally addressed using χPT. Lattice simulations are usually carried out in a hypercubic box of volume $L^3 \times \beta$, where L is the length of the spatial direction, and β is the length of the Euclidean time direction. We consider $\beta \gg L$ so that there is no effect from the finite temporal extent of the lattice. With periodic boundary conditions on the quark fields in each of the spatial directions, the momentum modes on the lattice are $\boldsymbol{p} = 2\pi\boldsymbol{n}/L$, with $\boldsymbol{n}$ a triplet of integers. The ordinary power

counting for χPT

$$|\boldsymbol{p}| \lesssim m_\pi \ll \Lambda_\chi \tag{C.13}$$

can be applied in a box of finite size provided $2fL \gg 1$ and $m_\pi L \gtrsim 2\pi$. These two conditions constitute what is called the p-regime of chiral perturbation theory. The first condition is required in order to use chiral perturbation theory at all, while the second condition maintains that pionic zero modes remain perturbative [96, 97]. As the power counting in this regime remains the same as in infinite volume [98], the same diagrams depicted in Figures C.1-C.4 contribute to the pion Compton tensor. It is straightforward to perform the loop calculations in a finite box, we merely replace integrals over virtual four-momenta by integrals over energy and sums over spatial momentum modes permitted by periodicity.

Consider an observable X calculated in both finite and infinite volume. Let $X(L)$ denote the value of the observable in finite volume, and $X(\infty)$ denote its value in infinite volume. The finite and infinite volume theories share exactly the same ultraviolet divergences, thus the volume effect can be determined from matching the two theories in the infrared,

$$X(L) = X(\infty) + \Delta X(L). \tag{C.14}$$

The volume effect is given by the matching term $\Delta X(L)$ which is ultraviolet finite. A salient feature of such matching is that it allows us to retain our infinite volume regularization scheme and values of low-energy constants.

Calculating the finite volume matching for the Compton scattering amplitude,

while straightforward, is quite involved in practice. We first remark that the decomposition of the Compton tensor in Eq. (C.1) is no longer valid. That decomposition makes use of the center-of-momentum frame. Finite volume results on a torus have only an S_4 cubic subgroup of the infinite volume $SO(4)$ invariance. Results will thus be frame dependent, and hence, to be general, we must not make recourse to a particular frame. Furthermore, as shown in [79], there are more gauge invariant structures allowed on a torus. Thus more terms than shown in Eq. (C.1) are allowed at second order in the field strength.

C.3.1 Neutral Pion

Carrying out the finite volume matching on the neutral pion Compton amplitude without recourse to a particular frame or gauge, we find

$$
\begin{aligned}
\Delta T_{\pi^0}^{\mu\nu}(L) \quad = \quad & \frac{e^2}{f^2} \sum_\phi \mathcal{C}_\phi^{\pi^0} \Bigg[-\frac{1}{6} g^{\mu\nu} \int_0^1 dx I_{3/2}(x\boldsymbol{r}, m_\phi^2 - x(1-x)r^2) \\
& + \delta^{\mu 0} \delta^{\nu 0} \Bigg(\frac{1}{3} \int_0^1 dx \int_0^{1-x} dy I_{3/2}(x\boldsymbol{k} + y\boldsymbol{k}', m_\phi^2 - xyr^2) \\
& \qquad - \frac{1}{4} \int_0^1 dx \int_0^{1-x} dy[(2x-1)\omega + 2y\omega'][2x\omega + (2y-1)\omega']I_{5/2}(x\boldsymbol{k} + y\boldsymbol{k}', m_\phi^2 - xyr^2) \Bigg) \\
& + \frac{1}{4} \delta^{\mu 0} \delta^{\nu j} \int_0^1 dx \int_0^{1-x} dy[(2x-1)\omega + 2y\omega']\Big\{ k'^j I_{5/2}(x\boldsymbol{k} + y\boldsymbol{k}', m_\phi^2 - xyr^2) \\
& \qquad + 2I_{5/2}^j(x\boldsymbol{k} + y\boldsymbol{k}', m_\phi^2 - xyr^2)\Big\} \\
& + \frac{1}{4} \delta^{\mu i} \delta^{\nu 0} \int_0^1 dx \int_0^{1-x} dy[(2y-1)\omega' + 2x\omega]\Big\{ k^i I_{5/2}(x\boldsymbol{k} + y\boldsymbol{k}', m_\phi^2 - xyr^2) \\
& \qquad + 2I_{5/2}^i(x\boldsymbol{k} + y\boldsymbol{k}', m_\phi^2 - xyr^2)\Big\} \\
& - \frac{1}{4} \delta^{\mu i} \delta^{\nu j} \int_0^1 dx \int_0^{1-x} dy[4I_{5/2}^{ij}(x\boldsymbol{k} + y\boldsymbol{k}', m_\phi^2 - xyr^2) + 2k^i I_{5/2}^j(x\boldsymbol{k} + y\boldsymbol{k}', m_\phi^2 - xyr^2) \\
& \qquad + 2k'^j I_{5/2}^i(x\boldsymbol{k} + y\boldsymbol{k}', m_\phi^2 - xyr^2) + k^i k'^j I_{5/2}(x\boldsymbol{k} + y\boldsymbol{k}', m_\phi^2 - xyr^2)] \Bigg] .
\end{aligned} \tag{C.15}
$$

Above we have employed $r_\mu = (k - k')_\mu$ for the momentum transfer, with $k_\mu = (\omega, \omega\hat{\boldsymbol{k}})$, and $k'_\mu = (\omega', \omega'\hat{\boldsymbol{k}}')$ for the photon momenta. To derive the above result, we have employed the reality of initial and final state photons, and taken their spatial momenta to be quantized. The finite volume functions $I_\beta(\boldsymbol{\theta}, m^2)$, $I_\beta^i(\boldsymbol{\theta}, m^2)$, and $I_\beta^{ij}(\boldsymbol{\theta}, m^2)$ are defined in Appendix C.6. The coefficient for contributing loop mesons $\mathcal{C}_\phi^{\pi^0}$ is given by

$$\mathcal{C}_\phi^{\pi^0} = 3Q_\pi^2 \left(2m_\pi^2 - r^2\right) \delta_{\phi,\pi} - \frac{3}{2}\Delta Q^2 r^2 \delta_{\phi,ju}. \tag{C.16}$$

While we have only given the PQχPT coefficients, the χPT, and QχPT results can be trivially deduced from Eq. (C.16). The latter is possible because there are no hairpin contributions. At zero frequency, the finite volume Compton amplitude for the neutral pion is non-vanishing. This is because the Thomson cross-section is not protected from renormalization in finite volume [79].

C.3.2 Charged Pion

The charged pion Compton amplitude at finite volume is even more involved than the neutral result as we must determine both reducible and irreducible contributions.

To one-loop order, the result is

$$
\begin{aligned}
\Delta T_{\pi\pm}^{\mu\nu}(L) &= -\frac{3e^2\Delta Q^2}{2f^2}r^2\Bigg\{ -\frac{1}{6}g^{\mu\nu}\int_0^1 dx\, I_{3/2}(x\bm{r}, m_{ju}^2 - x(1-x)r^2) \\
&\quad + \delta^{\mu 0}\delta^{\nu 0}\int_0^1 dx \int_0^{1-x} dy\Bigg[\frac{1}{3}I_{3/2}(x\bm{k}+y\bm{k}', m_{ju}^2 - xyr^2) \\
&\qquad -\frac{1}{4}[(2x-1)\omega + 2y\omega'][2x\omega + (2y-1)\omega']I_{5/2}(x\bm{k}+y\bm{k}', m_{ju}^2 - xyr^2)\Bigg] \\
&\quad + \frac{1}{4}\delta^{\mu 0}\delta^{\nu j}\int_0^1 dx\int_0^{1-x}dy[(2x-1)\omega + 2y\omega'] \\
&\qquad \times \Big[k'^j I_{5/2}(x\bm{k}+y\bm{k}', m_{ju}^2 - xyr^2) + 2I_{5/2}^j(x\bm{k}+y\bm{k}', m_{ju}^2 - xyr^2)\Big] \\
&\quad + \frac{1}{4}\delta^{\mu i}\delta^{\nu 0}\int_0^1 dx\int_0^{1-x}dy[(2y-1)\omega' + 2x\omega] \\
&\qquad \times \Big[k^i I_{5/2}(x\bm{k}+y\bm{k}', m_{ju}^2 - xyr^2) + 2I_{5/2}^i(x\bm{k}+y\bm{k}', m_{ju}^2 - xyr^2)\Big] \\
&\quad - \frac{1}{4}\delta^{\mu i}\delta^{\nu j}\int_0^1 dx\int_0^{1-x}dy\Big[4I_{5/2}^{ij}(x\bm{k}+y\bm{k}', m_{ju}^2 - xyr^2) + 2k^i I_{5/2}^j(x\bm{k}+y\bm{k}', m_{ju}^2 - xyr^2) \\
&\qquad + 2k'^j I_{5/2}^i(x\bm{k}+y\bm{k}', m_{ju}^2 - xyr^2) + k^i k'^j I_{5/2}(x\bm{k}+y\bm{k}', m_{ju}^2 - xyr^2)\Big]\Bigg\} \\
&\quad - \frac{2e^2 Q_\pi^2}{f^2}\Bigg[2g^{\mu\nu} - \frac{(2P+k)^\mu(P+P'+k)^\nu}{(P+k)^2 - m_\pi^2} - \frac{(2P-k')^\nu(P+P'-k')^\mu}{(P-k')^2 - m_\pi^2}\Bigg]I_{1/2}(m_{ju}^2) \\
&\quad - e^2 Q_\pi^2\Bigg[\frac{I^\mu(P, P+k)(P+P'+k)^\nu}{(P+k)^2 - m_\pi^2} + \frac{(2P+k)^\mu I^\nu(P+k, P')}{(P+k)^2 - m_\pi^2} \\
&\qquad + \frac{I^\mu(P-k', P')(2P-k')^\nu}{(P-k')^2 - m_\pi^2} + \frac{(P+P'-k')^\mu I^\nu(P, P-k')}{(P-k')^2 - m_\pi^2}\Bigg] \\
&\quad + \frac{e^2 Q_\pi^2}{f^2}\Bigg[\delta^{\mu 0}\delta^{\nu 0}\int_0^1 dx\Big[2I_{1/2}(x\bm{k}, m_{ju}^2) + 2I_{1/2}(x\bm{k}', m_{ju}^2) \\
&\qquad - x(2x-1)\left(\omega^2 I_{3/2}(x\bm{k}, m_{ju}^2) + \omega'^2 I_{3/2}(x\bm{k}', m_{ju}^2)\right)\Big] \\
&\quad + \delta^{\mu 0}\delta^{\nu j}\int_0^1 dx\,\Big[x\omega' k'^j I_{3/2}(x\bm{k}', m_{ju}^2) + 2x\omega' I_{3/2}^j(x\bm{k}', m_{ju}^2) + (2x-1)\omega I_{3/2}^j(x\bm{k}, m_{ju}^2)\Big] \\
&\quad + \delta^{\mu i}\delta^{\nu 0}\int_0^1 dx\,\Big[x\omega k^i I_{3/2}(x\bm{k}, m_{ju}^2) + 2x\omega I_{3/2}^j(x\bm{k}, m_{ju}^2) + (2x-1)\omega' I_{3/2}^i(x\bm{k}', m_{ju}^2)\Big] \\
&\quad - \delta^{\mu i}\delta^{\nu j}\int_0^1 dx\Big[2I_{3/2}^{ij}(x\bm{k}, m_{ju}^2) + 2I_{3/2}^{ij}(x\bm{k}', m_{ju}^2) \\
&\qquad + k^i I_{3/2}^j(x\bm{k}, m_{ju}^2) + k'^j I_{3/2}^i(x\bm{k}', m_{ju}^2)\Big]\Bigg\}. \quad\text{(C.17)}
\end{aligned}
$$

In the above result, the initial (final) pion momentum has been denoted by P (P').
We have employed an abbreviation for the finite volume pion-photon vertex function,

$I^\mu(P_2, P_1)$, which arises from the one-pion reducible diagrams and is given by

$$
\begin{aligned}
I^\mu(P_2, P_1) &= \frac{1}{f^2}\delta^{\mu 0}\Bigg\{(P_2 + P_1)^0\Big[\int_0^1 dx I_{1/2}(x\boldsymbol{\Delta}, m_{ju}^2 - x(1-x)\Delta^2) \\
&\qquad - \frac{1}{2}(\Delta^0)^2\int_0^1 dx\, x(2x-1)I_{3/2}(x\boldsymbol{\Delta}, m_{ju}^2 - x(1-x)\Delta^2)\Big] \\
&\qquad + \frac{1}{2}\Delta^0\int_0^1 dx(1-2x)(\boldsymbol{P_2} + \boldsymbol{P_1})\cdot \boldsymbol{I}_{3/2}(x\boldsymbol{\Delta}, m_{ju}^2 - x(1-x)\Delta^2)\Bigg\} \\
&\quad + \frac{1}{f^2}\delta^{\mu j}\Bigg\{(P_2 + P_1)^i\Big[\int_0^1 dx I_{3/2}^{ij}(x\boldsymbol{\Delta}, m_{ju}^2 - x(1-x)\Delta^2) \\
&\qquad + \frac{1}{2}\Delta^j\int_0^1 dx I_{3/2}^i(x\boldsymbol{\Delta}, m_{ju}^2 - x(1-x)\Delta^2)\Big] \\
&\qquad + \Delta^0(P_2 + P_1)^0\Big[\int_0^1 dx\, x\Big[I_{3/2}^j(x\boldsymbol{\Delta}, m_{ju}^2 - x(1-x)\Delta^2) \\
&\qquad + \frac{1}{2}\Delta^j\int_0^1 dx I_{3/2}(x\boldsymbol{\Delta}, m_{ju}^2 - x(1-x)\Delta^2)\Big]\Bigg\}, \quad\quad\text{(C.18)}
\end{aligned}
$$

with $\Delta^\mu = (P_2 - P_1)^\mu$. At zero frequency, we recover the results of [79]. Specifically from the one-pion reducible terms, we see that the current is renormalized. This is possible at finite volume because of gauge invariant zero-mode interactions.

C.3.3 Discussion of Finite Volume Results

With Eqs. (C.15) and (C.17), we have deduced the finite volume modification to the pion Compton scattering tensor. These results show explicitly broken $SO(4)$ invariance as well as additional structures not anticipated by infinite volume gauge invariance. The finite volume modifications can be directly utilized if two-current, two-pion correlation functions are calculated on the lattice. One merely removes the finite volume effects determined above to isolate the infinite volume physics. Such lattice calculations of the Compton tensor are, however, prohibitively expensive time wise, and will not be performed in the foreseeable future. A practical alternative to

these calculations is provided by the background field method. In this approach, a classical electromagnetic field is gauged into the QCD action.[4] One then studies the external field dependence of correlation functions to deduce electromagnetic observables. For example, at infinite volume the energy of a neutral pion in a weak external electric field is

$$E_\pi(\boldsymbol{p} = \boldsymbol{0}) = m_\pi - \frac{1}{2}\alpha_E^\pi \boldsymbol{E}^2 + \mathcal{O}(\boldsymbol{E}^4). \tag{C.19}$$

Thus by measuring the quadratic energy shift in the external field strength $|\boldsymbol{E}|$, one can deduce the electric polarizability. A practical question is then how to deduce volume corrections to polarizabilities determined from background field methods. Given the relation of the infinite volume Compton tensor to the polarizabilities, one might suspect that the finite volume Compton tensor in Eqs. (C.15) and (C.17) contains the finite volume corrections to the polarizabilities. We argue that the finite volume Compton tensor has no relevance to volume effects in background field methods. At finite volume, there is no longer a discernible relation between polarizabilities and the Compton tensor.

An analysis of finite volume effects for nucleon polarizabilities for background field methods derived from the Compton tensor, however, was presented in [81]. That analysis employed the Breit frame decomposition of the nucleon Compton tensor in Coulomb gauge. Such results surely cannot be utilized for background field

---

[4]Implementing this method currently suffers the need to quench effects of the background field. In principle, there is no impediment to coupling a suitably weak background field to sea quarks other than time cost.

calculations because such calculations are typically done in the rest frame. The finite volume modifications derived, moreover, are polluted by subtle effects from the gauge field due to the nature of gauge invariance on a torus. These effects have nothing to do with polarizabilities. For example, in the center-of-momentum frame, where $k^0 = k'^0 = \omega$, we may encounter a term in the amplitude of the form

$$\mathcal{M} = \ldots + \frac{1}{2}\omega^2\alpha(L)\,\boldsymbol{\varepsilon}'^* \cdot \boldsymbol{\varepsilon} + \ldots, \tag{C.20}$$

and be tempted to conclude that $\alpha(L)$ is a finite volume correction to the electric polarizability. In a general frame, however, this term could stem from any combination of ω^2, ω'^2, and $\omega\omega'$ structures. In infinite volume only the last term is allowed by gauge invariance, specifically by an operator $\propto \boldsymbol{E}^2$ with a coefficient proportional to the electric polarizability. In finite volume, however, the additional structures ω^2 and ω'^2 are allowed. They stem from single-particle effective theory operators of the form

$$\mathcal{L} = \frac{i}{2}\overline{\alpha}(L)\,\boldsymbol{W}^{(-)} \cdot \frac{\partial \boldsymbol{E}}{\partial t}\,\mathrm{tr}(Q^2\Phi^2), \tag{C.21}$$

for example, where $W_i^{(-)}$ is the negative parity part of the zero-mode Wilson line W_i, given by

$$W_i = \mathcal{P}_{\boldsymbol{0}}\mathcal{W}_i\mathcal{P}_{\boldsymbol{0}}^\dagger, \tag{C.22}$$

with the Wilson line $\mathcal{W}_i$ as

$$\mathcal{W}_i = \exp\left(\frac{ie}{3}\oint dx_i A_i\right), \tag{C.23}$$

and $\mathcal{P}_{\boldsymbol{0}}$ as the zero-mode projection operator. The operator in Eq. (C.21) respects C, P, and T, as well as the cubic symmetry of the torus. Furthermore it is gauge

invariant because the zero mode has a periodicity constraint under gauge transformations, see [79]. From Eq. (C.20), we cannot deduce that $\alpha(L)$ is a finite volume correction to the electric polarizability. In general, one must work in an arbitrary frame to disentangle the zero-mode electric coupling in Eq. (C.21) from the electric polarizability. An analogous situation exists for magnetic interactions, because the operator,

$$\boldsymbol{\nabla} \cdot \left(\boldsymbol{W}^{(-)} \times \boldsymbol{B}\right) \text{tr}(Q^2 \Phi^2), \tag{C.24}$$

for example, is allowed by symmetries.

The frame and gauge dependence notwithstanding, finite volume modifications to polarizabilities were determined in [81] from Taylor series expanding the Compton amplitude in photon frequency. That procedure is also invalid as we now demonstrate. For simplicity, consider the following finite volume difference function, $I_{1/2}(\boldsymbol{k}, m^2)$, where $\boldsymbol{k}$ is an external photon momentum. To determine finite volume corrections to polarizabilities stemming from this term, we perform a Taylor series expansion in the external momentum and arrive at

$$I_{1/2}(\boldsymbol{k}, m^2) = I_{1/2}(\boldsymbol{0}, m^2) - \frac{1}{2}\boldsymbol{k}^2 m^2 I_{5/2}(\boldsymbol{0}, m^2) + \mathcal{O}(\boldsymbol{k}^4). \tag{C.25}$$

If we were interested in determining a hypothetical polarizability X entering the amplitude in the form

$$\mathcal{M} = \ldots + \frac{1}{2}\boldsymbol{k}^2 X + \ldots, \tag{C.26}$$

then we would be tempted to conclude that the finite volume effect $\Delta X(L)$ is given

by

$$\Delta X(L) = -m^2 I_{5/2}(\mathbf{0}, m^2). \tag{C.27}$$

Because the external momentum is itself quantized, instead of Eq. (C.25) we actually have the exact relation

$$I_{1/2}(\mathbf{k}, m^2) = I_{1/2}(\mathbf{0}, m^2). \tag{C.28}$$

This follows trivially from re-indexing the summation over loop momentum modes, or from the periodicity of the elliptic-theta function, see Appendix C.6. Hence the volume effect for our example is actually $\Delta X(L) = 0$. The reason for this discrepancy is a poorly convergent series expansion.[5] Naively the expansion is in $\mathbf{k}^2 = 4\pi^2 \mathbf{n}^2/L^2$, and thus for large enough box size the finite volume effect should be well approximated by the first few terms in the Taylor series. This is not the case. Because higher-order terms have more derivatives, these contributions effectively have more propagators and hence more sensitivity to the infrared. While we would expect the second term in Eq. (C.25) to be $1/L^2$ suppressed relative to the first term, the asymptotics show that the volume effect is L^2 enhanced

$$\lim_{L \to \infty} m^2 I_{5/2}(\mathbf{0}, m^2)/I_{1/2}(\mathbf{0}, m^2) = \frac{1}{3}L^2. \tag{C.29}$$

The series expansion continues in this fashion: all terms are order one. We can see the same effect more directly by expressing the finite volume difference in terms of

---

[5]Another difference between Eqs. (C.25) and (C.28) is that the order of summation and differentiation has been interchanged. One can easily show, however, that the summation over modes is uniformly convergent by using the Weierstrass M-test.

the elliptic-theta function, namely

$$I_{1/2}(\boldsymbol{k}, m^2) = \frac{1}{\pi^2 L^2} \int_0^\infty d\lambda e^{-m^2 L^2/4\lambda} \Big[\vartheta_3(\pi n, e^{-\lambda}) \vartheta_3(0, e^{-\lambda})^2 - 1 \Big], \qquad \text{(C.30)}$$

for the choice $\boldsymbol{k} = (2\pi n/L, 0, 0)$. A series expansion in $\boldsymbol{k}$ is thus effectively the same as expanding in πn.

Returning to Eqs. (C.15) and (C.17), we must ascertain whether we can make sense of a series expansion in frequency for the Compton tensor. Terms of the form

$$r^2 \int_0^1 dx I_{3/2}(x\boldsymbol{r}, m^2 - x(1-x)r^2), \qquad \text{(C.31)}$$

for example, can be plausibly expanded to second order because this requires only evaluation of the finite volume function at $\boldsymbol{r} = 0$. This was the logic employed in [125] to deduce finite volume corrections to the nucleon magnetic moment. As $\boldsymbol{r}$ is not continuous, however, one cannot deduce the small momentum behavior of this term from evaluation at $\boldsymbol{r} = 0$, nor can one deduce the small momentum behavior from Taylor series expanding other terms like

$$\int_0^1 dx I_{3/2}(x\boldsymbol{r}, m^2 - x(1-x)r^2), \qquad \text{(C.32)}$$

in the Compton tensor, for example. Series expanding in $\boldsymbol{r}L = 2\pi\boldsymbol{n}$ is nonsense no matter the size of the box length L.[6]

At finite volume, one must treat the terms in the amplitude as form factors in ωL. Thus for electromagnetic form factors at finite volume, for example, volume

---

[6]There is a putative improvement in the convergence of the last term due to the integral over the Feynman parameter. The L scaling of terms in the expansion, however, is unchanged.

corrections to electromagnetic moments cannot be deduced. Similarly we are unable to use our results for the finite volume modification of the Compton amplitude to deduce corrections to the pion polarizabilities. At second order in the field strength there are a myriad of new terms allowed by the less restrictive symmetries on a torus: cubic invariance and periodic zero-mode gauge invariance. Furthermore a small frequency expansion at finite volume does not make sense for quantized momenta. Said another way, periodic gauge potentials on a torus do not lead to electromagnetic multipole expansions.

C.4   Summary

Above we have investigated chiral and volume corrections to pion Compton scattering using χPT, PQχPT, and QχPT. In infinte volume, straightforward calculation of the Compton amplitude allows us to determine charged and neutral pion polarizabilities in these theories. Due to fortuitous cancellation there is no dependence on the sea quark masses, or sea quark charges at one-loop order in the chiral expansion. The Compton tensor itself does not have any quark mass dependence at this order. Consequently the quark mass dependence of the derived polarizabilities stems from a kinematical prefactor of the inverse target mass. As this valence pion mass is relatively inexpensive to dial, the chiral singularity should be discernible from lattice data at light quark masses. Thus as the chiral regime is approached, one can use the lattice as a diagnostic tool to study the chiral behavior of pion polarizabil-

ities. This can be done most easily for the charged pion. Whereas for the neutral pion, we demonstrated that the polarizabilities at one-loop order stem entirely from annihilation contractions which are notoriously difficult to calculate on the lattice.

When accounting for finite volume effects, however, the situation becomes more complicated. Breaking of $SO(4)$ invariance and the nature of gauge invariance on a torus lead to considerably complicated structure for the Compton tensor. Sea quark charge and mass dependence enter in the one-loop finite volume effects. One cannot unambiguously determine the volume effects for the polarizabilities from the Compton tensor because the Taylor series expansion in quantized momentum is poorly convergent. What was in infinte volume a series expansion in $\omega/m_\pi \ll 1$ that lead to the polarizabilities, now is accompanied by an ill-defined expansion in $\omega L \sim 1$ at finite volume. This means that even at low energies, the finite volume Compton amplitude is a form factor in ωL. Consequently connection of our finite volume results to background field lattice calculations is not possible. Similarly finite volume corrections to electromagnetic moments cannot be deduced from momentum expanding finite volume form factors. Further investigation is required to determine volume corrections relevant for observables determined with background field methods.

C.5 Appendix A: Quenched χPT

Here we give the relevant details needed in the calculation of quenched pion polarizabilities. In quenched QCD, contributions from sea quarks are completely neglected.

In a quenched theory of two flavors u and d, we additionally have two ghost quarks $\tilde{u}$ and $\tilde{d}$. The mass matrix is now

$$m_Q = \text{diag}\left(m_u, m_d, m_u, m_d\right), \tag{C.33}$$

where the final two entries are the masses of the ghost quarks. These equal mass ghost quarks are necessitated so that path integral determinants for the valence quarks are exactly canceled by those from the ghosts. The symmetry breaking pattern in QχPT schematically takes the form $U(2|2)_L \otimes U(2|2)_R \to U(2|2)_V$ because there is no axial anomaly in quenched QCD. The coset field Σ is hence a $U(2|2)$ matrix and the singlet component cannot be integrated out. The dynamics of the pseudo-Goldstone modes is described at leading-order by the QχPT Lagrangian

$$\mathcal{L} = \frac{f^2}{8}\text{str}\left(D_\mu \Sigma^\dagger D^\mu \Sigma\right) + \lambda\frac{f^2}{4}\text{str}\left(m_Q^\dagger \Sigma + \Sigma^\dagger m_Q\right) + \alpha_\Phi D_\mu \Phi_0 D^\mu \Phi_0 - m_0^2 \Phi_0^2. \tag{C.34}$$

While propagators for flavor-neutral mesons have double poles, these are not encountered explicitly in expressions for the pion polarizabilities at next-to-leading order. Quenched observables are in general unrelated to their unquenched counterparts, for example, the constants α_Φ and m_0 have no analogs in χPT, moreover, arbitrary polynomial functions of Φ_0^2 can multiply any term in the Lagrangian and the low-energy constants in the quenched chiral Lagrangian above result from treating these polynomial terms in mean-field approximation.

For the quenched electric charge matrix of the quarks, we must have

$$\mathcal{Q} = \text{diag}\left(q_u, q_d, q_u, q_d\right), \tag{C.35}$$

for which the condition $\mathrm{str}\mathcal{Q} = 0$ is unavoidable. In general there are fewer local electromagnetic terms in QχPT as compared to χPT. At next-to-leading order, however, both the α_9 and α_{10} terms remain. We must keep in mind that the numerical values of these coefficients are unrelated to their values in χPT. Calculation of the pion polarizabilities then proceeds analogously to the partially quenched case. Results for the quenched polarizabilities have been given for infinite and finite volume in the main text.

C.6   Appendix B: Finite Volume Functions

Above we have determined the finite volume modification to the Compton scattering tensor. In this Appendix, we give explicit formulae for the finite volume functions used to express finite volume differences. We use similar notation for these functions as [126, 127], where further discussion can be found.

In evaluating a Feynman diagram in finite volume, the loop integral is converted into a sum over the allowed Fourier modes in a periodic box. The difference of this sum and the infinite volume result is the finite volume effect. As is customary, we treat the length of the time direction as infinite. All finite volume differences with momentum insertion can be cast in terms of the function $I_\beta^{i_1 \cdots i_j}(\boldsymbol{\theta}, m^2)$, defined by

$$I_\beta^{i_1 \cdots i_j}(\boldsymbol{\theta}, m^2) = \frac{1}{L^3} \sum_{\boldsymbol{n}} \frac{q^{i_1} \cdots q^{i_j}}{[(\boldsymbol{q} + \boldsymbol{\theta})^2 + m^2]^\beta} - \int \frac{d\boldsymbol{q}}{(2\pi)^3} \frac{q^{i_1} \cdots q^{i_j}}{[(\boldsymbol{q} + \boldsymbol{\theta})^2 + m^2]^\beta}, \qquad \text{(C.36)}$$

where the sum on $\boldsymbol{n}$ is over triplets of integers, and the loop momentum modes are quantized as $\boldsymbol{q} = 2\pi\boldsymbol{n}/L$ in a periodic box. While a general expression for the

exponentially convergent form of $I_\beta^{i_1\cdots i_j}(\boldsymbol{\theta}, m^2)$ exists, it is easiest merely to cite the

required cases for our work. These are

$$
\begin{aligned}
I_\beta(\boldsymbol{\theta}, m^2) &= \frac{(L^2/4)^{\beta-3/2}}{(4\pi)^{3/2}\Gamma(\beta)} \int_0^\infty d\lambda\, \lambda^{1/2-\beta} e^{-m^2 L^2/4\lambda} \left[\prod_{j=1}^3 \vartheta_3(\theta_j L/2, e^{-\lambda}) - 1\right] \quad \text{(C.37)}\\
I_\beta^{i_1}(\boldsymbol{\theta}, m^2) &= -\frac{1}{2(\beta-1)}\frac{d}{d\theta^{i_1}} I_\beta(\boldsymbol{\theta}, m^2) - \theta^{i_1} I_\beta(\boldsymbol{\theta}, m^2) \quad \text{(C.38)}\\
I_\beta^{i_1 i_2}(\boldsymbol{\theta}, m^2) &= \frac{1}{4(\beta-2)(\beta-1)}\frac{d^2}{d\theta^{i_1} d\theta^{i_2}} I_{\beta-2}(\boldsymbol{\theta}, m^2) + \frac{1}{2(\beta-1)} \delta^{i_1 i_2} I_{\beta-1}(\boldsymbol{\theta}, m^2)\\
&\quad - \theta^{i_1} I_\beta^{i_2}(\boldsymbol{\theta}, m^2) - \theta^{i_2} I_\beta^{i_1}(\boldsymbol{\theta}, m^2) - \theta^{i_1}\theta^{i_2} I_\beta(\boldsymbol{\theta}, m^2) \quad \text{(C.39)}
\end{aligned}
$$

where $\vartheta_3(z, q)$ is a Jacobi elliptic-theta function of the third kind, see, e.g. [100].

Bibliography

[1] D. J. Gross and Frank Wilczek. Ultraviolet behavior of non-abelian gauge theories. *Phys. Rev. Lett.*, 30:1343–1346, 1973.

[2] Howard Georgi. *Weak Interactions and Modern Particle Theory*. Benjamin/Cummings, 1984.

[3] J. Goldstone. Field Theories with Superconductor Solutions. *Nuovo Cim.*, 19:154–164, 1961.

[4] Jeffrey Goldstone, Abdus Salam, and Steven Weinberg. Broken Symmetries. *Phys. Rev.*, 127:965–970, 1962.

[5] Mark B. Wise. Combining chiral and heavy quark symmetries. *arXiv:hep-ph/9306277v1*, 1993.

[6] Aneesh V. Manohar and Mark B. Wise. *Heavy quark physics*, volume 10. 2000.

[7] Nathan Isgur and Mark B. Wise. Weak Decays of Heavy Mesons in the Static Quark Approximation. *Phys. Lett.*, B232:113, 1989.

[8] Estia Eichten and Brian Russell Hill. An Effective Field Theory for the Calculation of Matrix Elements Involving Heavy Quarks. *Phys. Lett.*, B234:511, 1990.

[9] Howard Georgi. An effective field theory for heavy quarks at low energies. *Phys. Lett.*, B240:447–450, 1990.

[10] Adam F. Falk. Hadrons of arbitrary spin in the heavy quark effective theory. *Nucl. Phys.*, B378:79–94, 1992.

[11] Mark B. Wise. Chiral perturbation theory for hadrons containing a heavy quark. *Phys. Rev.*, D45:2188–2191, 1992.

[12] Gustavo Burdman and John F. Donoghue. Union of chiral and heavy quark symmetries. *Phys. Lett.*, B280:287–291, 1992.

[13] T. M. Yan, H. Y. Cheng, C. Y. Cheung, G. L. Lin, Y. C. Lin, and H. L. Yu. Heavy quark symmetry and chiral dynamics. *Phys. Rev.*, D46:1148–1164, 1992.

[14] Iain W. Stewart. Extraction of the $D^*D\pi$ coupling from D^* decays. *Nucl. Phys.*, B529:62–80, 1998.

[15] Geoffrey T. Bodwin, Eric Braaten, and G. Peter Lepage. Rigorous QCD analysis of inclusive annihilation and production of heavy quarkonium. *Phys. Rev.*, D51:1125–1171, 1995.

[16] Michael E. Luke, Aneesh V. Manohar, and Ira Z. Rothstein. Renormalization group scaling in nonrelativistic QCD. *Phys. Rev.*, D61:074025, 2000.

[17] Nora Brambilla, Antonio Vairo, and Thomas Rosch. Effective field theory Lagrangians for baryons with two and three heavy quarks. *Phys. Rev.*, D72:034021, 2005.

[18] Sean Fleming and Thomas Mehen. Doubly Heavy Baryons, Heavy Quark-DiQuark Symmetry and NRQCD. *Phys. Rev.*, D73:034502, 2006.

[19] Nora Brambilla, Antonio Pineda, Joan Soto, and Antonio Vairo. Potential NRQCD: An effective theory for heavy quarkonium. *Nucl. Phys.*, B566:275, 2000.

[20] Martin J. Savage and Mark B. Wise. Spectrum of baryons with two heavy quarks. *Phys. Lett.*, B248:177–180, 1990.

[21] Kenneth G. Wilson. Confinement of quarks. *Phys. Rev.*, D10:2445–2459, 1974.

[22] Jie Hu and Thomas Mehen. Chiral Lagrangian with heavy quark-diquark symmetry. *Phys. Rev.*, D73:054003, 2006.

[23] M. Mattson et al. First observation of the doubly charmed baryon Ξ_{cc}^+. *Phys. Rev. Lett.*, 89:112001, 2002.

[24] M. A. Moinester et al. First observation of doubly charmed baryons. ((B)). *Czech. J. PHys.*, 53:B201–B213, 2003.

[25] A. Ocherashvili et al. Confirmation of the double charm baryon $\Xi_{cc}^+(3520)$ via its decay to pD^+K^-. *Phys. Lett.*, B628:18–24, 2005.

[26] L. Schmitt, S. Paul, R. Kuhn, and M. A. Moinester. Doubly charmed baryons in COMPASS. 2003.

[27] J. S. Russ. The double charm baryon family at selex: An update. *http://www-selex.fnal.gov/Welcome.html*.

[28] J. S. Russ. Recent hadron physics results from Fermilab. *AIP Conf. Proc.*, 717:507–514, 2004.

[29] Randy Lewis, Nilmani Mathur, and R. M. Woloshyn. Charmed baryons in lattice QCD. *Phys. Rev.*, D64:094509, 2001.

[30] Nilmani Mathur, Randy Lewis, and R. M. Woloshyn. Charmed and bottom baryons from lattice NRQCD. *Phys. Rev.*, D66:014502, 2002.

[31] J. M. Flynn, F. Mescia, and Abdullah Shams Bin Tariq. Spectroscopy of doubly-charmed baryons in lattice QCD. *JHEP*, 07:066, 2003.

[32] D. Ebert, R. N. Faustov, V. O. Galkin, and A. P. Martynenko. Mass spectra of doubly heavy baryons in the relativistic quark model. *Phys. Rev.*, D66:014008, 2002.

[33] A. K. Likhoded and A. I. Onishchenko. Lifetimes of doubly heavy baryons. 1999.

[34] B. Guberina, B. Melic, and H. Stefancic. Inclusive decays and lifetimes of doubly charmed baryons. *Eur. Phys. J.*, C9:213–219, 1999.

[35] V. V. Kiselev, A. K. Likhoded, and A. I. Onishchenko. Lifetimes of doubly charmed baryons: Ξ_{cc}^+ and Ξ_{cc}^{++}. *Phys. Rev.*, D60:014007, 1999.

[36] V. V. Kiselev and A. K. Likhoded. Baryons with two heavy quarks. *Phys. Usp.*, 45:455–506, 2002.

[37] V. V. Kiselev and A. K. Likhoded. Comment on "First observation of doubly charmed baryon Ξ_{cc}^+". 2002.

[38] R. Vogt and S. J. Brodsky. Charmed Hadron Asymmetries in the Intrinsic Charm Coalescence Model. *Nucl. Phys.*, B478:311–334, 1996.

[39] R. Vogt and S. J. Brodsky. Intrinsic charm contribution to double quarkonium hadroproduction. *Phys. Lett.*, B349:569–575, 1995.

[40] R. Vogt and S. J. Brodsky. QCD and intrinsic heavy quark predictions for leading charm and beauty hadroproduction. *Nucl. Phys.*, B438:261–277, 1995.

[41] Eric Braaten, Masaoki Kusunoki, Yu Jia, and Thomas Mehen. Λ_c^+/Λ_c^- asymmetry in hadroproduction from heavy-quark recombination. *Phys. Rev.*, D70:054021, 2004.

[42] Eric Braaten, Yu Jia, and Thomas Mehen. The leading particle effect from heavy-quark recombination. *Phys. Rev. Lett.*, 89:122002, 2002.

[43] J. G. Korner, M. Kramer, and D. Pirjol. Heavy baryons. *Prog. Part. Nucl. Phys.*, 33:787–868, 1994.

[44] R. Roncaglia, D. B. Lichtenberg, and E. Predazzi. Predicting the masses of baryons containing one or two heavy quarks. *Phys. Rev.*, D52:1722–1725, 1995.

[45] D. Ebert, R. N. Faustov, V. O. Galkin, A. P. Martynenko, and V. A. Saleev. Heavy baryons in the relativistic quark model. *Zeitschrift fr Physik C Particles and Fields*, 76, 1997.

[46] V. V. Kiselev and A. I. Onishchenko. Doubly heavy baryons in sum rules of NRQCD. *Nucl. Phys.*, B581:432–448, 2000.

[47] S. S. Gershtein, V. V. Kiselev, A. K. Likhoded, and A. I. Onishchenko. Spectroscopy of doubly heavy baryons. *Phys. Rev.*, D62:054021, 2000.

[48] V. V. Kiselev and A. E. Kovalsky. Doubly heavy baryons $\Omega_{QQ'}$ versus $\Xi_{QQ'}$ in sum rules of NRQCD. *Phys. Rev.*, D64:014002, 2001.

[49] James F. Amundson et al. Radiative D^* Decay Using Heavy Quark and Chiral Symmetry. *Phys. Lett.*, B296:415–419, 1992.

[50] Thomas Mehen and Roxanne P. Springer. Even- and odd-parity charmed meson masses in heavy hadron chiral perturbation theory. *Phys. Rev.*, D72:034006, 2005.

[51] S. Anderson et al. Observation of a broad L = 1 $c\bar{q}$ state in $B^- \to D^{*+}\pi^-\pi^-$ at CLEO. *Nucl. Phys.*, A663:647–650, 2000.

[52] K. Abe et al. Study of $B^- \to D^{**0}\pi^-(D^{**0} \to D^{(*)+}\pi^-)$ decays. *Phys. Rev.*, D69:112002, 2004.

[53] J. M. Link et al. Measurement of masses and widths of excited charm mesons D_2^* and evidence for broad states. *Phys. Lett.*, B586:11–20, 2004.

[54] B. Aubert et al. Observation of a narrow meson decaying to $D_s^+\pi^0$ at a mass of 2.32-GeV/c^2. *Phys. Rev. Lett.*, 90:242001, 2003.

[55] D. Besson et al. Observation of a narrow resonance of mass 2.46 GeV $/c^2$ in the $D_s^{*+}\pi^0$ final state, and confirmation of the D_{sJ}^* (2317). *AIP Conf. Proc.*, 698:497–502, 2004.

[56] V. V. Kiselev, A. K. Likhoded, O. N. Pakhomova, and V. A. Saleev. Mass spectra of doubly heavy $\Omega_{QQ'}$ baryons. *Phys. Rev.*, D66:034030, 2002.

[57] S. S. Gershtein, V. V. Kiselev, A. K. Likhoded, and A. I. Onishchenko. Spectroscopy of doubly charmed baryons: Ξ_{cc}^+ and Ξ_{cc}^{++}. *Mod. Phys. Lett.*, A14:135–146, 1999.

[58] S. S. Gershtein, V. V. Kiselev, A. K. Likhoded, and A. I. Onishchenko. Spectroscopy of doubly heavy baryons. *Heavy Ion Phys.*, 9:133–144, 1999.

[59] Nora Brambilla, Antonio Pineda, Joan Soto, and Antonio Vairo. Effective field theories for heavy quarkonium. *Rev. Mod. Phys.*, 77:1423, 2005.

[60] Peter L. Cho and Mark B. Wise. Comment on $D_s^* \to D_s\pi^0$ decay. *Phys. Rev.*, D49:6228–6231, 1994.

[61] P. Colangelo and F. De Fazio. Understanding $D_{sJ}(2317)$. *Phys. Lett.*, B570:180–184, 2003.

[62] Martin J. White and Martin J. Savage. Semileptonic decay of baryons with two heavy quarks. *Phys. Lett.*, B271:410–414, 1991.

[63] Jonathan M. Flynn and Juan Nieves. Semileptonic bc to cc Baryon Decay and Heavy Quark Spin Symmetry. *Phys. Rev.*, D76:017502, 2007.

[64] Svjetlana Fajfer and Jernej F. Kamenik. Chiral loop corrections to strong decays of positive and negative parity charmed mesons. *Phys. Rev.*, D74:074023, 2006.

[65] A. Morel. Chiral logarithms in quenched QCD. *J. Phys. (France)*, 48:1111–1119, 1987.

[66] Stephen R. Sharpe. Quenched chiral logarithms. *Phys. Rev.*, D46:3146–3168, 1992.

[67] Claude W. Bernard and Maarten F. L. Golterman. Chiral perturbation theory for the quenched approximation of QCD. *Phys. Rev.*, D46:853–857, 1992.

[68] Claude W. Bernard and Maarten F. L. Golterman. Partially quenched gauge theories and an application to staggered fermions. *Phys. Rev.*, D49:486–494, 1994.

[69] Stephen R. Sharpe. Enhanced chiral logarithms in partially quenched QCD. *Phys. Rev.*, D56:7052–7058, 1997.

[70] Maarten F. L. Golterman and Ka-Chun Leung. Applications of Partially Quenched Chiral Perturbation Theory. *Phys. Rev.*, D57:5703–5710, 1998.

[71] Stephen R. Sharpe and Noam Shoresh. Physical results from unphysical simulations. *Phys. Rev.*, D62:094503, 2000.

[72] Stephen R. Sharpe and Noam Shoresh. Partially quenched chiral perturbation theory without Φ_0. *Phys. Rev.*, D64:114510, 2001.

[73] Thomas Mehen and Brian C. Tiburzi. Doubly heavy baryons and quark-diquark symmetry in quenched and partially quenched chiral perturbation theory. *Phys. Rev.*, D74:054505, 2006.

[74] J. Ahrens et al. Measurement of the π^+ meson polarizabilities via the $\gamma p \to \gamma \pi^+ n$ reaction. *Eur. Phys. J.*, A23:113–127, 2005.

[75] Barry R. Holstein. Pion polarizability and chiral symmetry. *Comments Nucl. Part. Phys.*, A19:221–238, 1990.

[76] Juerg Gasser, Mikhail A. Ivanov, and Mikko E. Sainio. Revisiting $\gamma\gamma \to \pi^+\pi^-$ at low energies. *Nucl. Phys.*, B745:84–108, 2006.

[77] Frank X. Lee, Leming Zhou, Walter Wilcox, and Joseph C. Christensen. Magnetic polarizability of hadrons from lattice QCD in the background field method. *Phys. Rev.*, D73:034503, 2006.

[78] Jie Hu, Fu-Jiun Jiang, and Brian C. Tiburzi. Pion Polarizabilities and Volume Effects in Lattice QCD. *Phys. Rev.*, D77:014502, 2008.

[79] Jie Hu, Fu-Jiun Jiang, and Brian C. Tiburzi. Current Renormalization in Finite Volume. *Phys. Lett.*, B653:350–357, 2007.

[80] T DeGrand and C. DeTar. *Lattice Methods for Quantum Chromodynamics.* World Scientific, 2006.

[81] W. Detmold, B. C. Tiburzi, and Andre Walker-Loud. Electromagnetic and spin polarisabilities in lattice QCD. *Phys. Rev.*, D73:114505, 2006.

[82] Charles Earl Hyde and Kees de Jager. Electromagnetic Form Factors of the Nucleon and Compton Scattering. *Ann. Rev. Nucl. Part. Sci.*, 54:217–267, 2004.

[83] Martin Schumacher. Polarizability of the Nucleon and Compton Scattering. *Prog. Part. Nucl. Phys.*, 55:567–646, 2005.

[84] F. Fucito, G. Parisi, and S. Petrarca. First evaluation of g_A/g_V in lattice QCD in the quenched approximation. *Phys. Lett.*, B115:148–150, 1982.

[85] G. Martinelli, G. Parisi, R. Petronzio, and F. Rapuano. The proton and neutron magnetic moments in lattice QCD. *Phys. Lett.*, B116:434, 1982.

[86] Claude W. Bernard, Terrence Draper, Kirk Olynyk, and Minick Rushton. Lattice QCD calculation of some baryon magnetic moments. *Phys. Rev. Lett.*, 49:1076, 1982.

[87] H. R. Fiebig, W. Wilcox, and R. M. Woloshyn. A study of hadron electric polarizability in quenched lattice QCD. *Nucl. Phys.*, B324:47, 1989.

[88] Sinya Aoki and Andreas Gocksch. The neutron electric dipole moment in lattice QCD. *Phys. Rev. Lett.*, 63:1125, 1989.

[89] S. Aoki, A. Gocksch, A. V. Manohar, and Stephen R. Sharpe. Calculating the neutron electric dipole moment on the lattice. *Phys. Rev. Lett.*, 65:1092–1095, 1990.

[90] Matthias Burkardt, Derek B. Leinweber, and Xue-min Jin. Background-Field Formalism in Quantum Systems. *Phys. Lett.*, B385:52–56, 1996.

[91] Joseph C. Christensen, Walter Wilcox, Frank X. Lee, and Le-ming Zhou. Electric polarizability of neutral hadrons from lattice QCD. *Phys. Rev.*, D72:034503, 2005.

[92] W. Detmold. Flavour singlet physics in lattice QCD with background fields. *Phys. Rev.*, D71:054506, 2005.

[93] E. Shintani et al. Neutron electric dipole moment with external electric field method in lattice QCD. *Phys. Rev.*, D75:034507, 2007.

[94] J. Gasser and H. Leutwyler. Chiral Perturbation Theory to One Loop. *Ann. Phys.*, 158:142, 1984.

[95] J. Gasser and H. Leutwyler. Low-Energy Expansion of Meson Form-Factors. *Nucl. Phys.*, B250:517–538, 1985.

[96] J. Gasser and H. Leutwyler. Light Quarks at Low Temperatures. *Phys. Lett.*, B184:83, 1987.

[97] J. Gasser and H. Leutwyler. Thermodynamics of Chiral Symmetry. *Phys. Lett.*, B188:477, 1987.

[98] J. Gasser and H. Leutwyler. Spontaneously Broken Symmetries: Eeffective Lagrangians at Finite Volume. *Nucl. Phys.*, B307:763, 1988.

[99] Johan Bijnens and Fernando Cornet. Two Pion Production in Photon-Photon Collisions. *Nucl. Phys.*, B296:557, 1988.

[100] Jean Zinn-Justin. Quantum field theory and critical phenomena. *Int. Ser. Monogr. Phys.*, 92:1–1008, 1996.

[101] John C. Collins, Aneesh V. Manohar, and Mark B. Wise. Renormalization of the vector current in QED. *Phys. Rev.*, D73:105019, 2006.

[102] Martin Luscher. Two particle states on a torus and their relation to the scattering matrix. *Nucl. Phys.*, B354:531–578, 1991.

[103] Martin Luscher. Signatures of unstable particles in finite volume. *Nucl. Phys.*, B364:237–254, 1991.

[104] Laurent Lellouch and Martin Luscher. Weak transition matrix elements from finite-volume correlation functions. *Commun. Math. Phys.*, 219:31–44, 2001.

[105] John Clive Ward. An Identity in Quantum Electrodynamics. *Phys. Rev.*, 78:182, 1950.

[106] H. S. Green. A Pre-renormalized quantum electrodynamics. *Proc. Phys. Soc.*, A66:873–880, 1953.

[107] Y. Takahashi. *Nuovo Cimento*, 10:370, 1957.

[108] T. B. Bunton, F. J. Jiang, and B. C. Tiburzi. Extrapolations of lattice meson form factors. *Phys. Rev.*, D74:034514, 2006.

[109] F. J. Jiang and B. C. Tiburzi. Flavor Twisted Boundary Conditions, Pion Momentum, and the Pion Electromagnetic Form Factor. *Phys. Lett.*, B645:314–321, 2007.

[110] Murray Gell-Mann and M. L. Goldberger. Scattering of low-energy photons by particles of spin 1/2. *Phys. Rev.*, 96:1433–1438, 1954.

[111] F. E. Low. Scattering of light of very low frequency by systems of spin 1/2. *Phys. Rev.*, 96:1428–1432, 1954.

[112] H. Marsiske et al. A measurement of $\pi^0\pi^0$ production in two photon collisions. *Phys. Rev.*, D41:3324, 1990.

[113] M. Colantoni. Measurement of electric and magnetic polarizabilities with Primakoff reaction at COMPASS. *Czech. J. Phys.*, 55:A43–A54, 2005.

[114] Urs Burgi. Charged Pion Polarizabilities to two Loops. *Phys. Lett.*, B377:147–152, 1996.

[115] U. Burgi. Pion polarizabilities and charged pion pair production to two loops. *Nucl. Phys.*, B479:392–426, 1996.

[116] Juerg Gasser, Mikhail A. Ivanov, and Mikko E. Sainio. Low-energy photon photon collisions to two loops revisited. *Nucl. Phys.*, B728:31–54, 2005.

[117] L. V. Fil'kov and V. L. Kashevarov. Determination of π^0 meson quadrupole polarizabilities from the process $\gamma\gamma \to \pi^0\pi^0$. *Phys. Rev.*, C72:035211, 2005.

[118] L. V. Fil'kov and V. L. Kashevarov. Determination of $\pi^\pm$ meson polarizabilities from the $\gamma\gamma \to \pi^+\pi^-$ process. *Phys. Rev.*, C73:035210, 2006.

[119] Michael Engelhardt. Neutron electric polarizability from unquenched lattice QCD using the background field approach. *Phys. Rev.*, D76:114502, 2007.

[120] Brian C. Tiburzi. Baryon electromagnetic properties in partially quenched heavy hadron chiral perturbation theory. *Phys. Rev.*, D71:054504, 2005.

[121] William Detmold and C. J. David Lin. Twist-two matrix elements at finite and infinite volume. *Phys. Rev.*, D71:054510, 2005.

[122] J. F. Donoghue, E. Golowich, and Barry R. Holstein. Dynamics of the standard model. *Camb. Monogr. Part. Phys. Nucl. Phys. Cosmol.*, 2:1–540, 1992.

[123] Daniel Arndt and Brian C. Tiburzi. Charge radii of the meson and baryon octets in quenched and partially quenched chiral perturbation theory. *Phys. Rev.*, D68:094501, 2003.

[124] John F. Donoghue, Barry R. Holstein, and Y. C. Lin. The Reaction $\gamma\gamma \to \pi^0\pi^0$ and Chiral Loops. *Phys. Rev.*, D37:2423, 1988.

[125] Silas R. Beane. Nucleon masses and magnetic moments in a finite volume. *Phys. Rev.*, D70:034507, 2004.

[126] C. T. Sachrajda and G. Villadoro. Twisted boundary conditions in lattice simulations. *Phys. Lett.*, B609:73–85, 2005.

[127] Brian C. Tiburzi. Flavor twisted boundary conditions and isovector form factors. *Phys. Lett.*, B641:342–349, 2006.

Biography

Jie Hu was born in a beautiful city, Zhuzhou, in south China on February 17, 1979. In 1997, she graduated from No. 2 high school of Zhuzhou and left for Hefei when she entered the University of Science and Technology of China (USTC). She found her loves of theoretical physics and dance at USTC and graduated in 2002 with her bachelor's degree in physics. She then headed to Durham, NC to attend Duke University to pursue a Ph.D. in physics. She got married with Lingchu Yu in 2004 and their daughter, Xinyi Hu, was born in 2006.

PUBLICATIONS:

1. **J. Hu** and T. Mehen, "Doubly Heavy Baryons", Proceeding of the 34th International Conference on High Energy Physics, Jul. 29 - Aug. 5, 2008, Philadelphia, PA, will be published electronically by eConf: Electronics Conference Proceedings Archive.

2. **J. Hu**, F.-J. Jiang and B. C. Tiburzi, "Pion Physics at Finite Volume", Proceeding of the XXVI International Symposium on Lattice Field Theory, Jul. 14-19, 2008, College of William and Mary, Williamsburg, Virginia, will be published in the online journal, Proceedings of Science (PoS) organized by SISSA, the International School for Advanced Studies based in Trieste.

3. **J. Hu**, F.-J. Jiang and B. C. Tiburzi, "Pion Physics from Lattice QCD", In the Proceedings of 11th International Conference on Meson-Nucleon Physics and the Structure of the Nucleon (MENU 2007), Juelich, Germany, 10-14 Sep 2007, pp 237, published on the eConf archive at SLAC.

4. **J. Hu**, F.-J. Jiang and B. C. Tiburzi, "Pion Polarizabilities and Volume Effects in Lattice QCD", Phys. Rev. **D77**, 014502 (2008). arXiv:0709.1955 [hep-lat]

5. **J. Hu**, F.-J. Jiang and B. C. Tiburzi, "Current Renormalization in Finite Volume", Phys. Lett. **B653**, 350 (2007). arXiv:0706.3408 [hep-lat]

6. **J. Hu** and T. Mehen, "Chiral Lagrangian with Heavy Quark-Diquark Symmetry", Phys. Rev. **D73**, 054003 (2006). arXiv:hep-ph/0511321

PAPER IN SUBMISSION

1. **J. Hu**, "Doubly Heavy Baryon Zero-Recoil Semileptonic Decay with Heavy Quark-Diquark Symmetry".

AWARDS

2008   Students Award for 34th International Conference on High Energy
        Physics, ICHEP 2008, University of Pennsylvania,Philadelphia, PA,
        July 30 - August 5, 2008.

2008   Duke University Conference Travel Fellowship for Lattice 2008,
        The XXVI International Symposium on Lattice Field Theory,
        College of William and Mary, Williamsburg, Virginia, July 14-19, 2008.

2007   Duke University Conference Travel Fellowship for 11th International
        Conference on Meson-Nucleon Physics and the Structure of the Nucleon,
        IKP, Forschungzentrum Juelich, Germany, September 10-14, 2007.

2007   APS Supplemental Travel Grant for the CAM2007 Conference,
        August 8-11, 2007.

2007   DNP Travel and Registration Grant for the 2007 APS April Meeting,
        April 14-17, 2007.

2007   Duke University Conference Travel Fellowship for 2007 APS April
        Meeting in Florida.

2005   Duke University Conference Travel Fellowship for Introduction to Collider
        Physics Program in IAS, New Jersey.

2004   Duke University Conference Travel Fellowship for 17th National Nuclear
        Physics Summer School in California.

PRESENTATIONS

1. "Pion Physics at Finite Volume", Lattice 2008, The XXVI International Symposium on Lattice Field Theory, College of William and Mary, Williamsburg, Virginia, July 16, 2008.

2. "Pion Charge at Finite Volume", 2008 Duke Graduate Research Day, Duke University, April 2, 2008.

3. "Pion Physics at Finite Volume", Invited seminar talk at the University of Maryland, January 22, 2008.

4. "Doubly Heavy Baryons", 5th International Workshop on Heavy Quarkonia, DESY, Hamburg, Germany, October 19, 2007.

5. "Pion Physics from Lattice QCD", 11th International Conference on Meson-Nucleon Physics and the Structure of the Nucleon, IKP, Forschungzentrum Juelich, Germany, September 13, 2007.

6. "Getting Predictions from Lattice QCD", 3rd Canada-America-Mexico Graduate Student Physics Conference, McGill University, Montreal, Canada, August 9, 2007.

7. "Chiral Lagrangian with Heavy Quark-Diquark Symmetry", APS April Meeting, Jacksonville, Florida, April 15, 2007.

8. "Chiral Lagrangian with Heavy Quark-Diquark Symmetry", Duke Physics Nuclear and Particle Theory Seminar, Duke University, November 9, 2005.

9. "Pentaquark", Duke Physics Graduate Student Seminar, Duke University, August 20, 2004.

POSTERS

1. "Doubly Heavy Baryons", 34th International Conference on High Energy Physics (ICHEP 2008), University of Pennsylvania, 31 July 2008 (Invited).

2. "Excited Charmed Mesons in Heavy Hadron Chiral Perturbation Theory", 2005 Duke Graduate Research Day Poster Session, Duke University, March 30, 2005.

3. "Pentaquark, the Exotic Baryon", Duke Physics 2004 Poster Section, Duke University, April 14, 2004.